Alma Mater Studiorum – Università di Bologna

DOTTORATO DI RICERCA IN

Oncologia, Ematologia e Patologia Clinica

Ciclo XXXVI

Settore Concorsuale: MED-12

Settore Scientifico Disciplinare: 06/D4

A combination of Rapamycin, ω3-PUFA Docosahexaenoic Acid and Epigallocatechin-3-gallate for the simultaneous suppression of PI3K/mTOR pathway and Wnt/β-catenin signalling in colorectal carcinogenesis

Presentata da: **Chiara Alquati**

Coordinatore Dottorato

Prof. Manuela Ferracin

Supervisore

Prof. Luigi Ricciardiello

Co-supervisore

Prof. Lorenzo Montanaro

Esame finale anno 2024

TABLE OF CONTENT

ABSTRACT

Loss of function mutations in the APC gene represent a critical hit for colorectal cancer (CRC) onset in both sporadic and inherited settings (e.g. FAP). This gene encodes a tumor suppressor protein that regulates the Wnt/β-catenin pathway. Together with the PI3K/mTOR signalling, Wnt/β-catenin is frequently deregulated in the early stages of CRC development. Relevant cross-talks between the two pathways have been described, and over the years, numerous inhibitors of Wnt and mTOR signallings have been developed and tested against CRC. However, long-term treatment often fails due to the acquisition of resistance mechanisms, which are usually associated to the activation of the non-inhibited pathways. The aim of the study was to evaluate the effect of a combination (RDE) of Rapamycin, ω3-PUFA Docosahexaenoic Acid (DHA) and epigallocatechin-3-gallate (EGCG) on PI3K/mTOR and Wnt/β-catenin pathways to define an effective combinatorial approach against APC-driven CRC onset and progression. RDE was tested in selected different genetic backgrounds: (i) *APC-mutated background* consisting of intestinal organoids derived from FAP patients morphologically normal-appearing mucosa (NM) and adenomas (A); sporadic CRC-cancer (K) organoids, and the cell lines SW480 and HT-29; (ii) *non-APC-mutated CRC background* comprising HCT116 (CTNNB1 mutated) cell line; HEK293STF cell line and healthy FIT+ NM/ CRC-NM-derived organoids as *non-mutated backgrounds* (iii). Cells and organoids viability, markers of intestinal stemness (*LGR5*) and differentiation (*KRT20*), were evaluated together with expression of target genes and effector proteins of the Wnt/β-catenin and PI3K/mTOR pathways. We found that RDE strongly inhibited PI3K/mTOR by suppressing the activation of the downstream effectors protein P70S6K and S6R in a background-independent manner. Compared to the markedly inhibition of mTOR signalling, we observed that targeting Wnt/β-catenin pathway appeared more challenging and was mostly influenced by the intrinsic activation status of Wnt/β-catenin pathway. More specifically, in *pre-cancerous settings* comprising FAP NM/A and non-mutated organoids, RDE enhanced the Wnt signalling activation. In contrast, in both *APC-mutated and non-APC-mutated CRC settings* RDE, after activating the Wnt/β-catenin pathway, induced β-catenin protein degradation through non-canonical effectors involved in the modulation of the Wnt signalling. Despite the induction of Wnt/β-catenin pathway, RDE affected cell and organoids viability (20%) and significantly suppressed LGR5, promoting

a shift towards differentiation. Taken together our results suggests that RDE is a potential therapeutic approach for both preventive and therapeutic strategies against *APC*-driven CRC.

1. INTRODUCTION

1.1 Colorectal Cancer

Colorectal cancer (CRC) is the third most common type of tumor worldwide and accounts for the fourth most common cause of cancer-related deaths (Màrmol I. et al., 2017). Despite improvements in diagnoses and prevention, the incidence remains high (Brody H. et al., 2015). According to the cancer registries and mortality from the National Center for Health Statistics, in 2023, approximately 153,020 individuals will be diagnosed with CRC and 52,550 people will die for it. In addition, among those under 50 years of age, 19,550 people will develop CRC and 3,750 will die for it. However, it has been reported a decline in CRC incidence and mortality. Indeed, CRC incidence slowed from 3% to 4% per year in the 2000s to 1% per year between 2011 and 2019, while CRC mortality decreased by 2% per year compared to 2011–2020. Despite the overall decrease, CRC is rapidly moving toward younger age groups with more advanced stages in left colon/rectum at the diagnoses (Siegel R.L. et al., 2022). Indeed, it increased by 0.5%–3% annually in individuals younger than 50 years and in Native Americans younger than 65 years. A shift toward left-sided tumors, with the rate of rectal cancer increasing from 27% in 1995 to 31% in 2019, has also been reported too (Siegel R.L. et al., 2022).

In recent year, the improvement of CRC screening (e.g. stool-based tests and endoscopic methods) has led to the possibility of detecting and removing pre-cancerous lesions, contributing to a reduction in CRC mortality in a growing number of countries (Lauby-Secretan B. et al., 2018). The importance of CRC screening emerged during the SARS-CoV-2 pandemic in 2019-2020. Indeed, it has been estimated that the limited access to preventive health care and delayed screening with a growing number of non-diagnosed pre-cancerous lesions will increase the risk of mortality due to an increase in advanced CRC cases (Ricciardiello L. et al., 2021).

Intriguingly, it has been reported also a difference in CRC incidence between developed and developing nations, with the highest frequency occurring in economically developed countries, particularly Australia/New Zealand, United States, and Europe, and the lowest incidence occurring in Africa and South-Central Asia (Figure 1.1). Indeed, compared to less developed countries, more developed areas had a higher risk of developing CRC (Arnold M. et al., 2020).

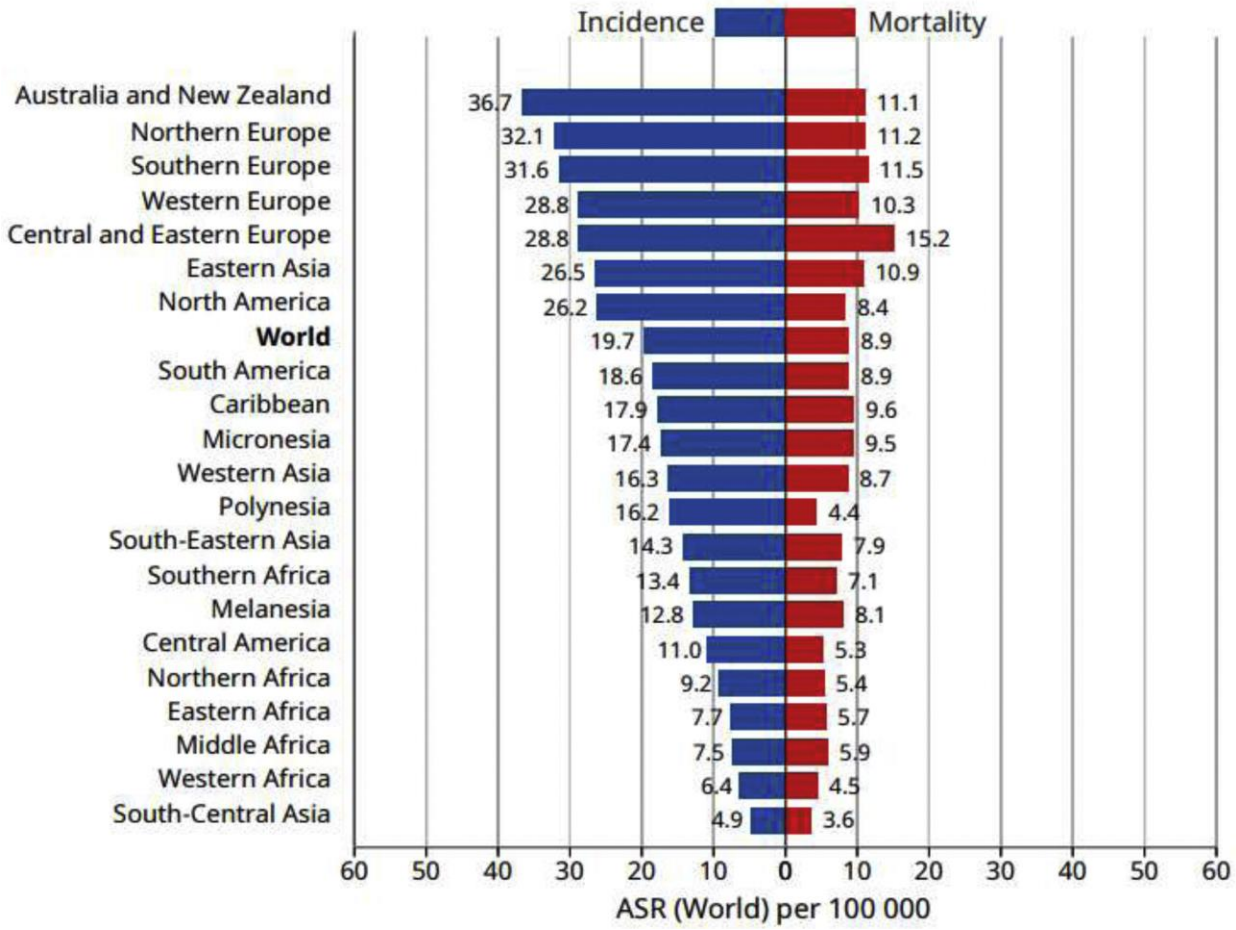

Figure 1.1 Estimated incidence and mortality rates by world region for colorectal cancer in 2018 (Arnold M. et al, 2020).

These differences in CRC incidence between countries highlighted the role of lifestyle and environment as relevant risk factors in the development of CRC. Among the modifiable factors contributing CRC onset the major determinants are diet, obesity, smoking, and alcohol abuse (Fiedler M.M. et al., 2017).

While environmental factors play a significant role in the etiology of colorectal cancer, hereditary or genetic predisposition can also influence the development and progression of the disease. Indeed, CRC can be classified, depending on the genetic of the mutation, as sporadic, hereditary, or familial.

1.1.1 **Sporadic Colorectal Cancer**

CRC is a heterogeneous disease that can occur in 70% of cases sporadically without a defined inherited or family-related component or a predisposing syndrome. The majority of sporadic CRC develops through a multistep process referred to as the 'adenoma-carcinoma sequence', during which a carcinoma develops from a pre-existing benign adenoma due to morphological transformations associated with an accumulation of both genetic and epigenetic alterations (Fearon and Vogelstein, 1990). Aberrant crypt foci (ACF) are known as the earliest histological changes that occur during the multi-step development of colorectal cancer (Clapper M.L. et al., 2020). In 1987, Bird described for the first time these lesions after observing clusters of crypts with a peculiar morphology in the colonic mucosa of C57BL/6 and CF1 mice treated with the colon carcinogen azoxymethane (AOM), a carcinogen commonly used to induce CRC (Bird R.P., 1987). Indeed, dysplastic ACFs are characterized by detectable epithelial alterations of a neoplastic nature, which includes hypercellularity with enlarged hyperchromatic nuclei, nuclear stratification, loss of polarity, high nuclear/cytoplasmic ratio, and increased mitotic index (Roncucci L. et al., 1991). Despite being generally identified as very early lesions, ACFs are known to regress spontaneously by 10 weeks (Choi J.W. et al., 2015), while only a small fraction turning into adenoma and ultimately to CRC, through the influence of a protumorigenic microenvironment that supports the acquisition of further mutations (Choi J.W. et al., 2015).

Tumor progression is enhanced by multiple genetic events. Among these, genomic instability represent a crucial cellular feature that follows the acquisition of mutations. The number of mutations needed for the development of cancer is hard to be accounted and defined by baseline mutation rates, and according to Loeb et al.'s hypothesis, cancer cells must develop a "mutator phenotype," which boosts their rate of new mutations (Loeb L.A., 2003).

Three main genetic pathways for the onset of CRC have been described: chromosomal instability (CIN), microsatellite instability (MSI), and CpG islands methylator phenotype (CIMP).

CIN is observed in 65-70% of sporadic colorectal cancers (Cho J. et al., 2022). The term describes an accelerated rate of gains or losses of whole chromosomes or large portions of them that causes karyotypic variability from cell to cell (Lengauer C. et al., 1998). The CIN phenotype may result from defective chromosome segregation, telomere dysfunction or impaired DNA damage response. As a result, the CIN phenotype is characterized by an unbalanced number of chromosomes (aneuploidy), sub-chromosomal genomic amplifications and a high rate of loss of heterozygosity (LOH) (Pino MS. e

Chung DC., 2010). The prevalent localization of these tumors is the left or distal side of the colon (Grady and Carethers, 2008). The canonical CIN pathway adheres to the model introduced by Fearon and Vogelstein in 1990, which outlined a well-defined temporal sequence of genetic mutations within the 'adenoma-carcinoma' progression (Fearon and Vogelstein, 1990; Figure 1.2).

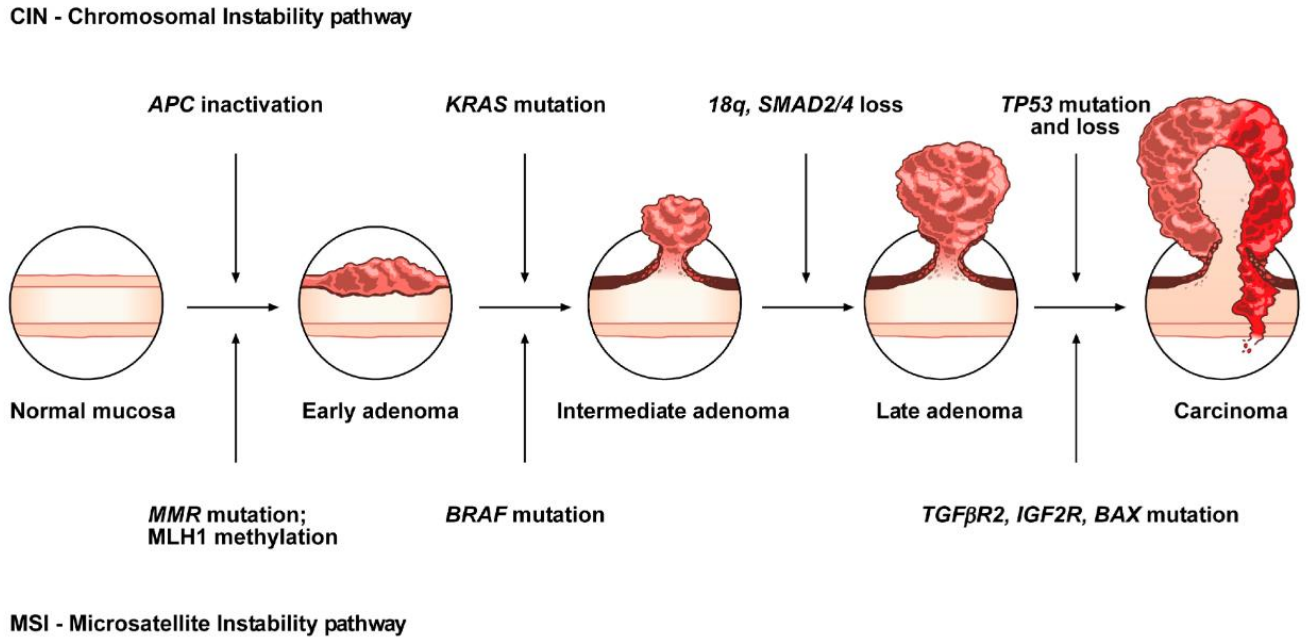

Figure 1.2 Conventional adenoma-to-carcinoma sequence, which includes the chromosomal instability (CIN) pathway and the microsatellite instability (MSI) pathway (De Palma F.D.E. et al., 2019).

According to this model, inactivating mutations in the Adenomatous polyposis coli (APC) gene or loss of chromosome 5q, which include the *APC* gene, are pivotal event in the onset of CRC. The relevance of the *APC* gene in the pathogenesis of CRC is attributable to its central role as tumor suppressor gene in the regulation of the canonical Wnt signalling pathway, that controls cell proliferation (Cadigan and Liu, 2006).

Mutations in the oncogene *KRAS* occur as the following step and characterize the intermediate adenoma stage (Fearon and Vogelstein, 1990). Aberrations in the *KRAS* gene, which encodes for a guanosine triphosphate/guanosine diphosphate binding protein, led to constitutive activation of the downstream Ras/Raf/Mek/Erk pathway, involved in the regulation of cell proliferation,

differentiation, invasion and apoptosis (Smith et al., 2002; Smith et al., 2010). Moreover, the advanced adenomas are usually distinguished by LOH which affect SMAD2, SMAD4 and DCC genes (Colussi D. et al., 2013).

Finally, mutations in the tumor-suppressor gene *TP53* or deletions of chromosome 17p harboring this gene, are commonly recognized as later event leading to in situ malignant transformation from adenoma to carcinoma (Fearon and Vogelstein, 1990). Even though it is more frequent in advanced stages of colorectal tumorigenesis, more recent evidences have demonstrated the existence of *TP53* mutations in both normal colonic epithelial stem cells (Lee-Six H. et al., 2019), and early/ premalignant colorectal adenomas (Alquati C. et al., 2021).

While the model proposed by Fearon and Vogelstein established the basis to understand the molecular mechanisms underlying sporadic CRC onset and progression, CRC develops through the interplay of a multitude of factors. Indeed, the advent of new and more advanced techniques has led to the identification of additional genetic pathways, epigenetic changes, and the modulation of non-coding RNAs that contribute significantly to the malignant transformation of the colonic tissues (Pancione M. et al., 2012).

As mentioned above, a different model of genetic instability is the MSI pathway (Figure 1.2) which is implicated in approximately 15-20% of sporadic cases of CRC (Ward R. et al., 2001).

Microsatellites are short tandem repeats distributed throughout the human genome, both in coding and non-coding regions. Such DNA sequences are susceptible to the occurrence of nucleotide mutations, which accumulate during the S-phase of the cell cycle. In normal conditions, these aberrations are repaired by the activity of the MMR system (Mismatch Repair System), a mechanism involved in DNA damage repair together with the Base Excision Repair System (BER), the Nucleotide Excision Repair System (NER), and the Non-Homologous End-Joining System(NHEJ) (Vilar E. and Gruber S.B., 2010). Conversely, the MSI phenotype results from germline or somatic mutations in one or more of the genes encoding for components of the MMR system (hMLH1, hMSH2, hMSH6, and hPMS2) (Thibodeau S.N. et al., 1993). Particularly, germline inactivating mutations are causative of the CRC-predisposing Lynch syndrome, while epigenetic modifications (methylation in the promoter of MLH1 gene) are responsible for sporadic CRC cases. Defects in these genes are responsible for several insertions or deletions that affect microsatellite sequences in the DNA due to an improper recognition and elimination of the mispaired base-pairs (Ward R. et al., 2001).

A standard panel of five microsatellite markers is commonly used according to the Bethesda guidelines to determine the MSI status of a tumour (Bolonad C.R. et al., 1998). The panel includes the two mononucleotide markers (BAT26 and BAT25) and the three dinucleotide markers (D2S123, D5S346 and D17S250). According to the number of unstable microsatellites, tumours are classified as MSI high (MSI-H) when ≥ 30% of markers present instability, MSI low (MSI-L) when< 30% of markers are characterized by instability, and microsatellites stable (MSS) when no reported instability is present (Findeisen P. et al., 2005).

Compared to CIN and MSI, in the CIMP model the development of CRC is promoted by epigenetic events rather than changes in the DNA sequence. The DNA hypermethylation at the CpG island in the promoter of tumour suppressor genes, which causes gene silencing, is now recognized as an important mechanism in human carcinogenesis (Laird P.W. et al., 2005). The CIMP phenotype has been identified in 30-35% of colorectal adenomas and is considered as an early event and a hallmark of the serrated pathway (Samowitz W.S. et al., 2005). However, Ogino et al, through a quantitative DNA methylation study, demonstrated that CIMP accounted for 17% of CRC cases, a lower frequency compared to previously reported events, and that the clinical features of CIMP were similar to those of MSI-associated CRC (Ogino S. et al., 2006). Indeed, sporadic MSI colorectal cancers are mostly associated with CIMP-associated MLH1 methylation, which leads to inactivation of this gene (Boland C.R. and Goel A., 2010). Moreover, CIMP-positive colorectal tumors display a distinctive profile, characterized by the onset of the CRC in the proximal colon, poor differentiation, microsatellite instability (MSI), *BRAF* mutations, and *wild-type KRAS.* It should be noted that *BRAF* gene mutations are more common in CIMP-positive cancers than in CIMP-negative malignancies (Nguyen H.T. and Duong H.; 2018).

Additional CIMP loci include: CACNA1G, IGF2, NEUROG1, RUNX3, and SOCS1 (Weisenberger D.J. et al., 2006). The current evaluation of colorectal cancer's CIMP status relies on a panel of methylation markers, which categorizes CRC as either exhibiting or not exhibiting DNA methylation, based on predefined thresholds (Nguyen H.T. and Duong H.; 2018). According to Shen et al. it is possible to distinguish CIMP-high tumors which are strongly linked to MSI status (80%) and BRAF mutations (53%), compared to CIMP-low tumors, characterized by KRAS mutations (92%), and CIMP-negative tumors typically present a higher frequency of p53 mutations (71%) (Shen L. et al., 2007).

1.1.2 Hereditary Colorectal Cancer

As previously described, about 70% of CRCs are sporadic, whereas approximately 6-10% of cases are classified as inherited forms of CRC. The histologic subtype of the precancerous lesion and the presence of polyposis can both be used as features to classify hereditary colorectal cancer syndromes. Adenomatous syndromes include Lynch syndrome (which is not typically associated with polyposis and for this reason has been previously referred as hereditary non-polyposis colorectal cancer or HNPCC) and the polyposis syndrome, such as the familial adenomatous polyposis (FAP), the attenuated familial adenomatous polyposis (AFAP), MUTYH-associated polyposis (MAP), and other uncommon hereditary disorders like Peutz-Jeghers syndrome, Cowden syndrome, and juvenile polyposis. Germline mutations are a common feature of all of these syndromes, which significantly increase the risk of developing CRC at a younger age (Medina Pabón M.A. e Babiker H., 2022).

1.1.2.1 Familial Adenomatous Polyposis (FAP)

FAP is an inherited syndrome characterized by an autosomal dominant pattern, which affects both sexes equally and has an incidence rate of 1 in 1000 births. It is the second most common inherited colorectal cancer syndrome, yet contributes to only 1% of diagnosed CRC (Kant P. et al., 2017). The clinical phenotype is distinguished by the development of hundreds to thousands of adenomas throughout the colon and rectum at a young age (childhood or adolescence), anticipating the multifocal adenoma-carcinoma sequence and thus predisposing to a 100% risk of developing CRC at a median age of 35–45 years if untreated (Shussman and Wexner, 2014). FAP also correlates with other malignancies, including gastric, duodenal, hepatoblastoma, and desmoid tumors. Currently, prophylactic proctocolectomy represents the surgical standard of care for a substantial reduction in the risk of developing colorectal cancer. After colectomy, FAP patients undergo lifelong endoscopic surveillance since adenomas could arise and develop in the retained rectum or ileal pouch, as well as gastric and duodenal cancer can occur (Aelvoet A.S. et al., 2023).

Germline mutations in the tumour suppressor gene adenomatous polyposis coli (APC) are causative of the FAP syndrome. The *APC* gene encodes for a scaffold protein implicated in the negative regulation of the β-catenin, the main effector protein of the Wnt signalling, that, when aberrantly activated, leads to the malignant transformation of colonic epithelial cells (Morin et al., 1997). According to

several studies, nonsense or frameshift mutations are the most prevalent *APC* germline mutations reported in patients with classical FAP, occurring in up to 80% of cases and resulting in a modified truncated protein (Stekrova J. et al., 2007). In addition, the location of the mutation along the *APC* gene has been associated with distinctive clinical phenotypes. The altered functions of mutated-APC might promote and drive the development of CRC. However, the transition from an early adenoma to an aggressive carcinoma requires further mutations in other oncogenes or tumor-suppressor genes as for most of the sporadic CRCs. The two-hit hypothesis, proposed by Knudson, well describes how carcinogenesis proceeds when both *APC* alleles are inactivated, and, in FAP patients, the inherited germline mutation represents the first hit (Lamlum H. et al., 1999). Importantly, it has been demonstrated that the two *APC* hits are not fully independent from each other and do not occur randomly to avoid an uncontrolled activation of the Wnt signalling and a consequent uncontrolled replication that would cause cellular death, preventing the formation of the tumor (Albuquerque C. et al., 2002).

A hallmark of FAP patients is the co-existence of multiple and diffuse adenomas at different stages. Genomic and transcriptomic sequencing analysis revealed that adjacent spatially separated adenomas arose from the same cell, supporting the theory of field cancerization by crypt fission and the hypothesis that tumor's development begins before it manifests as a visible lesion (Li J. et al., 2019).

Despite technical progress, we are still unable to fully diagnose all FAP cases as those induced by mosaicisms or mutations in deep intronic promoter regions (Kerr S.E. et al., 2013).

It is to note that exists also a milder form of FAP, referred to as attenuated-FAP (AFAP), which is diagnosed when the number of colorectal adenomas ranges from ≥ 20 to ≤ 100. In contrast to the conventional FAP, in AFAP adenomatous polyps develop later and the lifelong cancer risk is lower. However, the genetics of AFAP has been poorly characterized, and mutations in the APC or MUTYH genes have been rarely found (Knudsen A.L. et al., 2003).

Further details on APC mutations will be discussed later (Section 1.2.1).

1.1.2.2 MUTYH – Associated Polyposis (MAP)

MUTYH-Associated Polyposis (MAP) is an autosomal recessive disease which appears in individuals with biallelic mutations in the *MUTYH* gene (Kantor M. et al., 2017). *MUTYH* encodes for a DNA glycolase, involved in the Base Excision Repair system and is crucial to avoid DNA transversion (G:C to

T:A), by removing guanine mispaired with 2-hydroxyadenine and adenine opposing 8-oxoguanine (8-oxoG), which are formed as a result of oxidative stress (Goodenberger M. and Lindor N.M., 2011). Accordingly, MAP is responsible for fewer than 1% of all CRCs and is linked to a 28-fold increase in the risk of CRC. Indeed, the risk is 48% in individuals under 60, and the lifetime risk is 80-90% in non-surveilled patients (Curia M.C. et al., 2020).

Similarly to AFAP, MAP is characterized by the growth of ten to hundreds of colorectal polyps in adulthood, however, it differs by an overall higher cancer susceptibility and peculiar features. Firstly, together with colorectal adenomas, hyperplastic polyps and sessile serrated lesions are also frequent in MAP and are thought to be part of the phenotype (Boparai K.S. et al., 2018). Further, the clinical spectrum of MAP is extensive and highly unpredictable, and even if in general the disease is mild with a low number of polyps, eventually, it could manifest in some individuals with a higher number of polyps. Moreover, the high mutational burden and *KRAS* gene mutations of MAP polyps seems to drive an accelerated carcinogenesis (Thomas L.E. et al., 2017). Additionally, whereas polyps of FAP patients (and eventually CRC) are typically detected on the left side of the colorectum, the preferred location for these lesions in MAP patients is the right colon. Moreover, Lynch-like extraintestinal malignancies like ovarian, endometrial, urinary, skin, thyroid, and breast cancers as well as sebaceous adenomas appear to be more common (Curia M. C. et al., 2020).

1.1.2.3 Lynch syndrome

Lynch Syndrome is an autosomal dominant disorder which predisposes subjects to an early onset of colorectal cancer (approximately 44 years) mainly in the right colon and typically without polyposis. Lynch syndrome is the most common form of hereditary CRC accounting for 3% of all CRCs and affects approximately 1/300 in the Western population, predisposing to an 80% lifetime risk to develop CRC (Win A.K. et al., 2017). A distinctive feature of Lynch syndrome is the occurrence of extracolonic malignancies in addition to CRC. Among these, we predominantly found endometrial cancer (average age of diagnosis 45-50 years), followed by other Lynch syndrome-associated tumours including those of the stomach, liver, biliary system, urinary tract, small intestine, pancreas, brain, and sebaceous glands, with a lifetime absolute risk ranging from 5% to 20%, depending on the genetic mutation (Dominguez-Valentin M. et al., 2020).

Lynch syndrome is defined by the presence of germline pathogenic variants in the DNA mismatch repair genes (MMR) *MLH1*, *MSH2*, *MSH6* and *PMS2* (de la Chapelle A., 2004), and, in a subset of cases, it is due to 3' end deletion of the *EPCAM* gene, with subsequent epigenetic silencing of MSH2 (Sehgal R. et al., 2014). Pathogenic variants in *MLH1* and *MSH2* are usually associated to a lifetime risk of a multitude of cancer-occurrence of approximately 43-46% with a median onset age around 48–54 years and few differences between sexes. Conversely, in *MSH6* pathogenic variant carriers the lifetime cancer risk is reduced to 29% in males and 55% in females with a median age of tumour onset of 56–57 years. Moreover, *PMS2* pathogenic variant subjects are not generally associated with early-onset cancers, and CRC develops mostly at a median age of 66–70 and 61 year (Peltomäki P. et al., 2023). As for the *APC* gene in FAP syndrome, the inactivation of the remaining *wild-type* allele is a later and somatic-related event in the majority of patients, after acquiring a germline mutation in one copy of the MMR genes. Because the MMR system's primary function is to detect and correct mispaired bases and potential insertion/deletion events during DNA replication, mutations in these genes result in an accumulation of replication errors in microsatellites sequences that leads to an MSI phenotype, which is the defining feature of Lynch syndrome (de la Chapelle A., 2004).

1.2 The canonical Wnt/β-catenin pathway

WNT proteins are ubiquitous and cross-species conserved growth factors that control different phases of the cell cycle and, together with cell proliferation, guide the correct allocation of different cell types within the tissue (Huang Y.L. and Niehrs C., 2014; Habib S.J. et al., 2013).

Genes encoding for WNT proteins (e.g., WNT1, WNT2, WNT3), which act as pathways activating ligands, are numerous within the animal genome, and 19 genes have been identified in mammals. With the aim of understanding whether individual proteins perform individual or redundant functions, the deletion of genes belonging to the WNT family has been found to lead to different phenotypes, indicating that each protein plays a specific role (Nusse R. and Clevers H., 2017).

WNT proteins act as intercellular signals, however the mechanisms involved in their synthesis and extracellular transport still need to be clarified. During their synthesis, the Wnt factors are 40KDa proteins rich in cysteines, which are post-translationally modified by Porcupine enzyme through the addition of the lipid palmitoleic acid (Rios-Esteves J. and Resh M.D., 2013) (Figure 1.3).

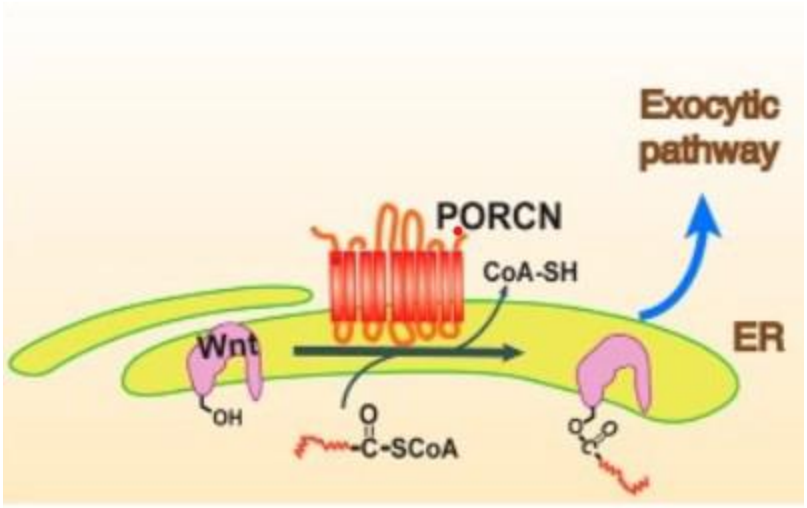

Figure 1.3 Porcupine enzyme reaction: acyl-CoA is transferred onto a conserved serine residue of the WNT (Ser209), which promotes the addition of the monounsaturated fatty acid to the signal protein (Lee C.J. et al., 2019).

This post-translational modification fulfills two main roles: firstly, the lipid gives the protein a hydrophobic nature required for its interaction with the plasma membrane; secondly, it acts as a binding motif between the WNT protein and the receptor FZD (Janda C.Y. et al., 2012).

During the maturation in the Golgi apparatus, the modified protein binds the transmembrane protein WNTLESS/EVI (WLS) (Yu J. et al., 2014; Nusse R. and Clevers H., 2017), whose role is to facilitate the exocytosis of the lipidated-WNT proteins. It is assumed that, once released into the extracellular environment through vesicles or exosomes, the WNT lipid-mature protein and the WLS protein form complexes with exosomes (Korkut C. et al., 2009). Within this structure, Wnt proteins exposed on the outside of the vesicle and can bind to the receptor FZD and the transmembrane E3 ligases Rnf43/Znrf3 on the cell surface (Fig 1.4).

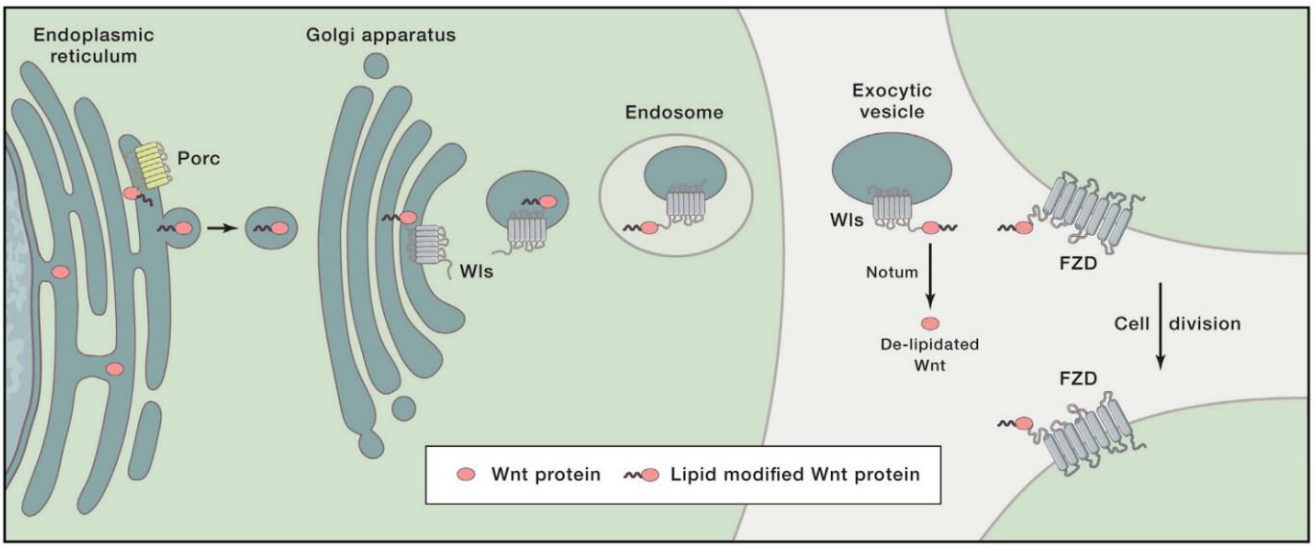

Figure 1.4 Mature-WNT protein secretion model (Nusse R. and Clevers H., 2017).

The triggering event for the activation of the Wnt/β-catenin pathway is the binding of the WNT protein to its own receptor complex, which consists of two components: the FZD (Frizzled protein) and LRP5/6 (Low-density lipoprotein receptor-related protein 5 and 6) proteins. The FZD proteins are constituted by a 7-domain transmembrane receptors and an N-terminal cysteine-rich domain (CRD) (Bhanot P. et al., 1996), which interact with the C-terminal end of the WNT protein signal. The CRD domain contains different sites of interaction, including a hydrophobic lipid binding site (Janda C.Y. et al., 2012).

The binding of the WNT protein to its receptor induces a conformational change of both FZD and the single transmembrane domain receptor LRP5/6, resulting in its heterodimerization (Janda C.Y et al., 2017). Following the conformational changes of the receptor complex, the cytoplasmic component of LRP5/6 undergoes a phosphorylation process driven by several kinases, including GSK3β, which acts on a serine residue located within the "PPPSP" amino acid motif. The modified amino acids serve as a binding site for the scaffold protein AXIN1 (Stamos J.L. et al., 2014). β-catenin, Axin, and APC are some of the components of the Wnt signalling that share the same PPPSP motif (Stamos J.L. et. al., 2014).
The cytoplasmic component of the FZD receptor binds the DISHEVELLED (DVL) protein (Tauriello D.V.F. et al., 2012), which is able, through its DIX domain, to interact with AXIN1 (Schwartz-Romond T.

et al., 2007; Fiedler M. et al., 2011). It has been proposed that the multimerization of receptor-bound DVL and Axin molecules facilitates LRP-FZD dimer formations (Gammons M.V. et al., 2016).

The downstream effector of the Wnt pathway is the β-catenin protein, whose concentration is closely dependent on the activation of the destruction complex, now referred to as degradosome. The degradosome consists of the tumor suppressor AXIN1, a scaffold protein that binds to the β-catenin, together with the APC protein and two serine-threonine-dependent kinases, CSK1α/δ and GSK3α/β. The APC protein contains three binding domains for AXIN1, alternately spaced by a series of 15-20 amino acid repeats that interact with β-catenin (Nusse R. and Clevers H., 2017). Several studies identified in APC a conserved domain called "CID" (β-catenin inhibitory domain), located between the second and the third repeats (Kohler E.M. et al., 2009; Roberts D.M. et al., 2011), which seems to be involved in the downregulation of the β-catenin. According to previous findings, the domain stabilizes the binding between APC and β-catenin, promoting the ubiquitination of the effector protein (Choi S.H. et al., 2013). Conversely, according to more recent studies, GSK3α/β-dependent phosphorylation of the CID domain triggers its conformational change, making the complex more accessible to the E3 ubiquitin-ligase enzymes (Pronobis M.I. et al., 2015).

When FZD/LRP receptors do not interact with the WNT ligands, the kinases CSK1α/δ and GSK3α/β phosphorylate the β-catenin protein on specific amino acids: CSK1α/δ phosphorylates the Ser45 residue while GSK3α/β phosphorylates Thr41, Ser37 and Ser33 (Liu C. et al., 2002). These phosphorylated residues serve as binding sites for the E3 ubiquitin-ligase b-TrCP enzymes, which are responsible for the ubiquitination of the β-catenin protein and lead to its subsequent degradation (Aberle H. et al., 1997; Kitagawa M. et al., 1999) (**Wnt OFF**, Fig. 1.6).

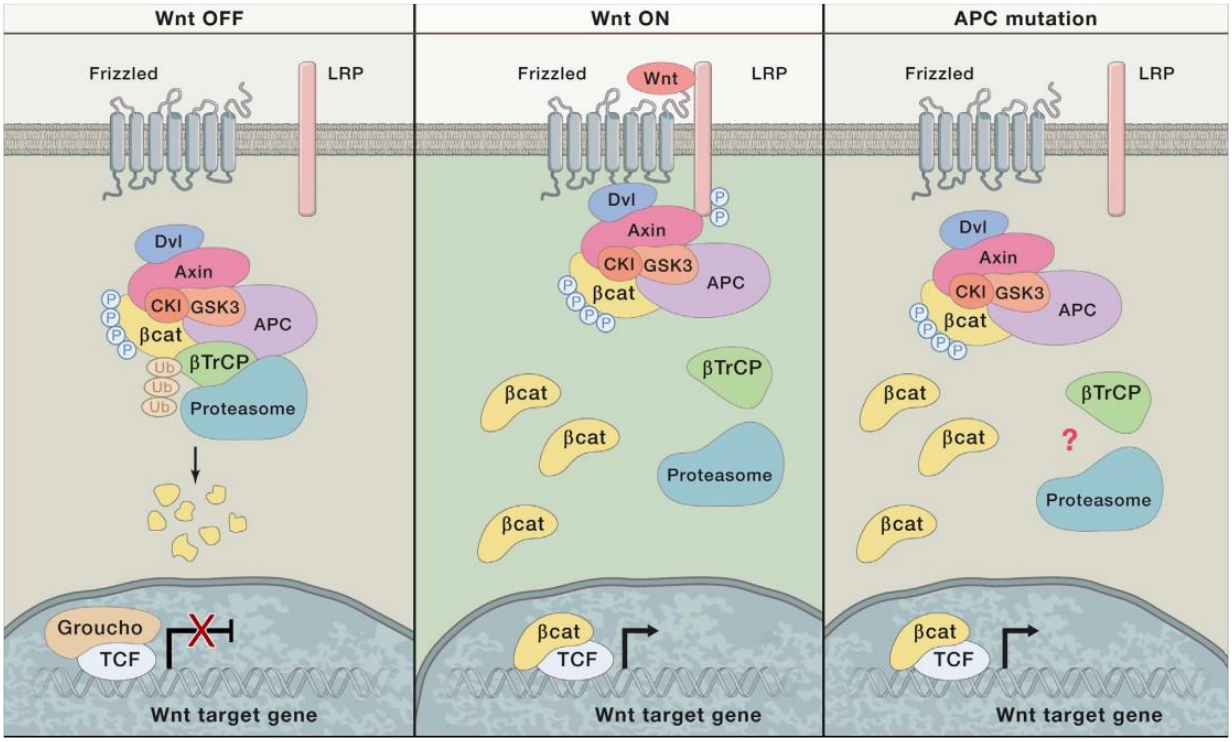

Figure 1.6 Schematic representation of the canonical Wnt pathway (Nusse R. and Clevers H., 2017).

Upon activation of the FZD/LRP receptors due to the binding with the Wnt proteins, the degradosome is recruited to the plasma membrane. As a result, the LRP-receptor's phosphorylated sites phosphorylate GSK3α/β, contributing to the negative regulation of the degradosome and promoting the intracellular accumulation of the β-catenin protein (Stamos J.L. et al., 2014). It has also been suggested that, when anchored to the FZD receptor through DVL, the degradosome inhibits the ubiquitination of the β-catenin, resulting in the accumulation also of its phosphorylated form in the proximity of the plasma membrane (Li V.S. et al., 2012; Azzolin L. et al., 2014) (**Wnt ON**, Fig. 1.6). However, this mechanism is much more complex. Indeed, it has been found that, after the signalling activation, ubiquitination of phosphorylated β-catenin is initially blocked within the intact degradosome. As a consequence, the phosphorylated form of the β-catenin saturates the degradosome, leading to the accumulation of newly synthesized non-phosphorylated β-catenin, free to translocate to the nucleus and to activate target genes (Li V.S. et al., 2012; Azzolin L. et al., 2014).

After Wnt activation, the accumulated and non-phosphorylated β-catenin translocates into the nucleus and binds the transcriptional factor TCF (Behrens J. et al., 1996; Molenaar M. et al., 1996) which promotes the transcription of the target genes (e.g *AXIN2, CCND1, C-MYC*) (Lusting B. et al.,

2002) (Fig. 1.6). Importantly, it has been suggested that low levels of nuclear β-catenin are sufficient to enhance the gene target activation (Goentoro L. and Kirschner M.W., 2009).

Two crucial steps inhibiting the β-catenin phosphorylation and/or ubiquitination have been proposed as essential drivers of the impairment of β-catenin degradation upon Wnt stimulation. Most of the evidence supports the idea that both the inhibition of β-catenin phosphorylation and the disassembly of the degradosome represent the crucial events during Wnt/β-catenin pathway activation.

Hernández et al. demonstrated by analysing the kinetics of the β-catenin turnover that, in the initial stages following Wnt stimulation, the reduced levels of GSK3-mediated β-catenin phosphorylation are responsible for inhibiting β-catenin degradation, whereas a subsequent recovery of β-catenin phosphorylation would restore its degradation. This model predicts that suppression of β-catenin phosphorylation causes an accumulation of β-catenin during Wnt activation (Hernandez A.R. et al, 2016).

Further, during the early phases of Wnt activation, it has been described an increase in AXIN1 protein stability, which contributes to the signalosome assembly and Wnt/β-catenin signalling initiation. However, upon prolonged Wnt stimulation, the enzyme poly (adenosine diphosphate-ribose) polymerase (TNKS) contributes to the proteolysis and degradation of AXIN1. This event enhances the disruption of the degradosome and results in sustained activation of the Wnt/β-catenin signalling (Yang E. et al., 2016).

Moreover, emerging evidence has shown that ring finger protein 43 (RNF43), the transmembrane E3 ubiquitin ligase zinc and ring finger 3 (ZNRF3) and DVL are critically involved in the regulation of the extrinsic Wnt/β-catenin pathway activation by modulating the levels of Wnt receptors on the cellular surface. Indeed, RNF43 and ZNRF3 promote a negative regulation of the pathway mediating the internalization and the subsequent degradation of the FZD and LRP6 receptors. Importantly, within this mechanism, it has been demonstrated that DVL is required also for RNF43 and ZNRF3-mediated degradation of FZD and LRP6 (Jiang X. et al, 2015). On the other hand, R-spondin, biding to the LGR5 receptor, via its second furin domain, and interacting with the RNF43 and ZNRF3 complex, inhibits them and enhances the activation of the Wnt/β-catenin signalling (de Lau W. et al., 2014) (Fig. 1.7).

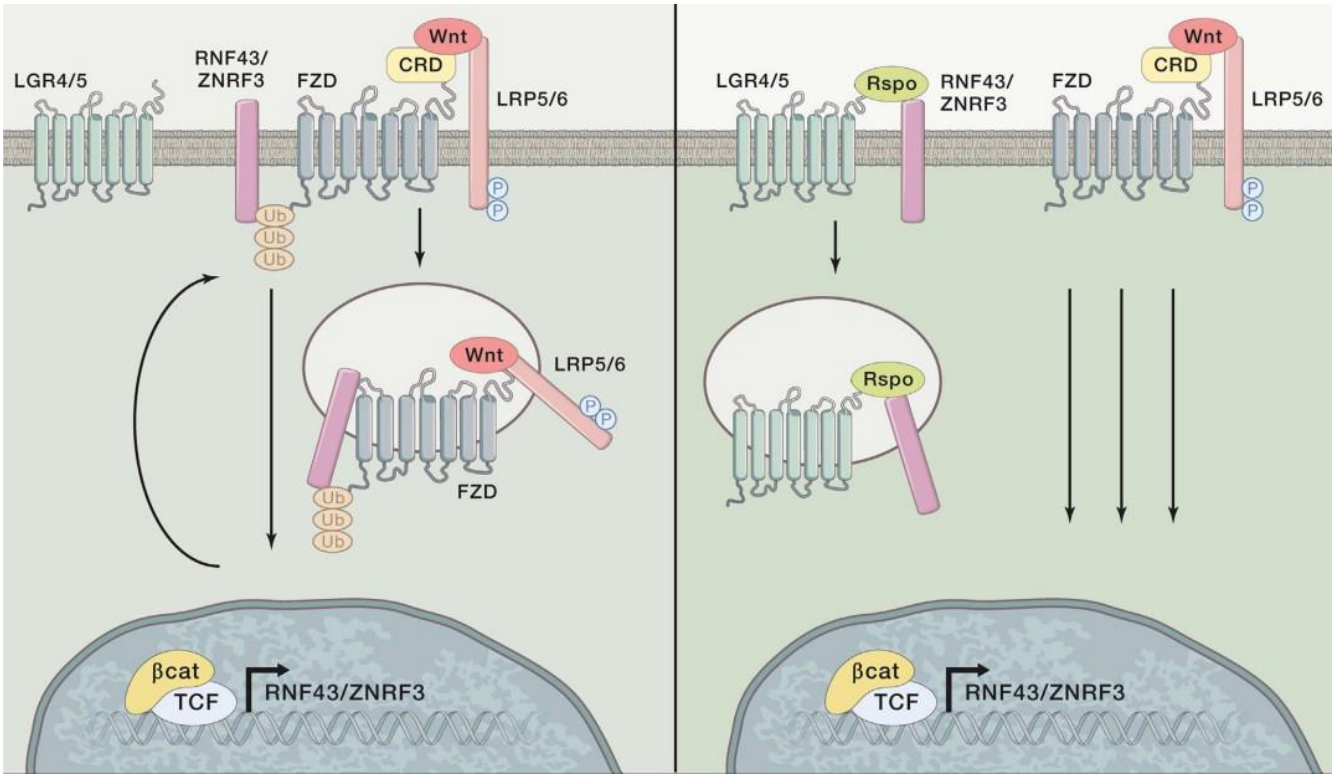

Figure 1.7 Wnt receptors and R-spondin positive regulation (Nusse R. and Clevers H., 2017).

1.2.1 The Wnt/β-catenin pathway in CRC

The Wnt/β-catenin signalling has been recognised as a highly conserved pathway involved in the regulation of cell growth, morphogenesis and maintenance of tissue homeostasis. As a result, any alteration of components of this pathway leads to a dysregulation in the activation of the signalling, which further leads to the initiation and progression of several cancers, including CRC.

As described above, Axin1 and β-catenin are two key elements of the Wnt/β-catenin pathway, whose mutation has been found to result in the acquisition of well-defined carcinogenic features that are associated with hyperactivation of the Wnt/β-catenin signalling during CRC development. Indeed, mutations in the *AXIN1* tumor suppressor gene (chromosome 16p13.3 – 10 exons) have been found in exons 1, 2, 3, 4, 5 and 10. In these regions are located site of interaction with APC (exon1, RGS domain), Mitogen-Activated Protein/Extracellular Regulated Kinase Kinase Kinase (MEKK), GSK3β (exon 3 and 4), β-catenin (exon5) and DVL (exon 10). Thus, Axin1 inactivating mutations result in aberrant activation of Wnt/β-catenin signaling (Salahashor S. et al., 2005).

CTNNB1 gene encodes for β-catenin and is located at 3p22.1. Exon 3 is the region of the gene in which most of CRC-associated β-catenin mutations occur and are associated to Wnt hyper-activation. Indeed, it contains the β-catenin-NH2-terminal regulatory domain which is essential for its phosphorylation by CK1α and GSK3β serine/threonine kinases (Krausova M. and Korinek V., 2014).

Moreover, we have previously described the involvement of R-spondin, Lgr5 and RNF43/ZNRF3 in the feedback mechanisms that regulates the Wnt signalling through the modulation of the receptors FZD and LRP5/6 on the cell surface. Consequently, somatic mutations of RNF43 have been found in more than 18% of colorectal adenocarcinomas and endometrial carcinomas (Giannakis M. et al., 2014). Gene fusions involving R-spondin2 or R-spondin3 had been observed in a small fraction of sporadic *APC*-wild-type-colon cancers (Seshagiri et al., 2012). Particularly, the fusions between the protein tyrosine phosphatase receptor type K and RSPO3 (PTPRK-RSPO3) or the eukaryotic translation initiation factor 3 subunit E and RSPO2 (EIF3E- RSPO2) enhance the sensitivity to low levels of WNT, correlating with hyperactivation of Wnt/β-catenin signaling (Sekine S. et al., 2016).

As previously mentioned, the loss of function of APC is one of the key driver events that disrupting Wnt/β-catenin signalling lead to CRC in both sporadic and hereditary settings. *In-vitro*, *ex-vivo*, and *in-vivo* studies had largely demonstrated that different mutations in the *APC* gene result in distinctive Wnt pathway activation statuses and are associated with different tumour features, as well as the locations within the large intestine (Christie M. et al., 2013). The *APC* gene is located on chromosome 5q21-22 and comprises of 16 coding and 3 noncoding exons that encodes a large protein of 310 KDa. Somatic APC mutations occur mainly in exon 16, which identify the mutation cluster region (MCR) that spans codons 1285 and 1580. It is to note that in this region occur 80% of all somatic mutations in CRC. Additional three mutational hotspots for somatic mutations are represented by the codons 1309, 1450 and 1554 corresponding to nearly 7%, 8% and 5% of all somatic mutations respectively (Sieber O.M. et al., 2000). Compared to somatic mutations, most of *APC* germline mutations in FAP patients are detected in the 5'-half of the APC gene. Nonsense (28%) or truncating frameshift (67%) mutations are responsible for almost 95% of all *APC* germline mutations in FAP disease (Sieber O.M. et al., 2000). Fearnhead et al. demonstrated that in classical FAP, germline mutations occur mainly within exons 6-9, 10-15 which include codons between 178 and 309 and codons between 409 and 1580 (Fearnhead N.S. et al., 2001). In addition, Lipton et al. demonstrated that the region of the APC gene between codons 1290 and 1400 is associated to a most severe polyposis phenotype in FAP

patients (Lipton L. and Tomlinson I., 2006), while codons 1061 and 1309 as two mutational hotspots which account for about 11% and 17% of all germline mutations, respectively (Sieber O.M. et al., 2000).

Mutations in the APC gene results generally to truncated and dysfunctional proteins. Recent findings have demonstrated that *APC* genetic alterations induce an autoassembly of the signalosome, constituted by the interaction between β-catenin and TCF, in the absence of Wnt ligands, leading an uncontrolled pathway activation (Saito-Diaz K. et al., 2018; McGough I.J. et al., 2018). Moreover, it has been demonstrated that the Wnt pathway can still be regulated by an intact degradosome containing the truncated form of APC. In this specific case, APC truncations induce activation of Wnt/β-catenin signalling by inhibiting the β-catenin ubiquitination within the destruction complex (Li V.S. et al., 2012). Indeed, Yang et al. showed that mutated-APC proteins inside an intact and functional degradosome impede the release of the phosphorylated-β-catenin from the complex. As a result, the proper assembly of the ubiquitin ligase complex is inhibited (Jang J. et al., 2006).

1.3 The mTOR signalling

The mammalian target of rapamycin (mTOR) is a serine/threonine kinase that play a central role in regulating many fundamental cell processes, including protein synthesis, cell survival, proliferation and metabolism, cell growth, and autophagy, thus highlights the physiological importance of this pathway (Saxton R.A. and Sabatini D.M., 2017).

The mTOR pathway is conserved among various organisms from yeast to humans. The main component involved in the mTOR signalling belongs to the phosphatidylinositol-3-kinase (PI3K) family. The mTOR forms two structurally and functionally distinct complexes called the mammalian target of rapamycin complex 1 (mTORC1) and mammalian target of rapamycin complex 2 (mTORC2) (Fig. 1.9).

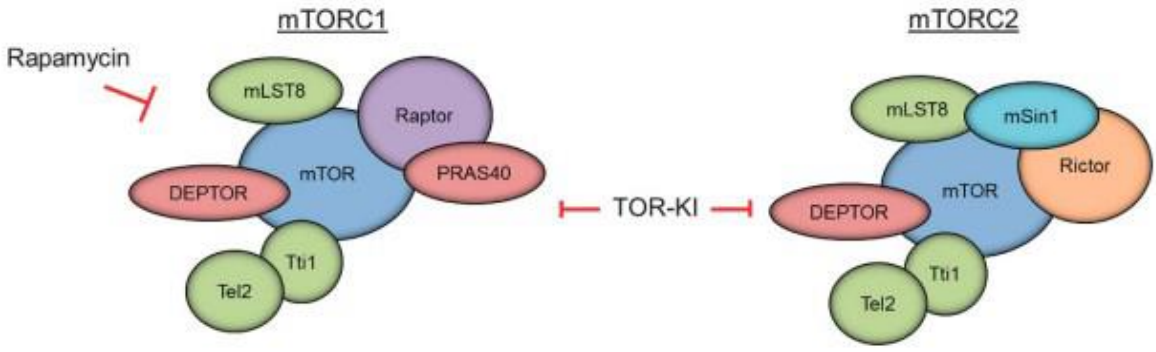

Figure 1.9 Representation of the mTOR complexes mTORC1 and mTORC2 (Kim L.C. et al., 2017).

Common proteins constitute both mTORC1 and mTORC2: among these we can find the mTOR central catalytic kinase, the scaffolding protein mLST8, DEPTOR, a regulatory subunit, and the complex Tti1/Tel2 responsible for the assembly and stability of the mTOR complex. Further, each complex harbours different subunits that ensure distinctive substrate specificity, subcellular localization and regulation. Indeed, mTORC1 binds to Raptor (Regulatory-associated protein of mammalian target of rapamycin), a scaffolding protein needed for the mTORC1 assembly, stability, substrate specificity and regulation, and PRAS40 (Proline-rich AKT substrate 40 kDa), involved in the inhibition of mTORC1 activity in the absence of activating signals (Aylett C.H.S. et al., 2015).
Conversely, mTORC2 comprises Rictor, required for mTORC2 assembly, stability, substrate identification and mSin1, which is required for subcellular localization. mSin1 functions also as a key negative regulator of mTORC2 kinase activity. Little is still known about the structure and functionality of mTORC2, as well as the upstream regulation mechanisms. The most certain information concerns the activation of the mTORC2 due to growth factor stimulation and ribosome association (Gaubitz C. et al., 2015). Through the known-mechanisms that regulates mTORC2 complex a positive feedback loop that involved AKT which direct phosphorylates mSin1 at T86 and sustains mTORC2-AKT signaling activation has been described, together with a negative regulation of mSin1 induced by S6K1 phosphorylation (Kim L.C. et al., 2017). Intracellular signalling is then mediated by PI3K (phosphatidylinositol-3-kinase), which recruits mTORC2 to the plasma membrane (Gaubitz C. et al., 2015).

The different components, structures and locations that characterize mTORC1 and mTORC2 give to these two complexes distinctive peculiarities. For instance, the active isoform of mTORC2 is located close to the plasma and ribosomal membranes, where it interacts with its main downstream effectors, comprising members of the AGC family of kinases, isoforms of SGK (serum glucose kinase) and several PKC (protein kinase C) (Zinzalla V. et al., 2011). Conversely, mTORC1 has mostly been observed in contiguity with the endosomal and lysosomal membranes, with the purpose of targeting its downstream effectors, which include the S6K1 (S6 kinase 1) and 4E-BP1 (4E-binding protein 1) proteins (Kim D.H. et al., 2002).

In addition to the different functional and structural components, another feature that distinguishes the two complexes is their response to Rapamycin inhibition: indeed, while mTORC1 is also referred to as Rapamycin-sensitive, mTORC2 is rather classified as Rapamycin-insensitive.

The PI3K pathway, which involved mTORC1, is frequently activated in response to growth factor's signals. *PIK3CA*-activating mutations, *RAS* mutations or *PTEN* loss have been found to increase the synthesis of the second messenger phosphatidylinositol (3,4,5)-triphosphate (PIP3) (Thorpe L.M. et al., 2014). Indirect activation of mTORC1 by PIP3 is usually mediated by AKT (protein kinase B), which in turn is activated as a result of phosphorylation of two amino acid residues, Ser473 and Thr308, modified by mTORC2 and PDK1 (pyruvate dehydrogenase kinase 1) respectively. The latter, similar to mTOR, is a serine/threonine kinase recruited to the plasma membrane by PIP3. Active-AKT phosphorylates TSC2 (tuberous sclerosis complex 2), preventing its association with TSC1. The TSC1/TSC2 heterodimer functions as a negative regulator of RHEB (Ras homolog enriched in brain) and prevents the binding of the guanosine-5'-triphosphate (GTP)-loaded RHEB to mTORC1. Therefore, TSC2 phosphorylation allows the guanosine-5'-triphosphate (GTP)-loaded RHEB to bind to mTORC1, leading to the activation of the signalling (Inoki K. et al., 2003; Tee A.R. et al., 2003).

Moreover, AKT directly activates mTORC1 by phosphorylating PRAS40, which dissociates from the complex to prevent the inhibition of the signalling (Sancak Y. et al., 2007).

One further signalling involved in the activation of mTORC1 is the Ras-MAPK (MAP kinase) pathway, in which ERK (extracellular signal-regulated-kinase) and RSK (Ribosomal S6 kinase) phosphorylate TSC2 on specific amino acid residues, triggering the activation of mTORC1 mediated by RHEB. In addition, similar to AKT, RSK phosphorylates PRAS40 resulting in its dissociation from the complex and mTORC1 activation (Carrière A. et al., 2008).

Although growth factors are primarily responsible for initiating the PI3K/AKT and Ras-MAPK pathways, which are mostly implicated in cell proliferation, the abundance of nutrients, energy, and macromolecules necessary to support the cell growth are rate limiting factors for the activation or inhibition of mechanisms that controls cell proliferation. This idea is supported by the fact that for example mTORC1 responds strongly to intracellular ATP, glucose, and certain amino acids including glutamine, leucine, and arginine. Indeed, low intracellular levels of ATP together with high amounts in AMP, activate AMPK (AMP kinase), which promotes the heterodimerization of TSC1 and TSC2, enhancing the inhibition of mTORC1 and blocking the cellular proliferation (Inoki K. et al., 2003). In

addition, when the level of amino acids is reduced, mTORC1 cannot be recruited to the lysosomal membrane, where the complex is activated by RHEB (Long X. et al., 2005).

It's interesting to note that cells can sense the intracellular type and localisation of amino acids to ascertain the mechanism governing the regulation of mTORC1. For example, RAG-GTPases are activated by intralysosomal arginine and cytoplasmic leucine, and after associating with RAPTOR, the RAG-GTPases enable mTORC1 localization on the lysosomal membrane. Conversely, cytoplasmic glutamine, through a RAG-independent mechanisms, coordinates the proper localization of mTORC1 to exert its catalytic activity (Stracka D. et al., 2014).

Activated-mTORC1 phosphorylates the eukaryotic translation initiation factor 4E (eIF4E) binding protein 1 (4E-BP1), and p70S6 ribosomal kinase 1 (S6 Kinase 1 [S6K1] or p70S6 ribosomal kinase 1), two downstream target of the pathway. Additional mTORC1 downstream effectors include 4E-BP1 (eukaryotic translation initiation factor 4E-binding protein 1) and S6K1 (ribosomal protein S6 kinase 1) proteins that are involved in the regulation of both cap-dependent and independent translation initiation. Interestingly, it has been observed that increased cap-dependent translation leads to typical carcinoma features, such as increased cell size and proliferation (Dowling R.J.O., 2010).

4E-BP1 and S6K1 phosphorylated by mTORC1 are no longer able to interact with eIF-4E and eIF-3, respectively, allowing the latter to carry on the formation of the translation initiation complex. S6K1, in turn, phosphorylates eIF-4B and S6R (S6 ribosomal) proteins, a component of the 40S ribosomal subunit, thus enabling translation initiation (Holz M.K. et al., 2005). Finally, S6K1, by phosphorylating eEF2 (eukaryotic elongation factor 2 kinase), also plays a key role in the positive regulation of the elongation stage (Browne G.J. and Prowd C.G., 2004) (Figure 1.10).

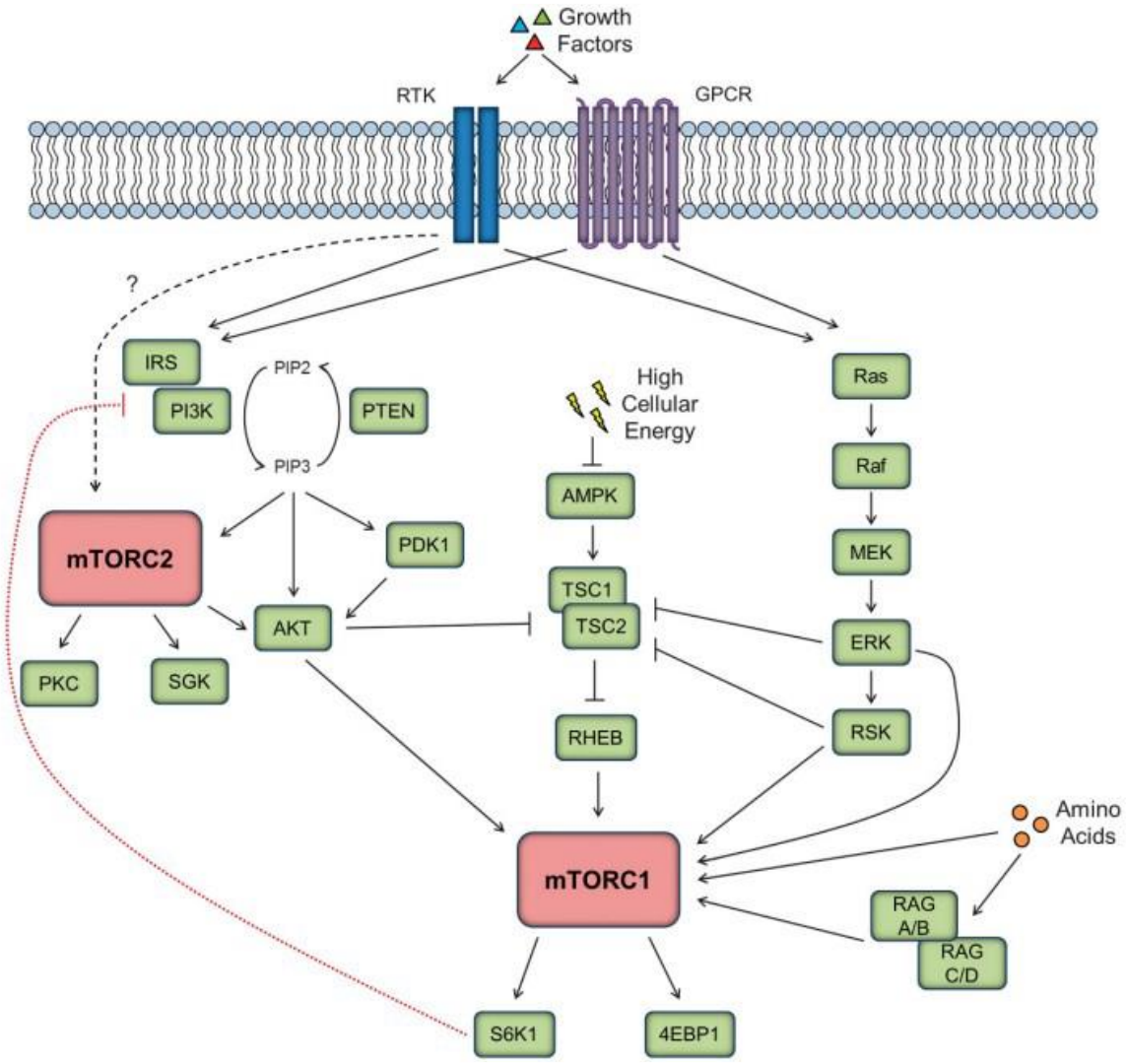

Figure 1.10 Summary of the mTOR pathway (Kim L.C. et al., 2017).

Compare to mTORC1, the mTORC2 downstream pathway is poorly characterized. Within the complex, the presence of mSin1 facilitates the localisation of the complex at the plasma membrane to ensure proximity to the mainly regulated targets: AKT, SGK (serum/glucocorticoid regulated kinase) and PKC (protein kinase C). Hence, the idea that the mTORC2 localisation is a key feature for its proper regulation (Liu P. et al., 2015). mSin1 is one of the main proteins involved in this regulation and is characterized by a PH (pleckstrin homology) domain that is responsible for anchoring the complex to the plasmalemma, after direct interaction with phosphatidylinositols. Mutations in this domain affect the mSin1-inhibitory activity toward mTORC2 and lead to constitutive activation of the mTORC2/AKT signalling (Liu P. et al., 2015). Furthermore, it has been observed that Akt-T86 residue-

phosphorylation of mSin1 trigger a positive feedback that sustain the mTORC2/AKT pathway activation. Recently, new regulatory functions of mSin1 involving the PH domain have been identified. Accordingly, the PH domain, part of the mSin1 structure, can bind to phosphorylated RB (retinoblastoma protein), a cytosolic component normally involved in cell cycle regulation and mutated in a variety of cancers. When mSin1 forms a complex with RB prevents the binding between mTORC2 and AKT, contributing to a negative regulation of the pathway (Thian T. et al., 2019) (Figure 1.10).

1.3.1 mTOR pathway in CRC

Several studies have demonstrated the contribution of mTOR pathway in the development of CRC, however mutation of the mTOR gene has been found only occasionally. Recently, Chang W.J. et al. reported that *MTOR* gene is aberrantly activated in more than 70% of cancers and plays a significant role in CRC tumorigenesis with a particular correlation with the ethnicity of patients. In the same study, altered expression of *MTOR* gene was also correlated with CRC with high-MSI, high tumour mutation burden and tumour-infiltrating immune cells features (Wang C. et al., 2022).

Despite these findings, the over-activation of the mTOR pathway is mostly due to genetic alterations in the upstream regulators of mTOR signalling. For example, both *PIK3CA* mutations and *PTEN* leads to mTOR over-activation. Indeed, members belonging to the PI3K family, through their catalytic activity, have been described to promote the conversion of PIP2 (phosphatidylinositol 4,5-bisphosphate) to PIP3 (phosphatidylinositol 3,4,5-trisphosphate), which in turn is responsible for the activation of PDK1 (phosphoinositide-dependent kinase-1) and mTORC2. PDK1 activation can be reverted by PTEN, which dephosphorylates PIP3 into PIP2 (Scheid M.P. et al., 2002). The interaction between an abnormal abundance or activation of insulin or insulin-like growth factors (IGF) and receptors such as EGFR (epidermal growth factor receptor), PDG-FR (platelet-derived growth factor receptor) and IGF-1R (insulin like growth factor-1 receptor) can also trigger the mTOR signalling, by activating the PI3K pathway, and consequently supporting cell proliferation, growth and survival (Vivanco I. and Sawyers C.L., 2002). Indeed, members belonging to the PI3K family, through their catalytic activity, have been described to promote the conversion of PIP2 (phosphatidylinositol 4,5-bisphosphate) to PIP3 (phosphatidylinositol 3,4,5-trisphosphate), which in turn is responsible for the

activation of PDK1 (phosphoinositide-dependent kinase-1) and mTOR. PDK1 activation can be reverted by PTEN, which dephosphorylates PIP3 into PIP2. (Scheid M.P. et al., 2002).

Mutations in the PI3K/PTEN/AKT pathway have been identified in several colorectal cancer cell lines (Ekstrand A.I. et al., 2010) and a high frequency of somatic mutations in the PI3K/AKT/mTORC1 pathway components has been reported in Lynch syndrome (Pandurangan A.K., 2013). Moreover, gain-of-function mutations in the *PIK3CA* gene have been linked to proximal colorectal cancer (CRC) and have been reported in 20%–25% of patients (Voutsadakis IA., 2021). Conversely, PI3K-negative regulator PTEN is usually affected by inactivating mutations, 10q23 loss of heterozygosis, or epigenetic silencing (e.g. promoter hypermethylation) and have been found mutated especially in CRC with MSI in both sporadic and hereditary settings (Molinari F. and Frattini M., 2014). Further, mutations in the Akt genes are rare event in CRC accounting for 1.73% of colorectal carcinoma (AACR project GENIE, 2017). AKT1 somatic missense mutation E17K is the most representative in CRC and other solid tumours (Carpten J.D. et al., 2007). This mutation causes mutated-Akt to be more easily phosphorylated in Ser473 and Thr308, resulting in a prolonged activation, which may lead to derangement of mTOR (Landgraf KE et al., 2008).

Moreover, TSC1/TSC2 deleting mutation are also rare event in CRC. Germline pathogenic mutations in *TSC1* and *TSC2* are mainly responsible for Tuberous Sclerosis Complex (TSC), an autosomal dominant and heterogeneous disease that have been associated with occurrence of gastrointestinal polyposis (most of them are hamartomatous) and pancreatic neuroendocrine tumours (Reis L. et al., 2020). Indeed, *TSC2* exon 2–16 deletion is the most representative mutation resulting in the complete removal of the TSC1 binding domain (T1BD) at the N-terminus of the TSC2 protein. This domain is critical for TSC1-TSC2 interaction (TSC complex formation), that, when altered, results in ubiquitination and degradation of TSC2, causing a the accumulation of Rheb-GTP and the subsequent activation of the mTORC1 pathway (Rosset C. et al., 2017). Moreover, with the occurrence of DNA damage or oxidative stress, p53 inhibited mTOR by promoting both SESTRIN1/2 activation, which is responsible for AMPK enhancement, and TSC2 expression (Budanov A.V. and Karin M., 2008). These evidence highlighted how aberrant activation of mTOR ,resulting from mutated-p53, leads to the transition from adenoma to carcinoma stage (Marcowitz S.D. et al., 2009).

Finally, RAS is a GTPase responsible for signal transduction triggered by activation of receptor tyrosine kinase (RTK) receptors. RAS protein affects downstream pathways involved in cell growth, survival,

and differentiation. The three most studied components belonging to the Ras family are H-RAS, N-RAS and K-RAS (Rajalingam K. et al., 2007); the latter has been classified as one of the most frequently mutated genes in colorectal cancer. RAS indirectly affects mTOR activity, both through the MAPK and PI3K/AKT cascades (Rajalingam K. et al., 2007).

1.4 The cross-talk between Wnt/β-catenin and mTOR in CRC

Most of the evidence demonstrating the involvement of the PI3K/AKT/mTORC1 signalling in the development of APC-driven CRC results from the study of murine models. Indeed, in intestinal polyps of the ApcΔ716 mouse model of FAP increased levels of mTORC1 signalling activation have been reported, and treatment of these mice with the mTORC1 inhibitor everolimus showed reduced tumour burden (Fujishita T. et al., 2008). Similar results have been observed in the ApcMin/+ mouse model of FAP and in the Apc conditional knock-out mouse model, following rapamycin treatment (Valvezan A.J. et al., 2014; Hardiman K.M. et al., 2014).

Further research elucidated the role of mTORC1 signalling in the process of APC inactivation. As a matter of fact, while mTORC1 activation is essential for maintaining the viability and growth of murine enterocytes, following *APC* gene deletion, its suppression has no discernible impact on the intestines of APC *wild-type* mice (Faller W.J. et al., 2015). Faller et al. outlined critical mechanisms that related *APC* loss-induced colorectal carcinogenesis to mTORC1 activation. Notably, after the deletion of the *APC* gene, they found that active mTORC1 increases the rate of elongation translation by activating eEF2 and blocking the elongation factor 2 kinase (eEF2K) via S6K. Significantly, the involvement of the mTORC1-S6K-eEF2K-eEF2 axis appears essential to ensuring the development and proliferation of *APC*-deficient enterocytes. Moreover, in a study crossing ApcMin/+ and FC PIK3ca* mice, the formation of colonic lesions was shown to be synergistically affected by the Wnt/β-catenin and PI3K/AKT/mTORC1 pathways. The simultaneous activation of both pathways, due to a germ-line mutation in the *APC* gene and the constitutive intestinal activation of PI3K, increased tumor initiation and progression (Deming D.A. et al., 2014). A different study demonstrated that while mTORC1 inhibition may prevent *APC* mutant colorectal cancer, it may also promote carcinogenesis in chronic inflammatory bowel disease. Indeed, mTORC1 signalling provides a protective function by promoting intestine regeneration after injury in an environment of chronic inflammation (Brandt M. et al., 2018).

Wnt/β-catenin and PI3K/AKT/mTORC1 pathways share some effectors critically involved in both signaling pathways. The most important are briefly described below.

1.4.1 GSK3β

GSK3 is a shared essential factor that participates in both PI3K/AKT/mTORC1 and Wnt/β-catenin signalling pathway and control numerous cellular functions. Because of its critical role in multiple cellular functions, GSK3 kinase protein is constitutively active and several feedback negative mechanisms are responsible for its modulation. Indeed, independent intracellular pools of GSK3β have been associated with the inhibition of PI3K/AKT/mTORC1 and Wnt/β-catenin pathways. Likewise, the activation of both signalling pathways leads to the inhibition of GSK3β activity through distinctive upstream events (Kadanovich-Beilin O. et al., 2011).

During the different stages of activation or inactivation of the Wnt pathway, GSK3 is mainly regulated via intracellular sequestration and protein–protein interactions. Indeed, as described above, the interaction between GSK3β, AXIN1 and APC plays a critical role in the regulation of β-catenin. While AXIN1 within the degradosome sustains GSK3β in phosphorylating the β-catenin in Wnt signalling-off conditions (Ikeda S. et al., 1998), the dissociation of APC from AXIN1 triggers the activation of the pathway and reduces the kinase activity of GSK3β, resulting in the stabilization and nuclear translocation of β-catenin (Valvezan A.J. et al., 2012).

Within the PI3K/AKT/mTORC1 pathway, upon activation of PI3K, active-phosphorylated AKT can inhibit the kinase activity of GSK3β through phosphorylation on Ser9. S6K can also phosphorylate GSK3β enhancing its inactivation when reduced active-AKT levels occur (Zhang H.H. et al., 2006). Importantly, the Wnt/β-catenin pathway is not directly influenced by AKT. Indeed, evidences have demonstrated that AKT-mediated phosphorylation at Ser9 is not a mechanism involved in GSK3β inactivation upon WNT stimulation (Prossomariti A. et al., 2020).

The mechanisms involving the regulation of GSK following activation of both Wnt and mTOR pathways do not always imply a direct effect on β-catenin accumulation. Indeed, Valvezan et al. showed that loss of *APC* resulted in dysregulation of GSK3β with reduced kinase activity in association with mTORC1 activation through a mechanism independent of β-catenin accumulation. This means that inhibition of APC is a crucial event for the simultaneous induction of β-catenin and mTORC1 signalling

through distinct downstream mechanisms that share upstream inhibition of GSK3β (Valvezan A.J. et al., 2012).

In addition, Wnt pathway has been found to influence protein synthesis by activating the mTORC1 signalling, leading to phosphorylation of S6K and 4E-BP1 through the axis APC-AXIN-GSK3β and TSC2, without affecting β-catenin accumulation or degradation (Inoki K. et al., 2006).

1.4.2 FZD and DVL

Zeng et al. demonstrated that mTORC1 had a negative regulatory effect on the Wnt/β-catenin signalling pathway, by modulating the expression of the Wnt receptor FZD with the involvement of the Wnt-positive regulator DVL and its association to the clathrin AP-2 adaptor (Zeng H. et al., 2018). They reported also that the mTORC1-driven inhibition of the Wnt signalling impaired intestinal organoids' stem cell functions, emphasizing the significance of reciprocal regulation for intestinal homeostasis maintenance.

1.4.3 DEPTOR

DEPTOR is mostly recognized as a suppressor of mTOR. However several studies have demonstrated that DEPTOR can contribute to cancer cell proliferation and survival in different cancer settings (Zhang H.R. et al., 2013; Parvani J.G. et al., 2015; Srinivas K.P. et al., 2016). Wang et al. demonstrated that DEPTOR is a direct target of the Wnt/β-catenin/c-Myc signalling in CRC cells. Indeed, they found increased DEPTOR expression after Wnt activation or c-Myc overexpression, and decreased expression in inhibited-Wnt/β-catenin or c-Myc settings. More importantly, the study showed that mTOR increase its activation after inhibiting Wnt/β-catenin/c-Myc signalling. These was found to be related to the ability of c-Myc to bind to the promoter of DEPTOR, influencing its transcription, thus, identifying DEPTOR as a downstream target of the Wnt/β-catenin/c-Myc signaling pathway (Wang Q. et al., 2018).

1.4.4 The cross-talk between Wnt/β-catenin and mTOR in drug resistance

Wnt and mTOR pathways control the homeostasis of intestinal and cellular functions. These pathways regulate each other to maintain cell function by preventing their overactivation or inhibition, thus the cross-talk between Wnt and mTOR signallings influence the effectiveness of target inhibitors.

- *mTOR Inhibitors resistance*

Everolimus and temsirolimus are two mTORC1 inhibitors whose efficacy have been evaluated in phase II clinical trials in metastatic CRC patients. *PIK3CA* mutations play a relevant role in mediating the effectiveness of these treatment in CRC. A small retrospective analysis of tumors with activating *PIK3CA* mutations showed that everolimus had no relevant effect. In contrast, the dual inhibition of both PI3K and mTOR resulted more effective in contrasting the occurrence of drug-resistance mechanism against mTORC1 inhibitors. In fact, it has been shown that the combination of an additional mTORC1/2 inhibitor to everolimus could restore sensitivity in PIK3CA-mutant CRC in preclinical models; accordingly, the dual PI3K/mTOR inhibitors PKI-587, XL765, BEZ235, and LY3023414 have successfully completed phase I clinical trials in patients with advanced solid tumors, including CRC. In addition, recent studies have revealed that activating the Wnt/β-catenin pathway can make PIK3CA-mutant CRC cells resistant to the dual PI3K/mTOR inhibitor PKI-587 (Park Y.-L. et al., 2019). Conversely, inactivated GSK3β can restore sensitivity to the same inhibitor. Although these results could appear contradictive considering the role of GSK3β as a negative regulator in the Wnt/β-catenin pathway, the presence of different and independent GSK3β pools can explain how the endogenous levels of GSK3β determine the efficacy of mTORC1 inhibitors in CRC. Indeed, lower levels of GSK3β have been linked to resistance to mTORC1 inhibitors. ù (Thorne C.A. et al., 2015). Recently, Foley et al. have suggested that targeting both PI3K and mTOR using BEZ235 and LY3023414 inhibitors could be an effective treatment strategy for CRC patients with concomitant APC and PIK3CA mutations (Foley T.M. et al., 2017).

- *Tankyrase inhibitors resistance*

Tankyrase inhibitors (TNKSi) stabilize AXIN1 and inhibit the Wnt signalling activation. Despite TNKSi like XAV939, IWR-1, JW74, and G007-LK showed effective inhibition of Wnt/β-catenin pathway in CRC-*in vitro* and -*in vivo* models, they also demonstrated intestinal cytotoxicity in a CRC cell line-

dependent manner (Mehta C.C. and Bhatt H., 2021). Recently, using the TNKSi-resistant cell line 320-IWR, it was reported activation mTORC1 as a mechanism of resistance to TNKSi IWR-1 and G007-LK (Mashima T. et al., 2017). This mechanism was found to be reversed after mTORC1 inhibition with temsirolimus. Taken together these data support the hypothesis that mTORC1 activates after Wnt/β-catenin signalling inhibition to ensure cancer cell survival, demonstrating how the two pathways are relevant and in close connection for cell growth in both healthy and cancer settings.

More recently, a combination of TNKSi inhibitor G007-LK, PI3K inhibitor NVP-BKM120, and the epidermal growth factor receptor (EGFR) inhibitor erlotinib was tested on TNKSi-sensitive COLO320 DM and TNKSi-insensitive HCT-15 cell lines CRC cell lines and xenografts. After treatment, they reduced cell growth *in-vitro* and tumour size *in vivo* by modulating multiple effectors of different cancer-related pathways including Wnt/β-catenin, AKT/mTOR, EGFR, and Rat Sarcoma (RAS) signalling. The effectiveness of the treatment was affected by the distinctive genetic background of the models selected for the study (Solberg N.T. et al., 2018).

1.5 Omega-3 Polyunsaturated Fatty Acids

Fatty acids (FAs) are carboxylic acids that consist of a long hydrocarbon chain. The two ends of the chain are characterized by a carboxylic (-COOH) and a methyl group (-CH3) respectively. The last carbon of the hydrocarbon chain can be identified as n or ω, based on the adopted nomenclature system.

FAs can be distinguished in: (i) the saturated fatty acids (SFAs), characterized by the presence of single bonds saturated with hydrogen atoms; (ii) the monounsaturated fatty acids (MUFAs), which contain only one double bond along the chain; and (iii) the polyunsaturated fatty acids (PUFAs), characterized by multiple double bonds not saturated with hydrogen atoms.

PUFAs are essential fatty acids that are crucial for human health, however, since the human body cannot produce them, they must be obtained through the diet (Kaur et al., 2014). There are two main families of essential PUFAs: ω-3 and ω-6, which are distinguished by the position of the first double bond in the chain starting from the methyl group (Wall R. et al., 2010). Linoleic acid (LA; C18:2 ω-6) is the precursor of ω-6 series fatty acids and can be found in vegetable oils (e.g. corn oil, safflower oil, and soybean oil) or nuts and sunflower seeds. Conversely, the ω-3 fatty acids derived from alpha-

linoleic acid (ALA; C18:3 ω-3), of which fish oil, flaxseeds, rapeseeds, hempseed, and canola oil are enriched (Calder P.C., 2009).

LA and ALA undergo a maturation process in the endoplasmic reticulum where they are elongated and further unsaturated into long chain (LC) PUFAs by the Δ6- and Δ5-desaturase enzymes and the Elovl-5 and Elovl-2 elongase. In addition, β-oxidation reaction occurring in the peroxisomes is required to shorten the fatty acid chain (Emery S. et al., 2013). The ω-6 arachidonic acid (AA 20:4 ω-6), and the ω-3s eicosapentaenoic acid (EPA 20:5 ω-3) and docosahexaenoic acid (DHA 22:6 ω-3) derived from the conversion of LA and ALA, respectively. Importantly, apart from their derivation, the ω-6 and ω-3 LC-PUFAs can be considered as two distinctive classes with opposite physiological functions. Importantly, ω-6 and ω-3 PUFAs competes for accessing the Δ6-desaturase, which demonstrates higher affinity for ALA. Given the importance of diet as a supply, especially in the Western diet, LA is the primary source of PUFA. As a result, the Δ6-desaturase enzyme typically uses it as a substrate (Harris W.S. et al., 2009). Therefore, the introduction of food enriched in EPA and DHA in the diet can help to reduce AA synthesis and the production of eicosanoids derived from ω-6 PUFA metabolism (Hull M.A., 2011).

PUFAs are then incorporated into cellular membranes as a lipid component of phospholipids, leading to changes in the membranes' physical and chemical properties as well as their function (Serhan C.N. and Chiang N., 2008). They also play a role in producing bioactive lipids known as eicosanoids, which have a multifaceted and complex function in the body (Larsson S.C. et al., 2004). Eicosanoid involves AA and EPA as precursors and are bioactive hormone-like lipids, that despite a short lifespan, are largely involved in pathophysiological processes (e.g. the regulation of cellular growth and differentiation and the modulation of inflammatory and immune responses)(Larsson S.C. et al., 2004).

The cyclooxygenases enzymes, COX-1 and COX-2 enzymes, respectively, the lipoxygenases (LOX) enzymes and cytochrome P450 monooxygenases (CYP) use AA and EPA for eicosanoid biosynthesis of prostaglandins (PGs) and thromboxanes (TXs), lipoxins (LXs), leukotrienes (LTs) and hydroxy fatty acids, hydroxy fatty acids, dihydroxy fatty acids, and epoxy fatty acids, respectively (Larsson et al., 2004).

Importantly, different LC-PUFAs were generated from AA or EPA. For example, the 2-series PGs and TXs, the 4-series LTs and the hydroxy and hydroperoxy derivatives (5-HETE and 5-HPETE) generate

from the metabolism of AA, while the 3-series PGs and TXs and the 5-series LTs were obtained from EPA as substrate (Lands B., 1992)

1.5.1 Antineoplastic properties of omega-3 PUFA

The anti-cancer properties of omega-3 polyunsaturated fatty acids (PUFAs) can be attributed to the regulation of several molecular and cellular mechanisms. Among these, the most recognized and described is the inhibition of COX-2 enzyme, involved in many inflammatory processes and often deranged in different types of cancer, including colorectal cancer (CRC). EPA and DHA can function as alternative substrates for COX-2 enzymes, which stimulates the synthesis of anti-inflammatory and anti-tumorigenic '3-series' PGs (PGE-3) instead of the pro-inflammatory and pro-tumorigenic '2-series' PGs (PGE-2) (Calviello G. et al., 2007).

Prostaglandins are a type of molecule found in the body that are categorized into different series. Prostaglandins belonging to the E-series, such as PGE2 and PGE3, are characterized by a carbonyl group on Carbon-9 and a hydroxyl group on Carbon-11. Additionally, all natural prostaglandins have a double bond between Carbon-13 and Carbon-14. However, the number of double bonds varies depending on the fatty acid from which they originate. PGE2 has two double bonds (between 13C-14C and 5C-6C), while PGE3 has three double bonds (between 13C-14C, 5C-6C, and 17C-18C).

In a study conducted by Hawcroft et al., it was observed that treating colorectal cancer (CRC) cell lines with ω-3 PUFA EPA in the FFA form resulted in a decrease in COX-2-driven PGE2 synthesis, leading to a "PGE2-to-PGE3 switch". The study also showed that in the presence of PGE-2, PGE-3 had the ability to counteract the protumorigenic signaling mediated by the EP4 receptor (Hawcroft G. et al., 2010). In addition, in nude mice inoculated with HT29 cells, EPA and DHA were found to significantly reduce PGE-2 synthesis and tumor growth (Jia G. et al., 2008; Calviello G. et al., 2004). Moreover, the presence of ω-3 PUFAs influences the production of resolvins and protectins. Indeed, EPA functions as a substrate for production of RvE1, while DHA leads to the production of D-series resolvins and protectins. These downstream effectors demonstrated important anti-inflammatory properties in animal models of acute inflammation (Serhan C.N. et al., 2008).

As mentioned previously, ω-3 PUFAs can induce changes into the organization of cell membranes, by altering the composition, structure, and function of lipid rafts or caveolae. These are small portions of the membrane that are enriched with cholesterol, sphingolipids, and saturated acyl chains. Lipid rafts

compartmentalize proteins and lipids, which functions as signaling scaffolds, thus the modulation of the lipid rafts could be relevant in mediating the anti-cancer activity of ω-3 PUFA (Turk H.F. and Chapkin R.S., 2013).

Together with the composition, ω-3 PUFA alter also the fluidity of the plasma membrane, impacting the location of cell surface receptors. Among these, the epidermal growth factor receptor (EGFR) is crucial in the development and progression of colon cancer. Turk et al. treated young adult mouse colonic (YAMC) cells with DHA. They found an EGFR displacement responsible for an altered signal transduction, which affected the cell proliferation. Same results were observed *in vivo* with decreased tumor incidence in a DHA-treated AOM-DSS mouse model (Turk H.F. et al., 2012).

ω-3 PUFAs may have an anti-tumorigenic effect also by altering the cellular redox state. Due to their high degree of unsaturation, LC-PUFAs are particularly susceptible to lipid peroxidation. When incorporated into the cellular membrane, they can stimulate the generation of reactive oxygen species (ROS) and cause oxidative stress. Enhanced oxidative stress induced by the fermentation product butyrate was observed in mouse colonocytes after DHA treatment. This was concomitant with an induction of apoptotic pathways (Ng Y. et al., 2005). Similar results were found in 7 solid tumor cell lines including SW620, HT-29 and LS147T CRC cell lines in response to arsenic trioxide (As2O3) combined with DHA. However, Baumgartner et al. didn't find toxic effects on cell deriving from healthy donor. They also found that the toxicity of the treatment was associated with an increase of intracellular lipid peroxidation (Baumgartner et al., 2004). Beneficial and harmful effects of lipid peroxidation on cancer development have been described. For example, a protective effects of ω-3 PUFAs in cancer had been linked to the ability to modulate gene expression by activating the peroxisome proliferator-activated receptors (PPARs). This family of nuclear receptors comprises three isoforms of PPARs, namely α, β/δ, and γ, all of which heterodimerize with retinoid X receptor α (RXRα). PPAR γ and δ are expressed in the colon, and EPA and DHA are natural ligands of these receptors. Thus, ω-3's anti-neoplastic characteristics may be linked to inhibit cell proliferation and induce apoptotic processes through PPAR γ activation (Edwards I.J. and O'Flaherty J.T., 2008).

1.6 Green Tea Catechins

Green tea is a widely consumed beverage that has been associated with reduced risk of several chronic diseases, such as cardiovascular diseases, metabolic syndrome such as diabetes, neurodegenerative disorders, inflammatory diseases, and different types of cancers. Catechins are mainly involved in the health benefits of green tea. They include catechin (C), epicatechin (EC), epigallocatechin (EGC), epicatechin gallate (ECG), and epigallocatechin gallate (EGCG). Among these five most representative catechins in the green tea, EGCG has been identified as the biologically active and most abundant, providing for at least 50% of the total catechin content in green tea leaves (Khan N. et al., 2006).

EGCG, when orally administered, is firstly absorbed in the intestine. However, its bioavailability resulted poor due to oxidation, metabolism, and efflux as reported by Kale A. et al. (Kale A. et al., 2010). Accordingly, the metabolism of EGCG in the intestine is highly dependent on the gut microbiota that plays a significant role in leading EGCG to several conversions, including hydrolysis. Indeed, by using a rat model, Takagaki et al., found that EGCG is first hydrolyzed to EGC and gallic acid by *Enterobacter aerogenes, Raoultella planticola, Klebsiella pneumoniae, and Bifidobacterium longum*. In this postulated microbiota-driven metabolic pathways it has been suggested that 5-(3,5-dihydroxyphenyl)-4-hydroxyvaleric acid is the primary metabolite of EGCG that can be found in both in rat cecal contents and feces and resulted after several conversions and degradation of EGC. Further conversion of this compounds has been described and a glucuronid form has been described as one of the most abundant EGCG metabolite in urines (Takagaki A., Nanjo F.et al., 2010). Importantly, the EGCG metabolic pathways appeared strictly dependent on the method of administration. Indeed, it was found that 4',4''-di-O-methyl-EGCG represent the main metabolite after EGCG intravenous administration, while 4''-O-methyl-EGCG was detected in the small intestine, colon, liver, and prostate of mice after intragastric administration (Lambert J.D. et al., 2006).

1.6.1. Cancer antineoplastic properties of catechins

EGCG exhibits versatile bioactivities and several *in-vitro*, *in-vivo*, and clinical studies, have demonstrated that EGCG exerts anti-cancer effects through the activation/inhibition of different signalling pathways, most of which are triggered by the direct interaction between EGCG and specific

protein targets. The main EGCG-antineoplastic mechanisms include the activation of anti-oxidant and detoxification systems (Lambert J.D. et al., 2010), alteration of the cell cycle (Gupta S. et al., 2004), suppression of mitogen-activated protein kinase (MAPK) and receptor protein kinase (RTKs) pathways, inhibition of clonal expansion of the tumour-initiating stem cell population, and production of epigenetic changes in gene expression (Alam M. et al., 2022).

The effects of EGCG on cancer stem cells have been documented in various malignancies, including breast, lung, and colorectal cancer. Several anticancer mechanisms have been described. For example, EGCG can modulate proteins involved in cell cycle regulation (e.g. cyclins, CDKs) or protein that activates or inhibit apoptosis (e.g. Bax, Bcl-2, and Bcl-XL). Many proteins control the cell cycle progression and consequently the cell proliferation. Cyclins, together with p53, p73 and Survivin are the some of those and most representative (Feitelson M.A. et al., 2015; Suzuki A. et al., 2000; Di Agostino S. et al., 2006). In human pancreatic cancer cells EGCG was found to arrest the cell cycle at G1 stage by suppressing Cyclins proteins such as Cyclin D1, CDK4 and CDK6 and increasing the expression of p21 and p27 (Shankar S. et al., 2007). EGCG has been demonstrated to trigger apoptosis through a broad spectrum of mechanisms. One of those is related to the production of reactive oxygen species (ROS) that inhibit the proliferation of cancer cells by enhancing apoptosis (Lambert J.D. et al., 2010). However it has been demonstrated that catechins, including EGCG, can acts also as radicals scavenger under conditions of heightened oxidative stress (Bernatoniene J. et al., 2018). EGCG has been found to trigger apoptosis in PC3 prostate cancer and MCF-7 breast cancer cells via the mitochondrial pathway, inducing the activation of Caspase-9 (Tang Y. et al., 2007; Hagen R.M. et al., 2013). Similar results have been reported by Shankar et al. in human pancreatic cancer cells (Shankar S. et al., 2007). Conversely, in another model of human pancreatic cancer cell line (MIA PaCa-2) EGCG demonstrated the ability to trigger the death receptor signaling through Fas and DR5, enhancing Caspase-8 activation (Basu A. et al., 2009). In addition, EGCG in some systems was found to activate apoptosis by triggering both the apoptotic pathways (Wu A.H. et al., 2009). Moreover, EGCG can modulated also several pro-apoptotic proteins, such as BAD, BAK, BAX, BCL-XS, BID, BIM, NOXA, PUMA and SMAC, and anti-apoptotic proteins, such as BCL-2, BCL-XL, c-FLIP, MCL-1 and XIAP to influence apoptosis progression (Alam M. et al., 2022), supporting the anti-cancer activity of EGCG.

2. AIM OF THE WORK

Although cancer development in patients with FAP and sporadic CRC is essentially driven by Wnt/β-catenin signaling alterations, relevant cross-talks with PI3K/mTOR pathway in *APC*-driven intestinal tumorigenesis has been largely described (Clevers H. et al., 2012; Gulhati P. et al., 2009; Kim L.C. et al., 2016), outlying the existence of an oncogenic network that dynamically involves both Wnt/β-catenin and mTOR signaling. PI3K inhibitors, the mTOR inhibitors Rapamycin and RAD001 demonstrated strong anti-neoplastic effects in *APC*-mutated CRCs and mouse models (Hardiman K.M. et al., 2014; Fujishita T. et al., 2008). Despite their effectiveness, long-term treatment often failed due to the acquisition of resistance mechanisms. Recent studies indicated that the combination of multiple inhibitors resulted in a more effective treatment (Prossomariti A. et al., 2020). Indeed, a combination of tankyrase, PI3K and EGFR inhibitors were found to be effective against CRC by modulating multiple pathways, including Wnt/β-CATENIN, AKT/mTOR, EGFR and RAS (Solberg N.T. et al., 2019). Noteworthy, bioactive molecules such as the ω3-Polyunsaturated fatty acid (PUFA) Eicosapentaenoic Acid (EPA) and the green catechin Epigallocatechin-3-Gallate (EGCG) showed preventive effects in CRC cell lines by inhibiting the PI3K/mTOR pathway and reducing β-CATENIN levels (Oh S. et al., 2014; Van Aller G.S. et al., 2011). We also previously tested the effects of EPA on *in vitro* and *in vivo* models, including the ApcMin/+, showing strong anti-cancer effects (Piazzi G. et al., 2014; Fazio C. et al., 2016), and we demonstrated that EPA in combination with proanthocyanidins (from grape seeds) and Epigallocatechin-3-Gallate (EGCG), resulted in a potent mTOR inhibitory effect in CRC cell lines (D'Angelo L. et al., 2014).

On the basis of these knowledge, this thesis aim at investigating in *in-vitro* and *ex-vivo* models how a combination of Rapamycin, ω3-PUFA Docosahexaenoic Acid (DHA) and EGCG influences the activation of Wnt/β-catenin and PI3K/mTOR pathway in several mutated settings (including the wild-type, the APC-mutated, and the non-APC-mutated), to delve into the mechanisms involved in the cross-talk of the two pathways and in drug-responsiveness, and to define an effective and synergic chemopreventive strategy against *APC*-driven CRC onset and progression in both hereditary (FAP) and sporadic settings.

3. MATERIALS AND METHODS

3.1 Patients' enrollment

Eight unoperated FAP (aged 19-57 years) and ten CRC patients (aged 51-80 years) together with twelve FIT+ subjects (aged 50-70 years) who resulted negative during screening colonoscopy, were enrolled at the IRCCS S.Orsola-Malpighi Hospital (Bologna, Italy). The study was conducted according to the Good Clinical Practice guidelines and the Declaration of Helsinki, and approved by the ethical committee of the S.Orsola-Malpighi Hospital (CE: 599/2018/Sper/AOUBo) (Bologna, Italy). All enrolled patients provided informed consent. Patients with history of inflammatory bowel disease, hereditary gastrointestinal syndromes different from FAP, those with inoperable metastatic CRC were excluded from the study.

3.2 Human Intestinal Organoids Culture

3.2.1 Tissues collection and cryopreservation

Six fresh biopsies were collected from FIT+, FAP normal appearing colonic mucosa (NM) and FAP adenomas (A; size < 5mm) during colonoscopy from the sigmoid colon, and placed into cold physiological solution. For patients with sporadic CRC, surgical resected colonic tissues (non-cancerous mucosa and tumor) were collected into cold physiological solution. Samples from non-cancerous mucosa (NM) were resected from a minimum distance of 5 cm from the tumor (K). Sporadic CRC tumors include CRC K tissues PT13 (*APC mutated*; *TP53 mutated*) and PT16 (*APC mutated; PI3KCA mutated; TP53 mutated*).

Biopsy samples and tissues specimens for organoids isolation were collected and cryopreserved according to Tsai H. et al. protocol (Tsai H. et al., 2018). Briefly, biopsies and tissues were washed three times in cold DPBS without Ca2+/Mg2+ (1X) (D-PBS) (Thermo Fisher Scientific, #14190144) with 100 U/mL penicillin, 100 µg/ml streptomycin. CRC non-cancerous mucosa were separated from fat and sub-mucosal residues. After washing, biopsies and tissues were cut into smaller fragments (2 to 3 mm) resuspended in 1mL freezing medium (80% Dulbecco's modified Eagle medium/F12 (DMEM-F12), 10% fetal bovine serum (FBS), and 10% dimethyl sulfoxide (DMSO)) and then transferred into a cryopreservation vial. By using a cell-freezing container filled with isopropanol, the biopsy fragments were frozen to -80°C overnight and then moved to liquid nitrogen for long-term storage.

3.2.2 Colonic crypt isolation

Colonic crypts were isolated and organoids were developed by modified Pleguezuelos-Manzano et al.; Tsai et al.; Soragni et. al protocols (Pleguezuelos-Manzano C. et al., 2020; Tsai Y.H. et al., 2018; Nguyen H.T.L. and Soragni A. et al., 2020). Intestinal frozen fragments were quickly thawed in water bath at 37°C and washed three times with D-PBS. CRC-tissue fragments were washed three times with D-PBS with 100 U/mL penicillin, 100 µg/ml streptomycin. Intestinal and tumoral fragments were cut into smaller pieces (1 to 2 mm), collected into a 15mL tube, then digested. CRC NM and K were digested for 1h at 37°C using 10 mL of 200 U/mL collagenase type II (Gibco, #17101-015) diluted in D-PBS. FIT+ and FAP tissues were digested with the Gentle Cell Dissociation Reagent (GCDR) (Stem Cell Technologies, #100-0485) at room temperature for 20 minutes on an orbital shaker.

After digestion, the intestinal fragments were centrifuged (CRC tissues: 600 g for 5 min; FAP and FIT+: 290 g for 5 min at 4°C), resuspended in 1mL DMEM-F12-1% BSA, syringed (21 G needle) and filtered through a 70 µm strainer into a new tube to isolate intestinal crypts. The suspension was centrifuged for 5 min, 200 g at 4°C. After removing the supernatant, intestinal crypts were resuspended in undiluted Corning® Matrigel® Growth Factor Reduced Basement Membrane Matrix, Phenol-Red Free, LDV-Free (Matrigel) (Corning, #356231). All the colonic crypts were seeded in a 24-well plate in 50µl Matrigel/well. After 20 minutes of polymerisation, Human Intesticult™ Organoid Complete Growth Medium (Basal+Supplement) (Stem Cell Technologies, #06010) supplemented with the Rho kinase inhibitor 2.5 µM Thiazovivin (Thz) (Sigma-Aldrich, #SML1045) was added in each well. Media was replaced every two-three days removing Thz.

Human Intesticult™ Organoid Complete Growth Medium was prepared according to the manufacturer instructions by adding the Supplement solution to the Basal media and adding 100 U/mL penicillin, 100 µg/ml streptomycin.

CRC-cancer (K)-organoids, after 2 days in Human Intesticult™ Organoid Complete Growth Medium, were tested for 2 weeks in different growth media compositions in accordance to cancer's mutations, in order to select the best culture conditions to unable their growth and expansion. After this evaluation, both the CRC-cancer (K)-organoids selected for the study were found to grow in Human Intesticult™ Organoid Complete Growth Medium.

3.2.3 Organoids expansion

- 24-well plate assay

Organoids were dissociated in a 15mL tubes with GCDR solution for 10 min at RT on an orbital shaker according to the manufacturer's procedures. After incubation, organoids were centrifuge (290 g for 5 min, at 4°C). The pellet containing the dissociated cells was then resuspended in 1mL cold DMEMF12-1% BSA and syringed (21 G needle). Organoids were filtered in a 70 µm strainer, collected in a new tube and centrifuged (200g for 5 min at 4°C). The pellet was resuspended in undiluted Matrigel and cells were seeded (expansion ratio 1:4) in a 24-well plate (50 µl Matrigel/well). After 20 minutes of polymerisation, Human Intesticult^{TM} Organoid Complete Growth Medium (Basal+Supplement) (Stem Cell Technologies, #06010) supplemented with Thz was added in each well.
Organoids were passaged every five–seven days, depending on their growth rate.
Media was replaced every two - three days removing Thz.

- 96-well plate assay

Organoids were washed with cold D-PBS, collected in a 15mL tube and centrifuge for 3 minutes, 500g at room temperature. Organoids were resuspended in ten volumes of TrypLE™ Express (Gibco, #12604-013). The final volume of TrypLE™ Express is calculated on the volume of Matrigel: 50µL Matrigel correspond to 500µL TrypLE™ Express. The solution was then syringed (21 G needle), incubated for 30 min at 37°C in water bath, and vortexed every five minutes to ensure a single-cell dissociation. The enzymatic reaction was stopped by adding 100µL FBS/mL TrypLE™ Express solution and organoids were dissociated into a single cell suspension through a second step of syringed (21 G needle). Cells were centrifuged at 500 g for 3 min at room temperature and counted in a Burker chamber with Trypan Blue solution. 10.000 cells/well were resuspended in 25 µl/well of undiluted Matrigel and seeded. After 20 minutes of polymerisation, Human Intesticult^{TM} Organoid Complete Growth Medium (Basal+Supplement) (Stem Cell Technologies, #06010) supplemented with Thz was added in each well.

3.2.4 Mature organoids cryopreservation and thawing

- Cryopreservation

After removing the Media, organoids were flushed with 1mL cold D-PBS and the Matrigel droplets were disrupted to release the organoids. Organoids were collected into a 15mL tube and centrifuge for 5 minutes, 290 g at 4°C. Pellets were then resuspended in 7 mL of cold DMEM/F12 with 15mM HEPES and syringed (21 G needle). After syringe, organoids were centrifuged for 5 minutes, 200 g, at 4°C. Pellets were then resuspended in 1mL cold freezing media (80% Advanced DMEM-F12; 10% FBS; 10% DMSO) and transferred into a cryopreservation vial. By using a cell-freezing container filled with isopropanol, the organoids were frozen to -80°C overnight and then moved to liquid nitrogen for long-term storage.

- Thawing

Frozen organoids were quickly thawed in water bath at 37°C, resuspended with DMEM-F12 with 15mM HEPES-1%BSA solution and transferred in a 15mL tube filled with additional 2mL of DMEM-F12 with 15mM HEPES-1%BSA solution. Organoids were centrifuged for 5 minutes, 200 g, at 4°C and then resuspended in undiluted Matrigel and seeded in a 24-well plate (50 µl Matrigel/well).

3.3. Human cell lines culture

We selected the human colorectal cancer cell lines HCT116 (MSI, *PIK3CA* mutant, *KRAS mutant, CTNNB1* mutant, *APC wild-type*), HT29 (*PIK3CA* mutant, *BRAF mutant*, *CTNNB1 wild-type* and *APC* mutant), SW480 (*PIK3CA wild-type*, *KRAS mutant*, *CTNNB1 wild-type*, *APC* mutant) and the human embryonic kidney SuperTOPFLASH HEK293 (STF) (*PIK3CA*, *KRAS*, *CTNNB1* and *APC wild-type*) cells.
All human cells were obtained from ATCC (Manassas, VA, USA) and maintained according to the following culture conditions:

- HCT116 and SW480 were cultured in Dulbecco's modified Eagle medium (DMEM) High glucose (Microgem, Naples, Italy), 10% FBS (Microgem, Naples, Italy), 100 U/mL penicillin, 100 µg/ml streptomycin, 2mM glutamine (Microgem, Naples, Italy).
- HT29 were cultured in RPMI-1640 (Microgem, Naples, Italy), 10% FBS (Microgem, Naples, Italy), 100 U/mL penicillin, 100 µg/ml streptomycin, 2mM glutamine (Microgem, Naples, Italy).

- HEK293STF were cultured in DMEM-F12 (Microgem, Naples, Italy). The culture media were supplemented with 20% FBS (Microgem, Naples, Italy), 100 U/mL penicillin, 100 µg/ml streptomycin, 2mM glutamine (Microgem, Naples, Italy) and 200 µg/ml G-418 (GoldBio).

Cells' identity was verified by STR profile analysis and cells were tested routinely for Mycoplasma contamination.

3.3.1 Cell lines expansion

Confluent-adherent cells in T75 flasks were washed with 5mL of 1X phosphate buffer saline (PBS) and dissociated with 1 mL of Trypsin-EDTA 1X (Sigma-Aldrich) for 5 minutes at 37°C and 5% CO2. After dissociation, 3 mL of complete growth medium was added to stop the enzymatic reaction. Trypsinized-cells were collected in a 15mL tube and centrifuged for 5 minutes, 1500 rpm, at room temperature. The pellets were resuspended in the appropriate complete growth media and $2x10^6$ cells were seeded in a new T75 flasks with 8 mL of appropriate complete growth media, then placed in a humidified incubator at 37% and 5% CO_2.

3.3.2 Cell lines cryopreservation and thawing

- <u>Cryopreservation</u>

Confluent-adherent cells in T75 flasks were washed with 5 mL 1X PBS and dissociated with 1 mL of Trypsin-EDTA 1X (Sigma-Aldrich) for 5 minutes at 37°C and 5% CO_2. After dissociation, 3mL of complete growth medium was added to stop the enzymatic reaction. Trypsinized-cells were collected in a 15mL tube and centrifuged for 5 minutes, 1500 rpm, at room temperature. Cells were then resuspended in 1mL of appropriate freezing media:

- 90% FBS (Microgem, Naples, Italy) and 10% DMSO for HCT116 and SW480;
- 95% RPMI-1640 (Microgem, Naples, Italy) complete growth media (supplemented with 100 U/mL penicillin, 100 µg/ml streptomycin, 2mM glutamine and 10% FBS), and 5% DMSO for HT-29;
- 50% FBS, 39% DMEM-F12 (Microgem, Naples, Italy) complete growth media (supplemented with 20% FBS, 100 U/mL penicillin, 100 µg/ml streptomycin, 2mM glutamine, and 200 µg/ml G-418), and 11% DMSO for HEK293-STF.

Cells were transferred into a cryopreservation vial, placed in a cell-freezing container filled with isopropanol, frozen to -80°C overnight, and then moved to liquid nitrogen for long-term storage.

- Thawing

Frozen cells were quickly thawed in water bath at 37°C, transferred in a 15mL tube and centrifuged for 5 minutes, 1500 rpm, at 4°C. After centrifuge, the pellet was resuspended in 1mL of appropriate growth media and seeded in a T75 flask with 8mL of growth media. Cells were grown in a humidified incubator at 37% and 5% CO_2.

3.4 Compounds and Treatments

- Stock Solutions

(-)-Epigallocatechin gallate (EGCG; E4143 purity ≥ 95%; Sigma-Aldrich, Milan, Italy) was dissolved in dimethyl sulfoxide (DMSO) to obtain a stock concentration of 54,54 mM.

Rapamycin (#9904; Cell Signaling Technology, MA, USA) was resuspended in DMSO to obtain a stock concentration of 100 µM according to the manufacturers' instructions.

Cis-4,7,10,13,16,19-Docosahexaenoic acid (DHA; D2534 purity ≥ 98%; Sigma-Aldrich, Milan, Italy) was dissolved in EtOH 96% in order to achieve a stock concentration of 121,77 mM. To prevent DHA oxidation, the anti-oxidant Butylhydroxytoluene (BHT; B1378; Sigma-Aldrich, Milan, Italy) was added to the DHA stock solution at 0.1% w/w.

- Treatments

Prior to cell culture treatments, to achieve a final vehicles concentration $\leq$ 0.1% (DMSO or EtOH 96%, respectively), EGCG and Rapamycin stock solutions were further diluted in PBS 1:10. DHA stock solution was further dissolved in PBS 1:4.

For cell lines treatment EGCG (E), DHA (D) and Rapamycin (R) were tested individually or in combination (RDE) at a final concentration of 60 µM, 150 µM and 20 nM, respectively for 24 hours. The compounds were dissolved in the appropriate culture medium for the corresponding-treated cell line.

For organoids treatment the compounds were tested only in combination (RDE) at the same final concentrations for 48 hours. The compounds were dissolved in Basal Human Intesticult™ Organoid Growth Medium (Stem Cell Technologies, #06010) diluted 1:1 with Advanced DMEM-F12. The Basal media, according to the manufacturer's instructions should not contain Wnt3A and R-spondin factors.

In each experiment, untreated cells or organoids (Negative control; NC) and cells or organoids treated with vehicles of the compounds (CTRL) have been included as negative controls.
In CTRL condition, DMSO and EtOH 96% were prior diluted in PBS (1:10 or 1:4, respectively) as the corresponding compound and then added to the media at the appropriate final volume.
The Glycogen synthase kinase 3 (GSK3) inhibitor CHIR99021 (SML1046; purity ≥ 98%; Sigma-Aldrich, Milan, Italy) was dissolved in DMSO to obtain a stock solution of 4mM and used as a positive control for Wnt signaling activation at a final concentration of 2.5 µM.

For the inhibition of the proteasome in HEK293STF cells, MG132 (Sigma-Aldrich) was added at a final concentration of 10µM, 4 hours prior the end of the treatment, directly into the media containing the different treatment conditions.

3.5 Molecular Evaluation of Wnt and mTOR activation

3.5.1 Assay

FIT+, FAP and CRC-organoids were seeded 1:4 into a 24-well plate as previously described (3.2.3) and treated following the protocol previously described (3.4). For each conditions 6 wells were seeded to achieve a sufficient volume of organoids for the following analysis.
HEK293STF, HCT116, HT29 and SW480 were seeded into 6-well plate ($4x10^5$ cells/well) as previously described (3.3.1) and treated following the protocol previously described (3.4). Three wells for each conditions were seeded to achieve a sufficient volume of cells for the following analysis.
Each experiment was repeated at least three times.

3.5.2 Organoids and Cells Harvesting

- Organoids Harvesting

After treatment, organoids were washed with cold D-PBS. Ten volumes of Cultrex™ Organoid Harvesting Solution (R&D, #3700-100-01) were added in each well and incubated at 4°C for 1h on an orbital shaker to depolymerize Matrigel, according to the manufacturers' instructions. The final volume of Cultrex™ Organoid Harvesting Solution is calculated on the volume of Matrigel: 50µL Matrigel correspond to 500µL Cultrex™ Organoid Harvesting Solution.

Once the Matrigel was completely depolymerized, organoids released from the 6 wells were collected together in a 15mL tube and centrifuged for 5 minutes, 500 g, at 4°C. Organoids were washed in 10mL cold D-PBS and centrifuged for 5 minutes, 500 g, at 4°C. The organoids' pellet was resuspended in 1mL cold D-PBS: 750µL were transferred in a new 1.5mL tube for proteins extraction and 350µL were transferred in a different 1.5mL tube for RNA extraction. Organoids were further centrifuged 3 minutes, 7500 rpm, at 4°C. All the supernatant was discarded and the pellets were quickly frozen in liquid nitrogen and then stored at -80°C until protein/RNA extraction.

- Cells Harvesting

After treatment, adherent cells were washed with cold PBS and dissociated with 500 µL/well of Trypsin-EDTA 1X (Sigma-Aldrich; #T2601) for 5 minutes at 37°C and 5% CO2. After dissociation, 1.5 mL of cold PBS was added to stop the enzymatic reaction. Trypsinized-cells from 3 wells were collected in a 15 mL tube and centrifuged for 5 minutes, 1500 rpm, at 4°C. The pellets were resuspended in 2 mL cold PBS: 1 mL was transferred in a new 1.5 mL tube for Cytosolic and Nuclear protein extraction, 750 µL were transferred in a new 1.5 mL tube for proteins extraction and 350 µL were transferred in a different 1.5 mL tube for RNA extraction. Cells were further centrifuged 3 minutes, 7500 rpm, at 4°C. All the supernatant was discarded and the pellets were quickly frozen in liquid nitrogen, and then stored at -80°C until protein/RNA extraction.

3.5.3 Protein expression analysis

3.5.3.1 Protein extraction

- Total Protein

Pellets containing organoids or cells were thawed on ice and resuspended in an appropriate volume (15-20 µL for organoids' pellets and 25 µL for cells' pellets) of cold RIPA Buffer solution (50 mM Tris-HCl (pH 7.4), 150 mM NaCl, 1mM EDTA, 1% NP-40, 1% Na-deoxycholate, 0.1% SDS, sterile-filtered) with 1:10 phosphatase and protease inhibitors, and 1 mM DL-Dithiothreitol (DTT). Pellets were vortexed twice for 20 seconds, incubated on ice for 15 minutes and finally centrifuged for 15 minutes, 13.000 g at +4°C. The extracted protein were collected into a new 1.5mL tube and stored at -80°C.

- Cytosolic and Nuclear protein extraction

Nuclear and cytoplasmic extracts were obtained using the NE-PER Nuclear and Cytoplasmic Extraction Kit (Thermo Fisher Scientific™, #78833) according to the datasheet's instructions for 1 X 10^6 cells. The nuclear and cytoplasmic protein extracts were collected into a new 1.5 mL tube and stored at -80°C.

All the protein lysates were quantified by Lowry-Assay performed with DC Protein Assay kit (Bio-Rad, #5000116) according to the manufacturer's instructions in a 96 well-plate. 750 nm absorbance was acquired in the multimode microplate reader Spark® (Tecan Trading AG, Switzerland).

3.5.3.2 SDS-PAGE and Western Blotting

Thirty micrograms of cell's total proteins (fifteen micrograms for organoids) and fifteen micrograms of nuclear and cytoplasmic extracts for each sample were separated on a 4-12% NuPAGE™ Novex Bis-Tris gels (Invitrogen™; Thermo Fisher Scientific) by using the NuPAGE™ MOPS SDS Running buffer (Invitrogen™; Thermo Fisher Scientific) and transferred onto nitrocellulose membrane. Membranes were blocked with 5% non-fat milk solution and then incubated overnight at +4°C with the following primary antibodies: APC (1:1,000, Cell Signaling Technology, CST #2504), AXIN1 (1:500, CST#2087), phospho-β-Catenin (1:500, CST #9561), Non-phospho (Active) β-Catenin (1:2,000, CST #9561), β-Catenin (1:2,000, CST #9562), phospho-GSK-3β (Ser9) (1:500, CST #9323), GSK-3β (1:4,000, CST #9315), phospho-mTOR (Ser2448) (1:1,000, CST#2971), mTOR (1:1,000, CST #2983), phospho-p70S6

Kinase (Thr389) (1:1,000, CST#9234), p70 S6 Kinase (1:2,000), phospho-S6 ribosomal protein (Ser235/236) (1:2,000, CST #2211), Cleaved and full-length PARP (1:2,000, CST #9542), Survivin (1:1,000, CST #2808), GAPDH (1:6,000, CST #2118), Lamin B1 (1:1,000, CST #12586). GAPDH was used as loading control for total protein and cytoplasmic extracts, while LAMINB1 was used as nuclear loading control. After the incubation with the primary antibody, membranes were washed and then incubated with the secondary antibody ECL™ anti-rabbit IgG (1:1,000; Amersham™; NA934VS ECLTM Peroxidase labelled anti-rabbit antibody) for 1 hour at room temperature. All antibodies were incubated in dried non-fat milk 5% diluted in PBS 1X with 0.05% Tween® 20. Signals were detected with WESTAR ECL chemiluminescent substrates (Cyanagen, #XLS0142 and #XLS075) and images were acquired with Chemidoc XRS+ (Bio-Rad Laboratories). Prior to re-probing with different antibodies, the membranes were stripped with Restore Western blot stripping buffer (Thermo Fisher Scientific, #21059), washed in PBS 1X with 0.05% Tween® 20 and blocked in non-fat milk 5% solution. Densitometric analyses were performed with the Image-Lab software (Bio-Rad Laboratories). Each signal intensity was normalized on GAPDH (or LAMINB1 for nuclear proteins) and then compared to CTRL to quantify fold differences in protein expression.

3.5.4 Gene expression analysis

3.5.4.1 RNA extraction

Total RNA was extracted from cell lines and organoids using the TRIzol® reagent (Invitrogen™; Thermo Fisher Scientific) according to the manufacturer's instructions. RNA quantification and purity evaluation was performed by using NanoDrop spectrophotometer (Thermo Fisher Scientific). Absorbance (optical density, OD) at 260 nm in relation to the absorbance at 280 nm (OD 260/280) or 230 nm (OD 260/230) was measured to evaluate respectively protein or ethanol contamination.

3.5.4.2 RNA to cDNA reverse transcription

Two micrograms of RNA were retrotranscribed using the High-Capacity cDNA Reverse Transcription Kit with RNase Inhibitor (Applied Biosystems; #4374966), according to the manufacturer's instructions. The reverse transcription reaction was performed in an GeneAmp PCR 9700 Thermal

Cycler (Applied Biosystems, Thermo Fisher Scientific) as follow: 10 minutes at 25°C, 37°C for 120 minutes, 85°C for 5 minutes, and 4°C. At the end of the cycle, cDNAs were stored at -20°C until use.

3.5.4.3 Quantitative real-time PCR (qPCR)

cDNA were diluted 1:5 with sterile H2O and 2 µl were used to performed the qPCR by using the TaqMan™ Fast Advanced Master Mix (Applied Biosystems™; Thermo Fisher Scientific, #4444965) and TaqMan™ Gene Expression Assays (Life Technologies, Monza, Italy) in a final volume of 20 µL following manufacturers' instructions. TaqMan™ Gene Expression Assays include: *AXIN1* (Assay ID: Hs00394718_m1), *AXIN2* (Assay ID: Hs00610344_m1), *MYC* (Assay ID: Hs00153408_m1), *CCND1* (Assay ID: Hs00765553_m1), *LGR5* (Assay ID: Hs00969422_m1), *RPS6* (Assay ID: Hs03044100_g1), *KRT20* (Assay ID: Hs00300643_m1)*, GAPDH (Assay ID: Hs03929097_g1).*

The qRT-PCR reaction was performed in a MicroAmp™ Fast Optical 96-Well Reaction Plate on a QuantStudio5 thermal cycler (Applied Biosystems™; Thermo Fisher Scientific) as follow: 50°C for 2 minutes for Uracil-DNA Glycosylase (UDG) incubation, 95°C for 10 minutes for TaqMan™ Fast Advanced enzyme activation followed by 40 cycles of denaturation at 95°C for 15 seconds and annealing/extension at 60°C for 1 minute. Reactions were performed in triplicate.

Fold induction levels for each gene were obtained using the 2-ΔΔCt method by normalizing against GAPDH used as endogenous control. Fold changes values were compared to the healthy mice group.

3.6 Organoids and Cells viability assay

- Organoids Viability Assay

Organoids viability was measured using the CellTiter-Glo® 3D Cell Viability Assay (Promega, #G9681), a luminescent metabolic assay based on quantitation of the ATP produced by cells. The amount of ATP is directly proportional to the number of viable cells present in culture. For this assay, organoids were dissociated into single cells (3.2.3) and 10.000 cells/well were seeded in a 96-well plate. After 4 days, growing-organoids were treated for 48h and the organoids viability was analyzed by CellTiter-Glo® 3D Cell Viability Assay according to the manufacturer's instructions. Each condition was evaluated in five different wells. Luminescent signals were measured by the multimode plate reader Spark® (Tecan Trading AG, Switzerland) (integration time 1,000 ms). Organoids viability was expressed

as percentage of the ratio of the mean luminescence of treated organoids/median luminescence of CTRL. Each experiment was repeated at least three times.

- Cells Viability Assay

$10x10^3$ cells/well were seeded into 96-well plate and after 24 hours were treated with EGCG (60 µM), DHA (150 µM) and Rapamycin (20 nM) individually or in combination for 24 hours. Cell viability was assessed by using alamarBlue™ Cell Viability Reagent (Invitrogen, Thermo Fisher Scientific, #DAL1025) following the manufacturer's instructions. The alamarBlue™ Cell Viability Reagent is a Resazurin-based dye, whose fluorescent color intensity is influenced by the reducing environment of viable cells. The fluorescence color changes and intensities were detected using the multimode plate reader Spark® (Tecan Trading AG, Switzerland) (Fluorescence Ex/Em = 530/580). To evaluate background signals, blank wells containing only the medium or tested compounds individually or in combination were introduced in each assay. Background fluorescence signals have been subtracted for normalization from the corresponding negative controls and treated samples during the analysis process. A positive control containing 100% of reduced alamarBlue™ reagent without cells has been also included in each assay. The experiments were performed independently three times in quadruplicate. Cell viability was expressed as percentage

$$\frac{\text{fluorescence of treated cells} - \text{fluorescence of background controls}}{\text{fluorescence of vehicles controls} - \text{fluorescence of background controls}}\ x100$$

3.7 Cells apoptosis assay

HCT116 were seeded 2,500 cells/well in a 96-well plate in Eagles MEM with low riboflavin (Microgem). After 24 hours cells were treated with EGCG (60 µM), DHA (150 µM) and Rapamycin (20 nM) individually or in combination for 24 hours and co-stained with the Incucyte® Caspase-3/7 Red Dye for Apoptosis (1:500, Sartorius, #4704) and Incucyte® AnnexinV Green Dye (1:200, Sartorius, #4642). Cells were directly incubated in Incucyte® Live-Cell Analysis System (Sartorius, Essen BioScience) at 37°C and 5% CO_2. Cell growth and the kinetic activation of apoptosis in the two different fluorescent channels were monitored for 36 hours using live cell imaging, and quantified using the Incucyte® Live-Cell Analysis System according to the manufacturer's instructions. The

apoptotic index were calculated on Incucyte® Live-Cell Analysis System using the Incucyte® Cell-by-Cell Analysis Software Module (Sartorius, #9600-0031) according to the manufacturers' instructions.

3.8 Statistical Analysis

Data were reported as mean ± SD of at least three independent experiments. Unpaired T-test was used to analyze differences between RDE and CTRL or CHIR. One-way ANOVA followed by Dunnett's test was used to compared differences between the mean of each single treatment or RDE and the mean of CTRL to analyze the contribution of each individual compound in the final effect of RDE. Statistical analysis was performed using GraphPad 8.0 software (GraphPad Software Inc., La Jolla, CA). P values < 0.05 were considered statistically significant.

4. RESULTS

4.1 RDE inhibits the mTOR pathway in a tissue-type independent manner.

In this study, we selected organoids and cell lines with different mutational settings to investigate if the effect of RDE was influenced by different statuses of Wnt/β-catenin or PI3K/mTOR activation, with a focus on *APC*-mutated settings. Due to the limited material in organoids' experiments, we used representative cell line models to investigate the contribution of the single compounds (Rapamycin, DHA, and EGCG). HEK293STF was used as a *wild-type* model; SW480 as Wnt/β-catenin dysregulated only (mutation in *APC*), HT-29 as Wnt/β-catenin and PI3K/mTOR (mutation in *APC* and *PI3KCA*) mutated, and HCT116 as Wnt/β-catenin and PI3K/mTOR (mutation in *PI3KCA*) dysregulated, but without *APC* gene mutations (mutation in *CTNNB1*). We also included CHIR99021 2.5 µM (CHIR), a GSK3β inhibitor, usually used as a positive control to monitor Wnt/β-catenin signalling induction.

After selecting sub-cytotoxic concentrations of Rapamycin (20nM), DHA (150µM), and EGCG (60µM), we treated patients-derived organoids and cell lines respectively for 48 and 24 hours. We found that, after 48 hours of treatment, compared to CTRL, RDE significantly inhibited the pathway, by downregulating the phosphorylation of the downstream proteins P70S6K (p-P70S6K) ($p<0.0001$, T-test vs CTRL, FIT+ NM; FAP NM, FAP A; CRC NM, CRC K) and S6 ribosomal protein (p-S6R) ($p<0.0001$, T-test vs CTRL, FIT+ NM; FAP NM, FAP A; CRC NM, CRC K) in all organoids in a mutations-independent manner (Fig.4.1 A-C). The expression of *RPS6* gene was not significantly affected by RDE treatment in most of the organoids ($p=0.0286$ T-test vs CTRL, FIT+NM; p=ns (non-significant) T-test vs CTRL, FAP NM, FAP A; CRC NM, CRC K); confirming that the modulation of mTOR occurred mainly at a post-translational level (Fig.4.1 D).

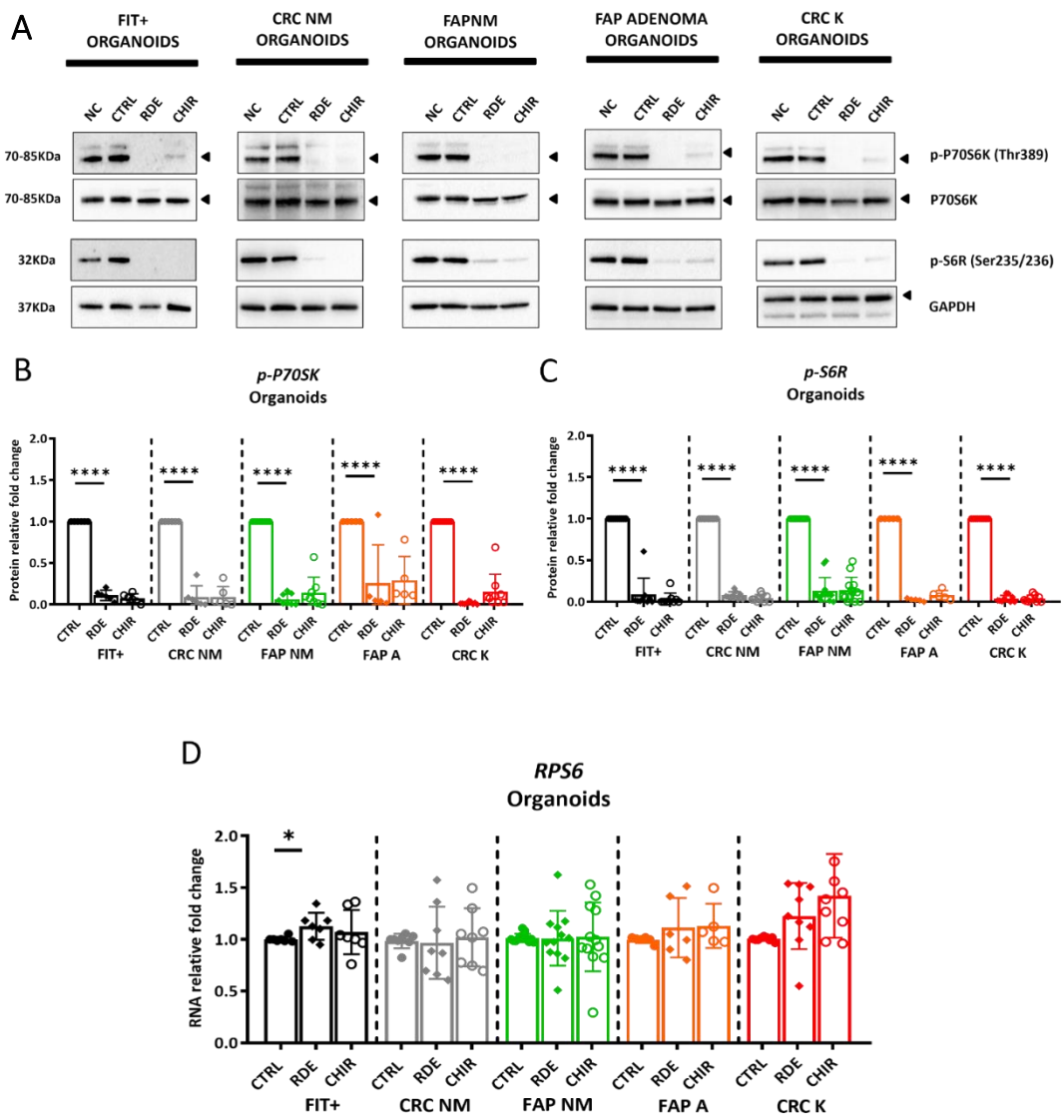

Figure 4.1. (A-C) Effect of RDE on mTOR down-stream target proteins expression p-P70S6K and p-S6R in intestinal organoids evaluated by Western Blot. p-P70S6K was normalized on the expression of total P70S6K protein; p-S6R was normalized to GAPDH protein. **(D)** Effect of RDE on *RPS6* mRNA expression assessed by qRT-PCR. *RPS6* mRNA expression was normalized to GAPDH mRNA expression. Proteins and RNA mean values relative fold changes were calculated using CTRL as reference sample. Data are expressed as means ± SD. Statistical significance was tested using unpaired T-test. FIT+ n=6; CRC NM n=6; FAP NM n=9; FAP A n=6; CRC K n=6. NC = Negative Control; CTRL = Control with vehicles; RDE = treatment; CHIR = Active-Wnt signalling positive control. *P<0.05; **P<0.010; ***P<0.001; ****P<0.0001.

Similar results on P70S6K and S6R phosphorylation were also observed in HEK293STF (p-P70S6K p=0.0175; p-S6R p<0.0001, *RPS6* ns, T-test vs CTRL), HCT116 (p-P70S6K p<0.0001; p-S6R p<0.0021, *RPS6* ns, T-test vs CTRL) and SW480 (p-P70S6K p<0.0002; p-S6R p<0.0001, *RPS6* p=ns, T-test vs CTRL) cell lines after 24 hours of treatment (Fig.4.2 A-D).

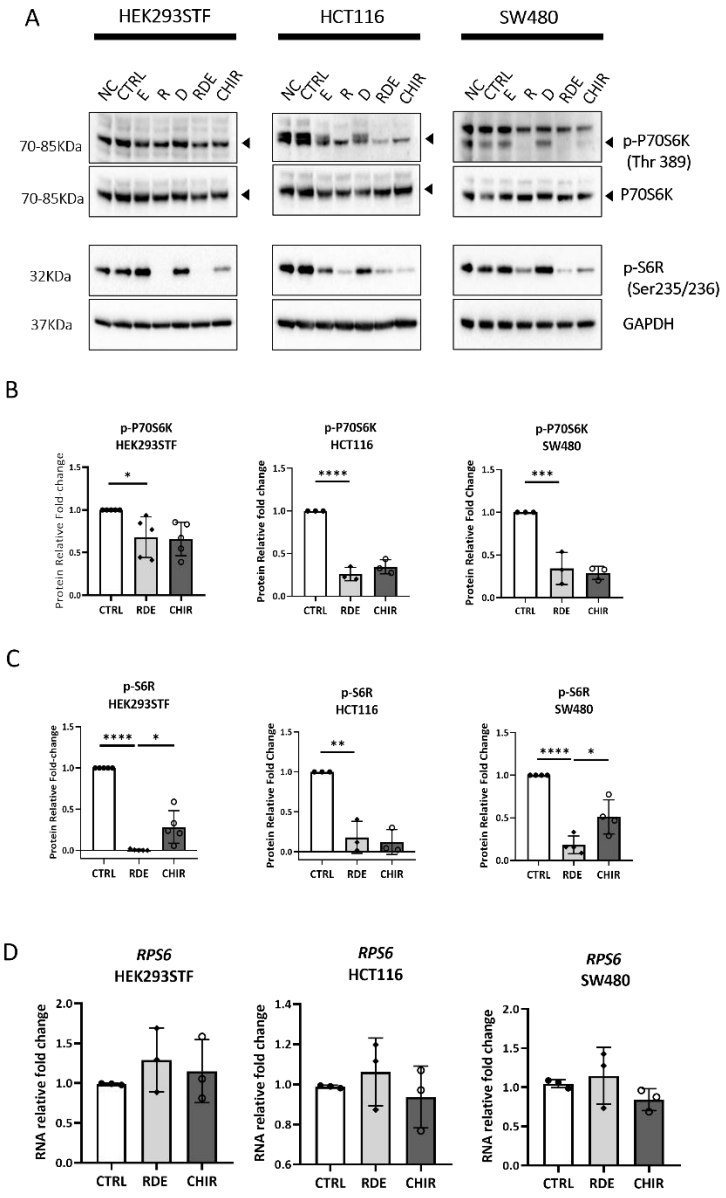

Figure 4.2. (A-C) Effect of RDE and the single treatments on mTOR down-stream target proteins expression p-P70S6K and p-S6R in HEK293STF, HCT116 and SW480 cell lines evaluated by Western Blot. p-P70S6K was normalized on the expression of total P70S6K protein; p-S6R was normalized to GAPDH protein. **(D)** Effect of RDE on *RPS6* mRNA expression assessed by qRT-PCR. *RPS6* mRNA expression was normalized to GAPDH mRNA expression. Proteins and RNA mean values relative fold changes were calculated using CTRL as reference sample. Data are expressed as means ± SD. Statistical significance was tested using unpaired T-test. HEK293STF n = 5; HCT116 n= 3; SW480 n = 4. NC = Negative Control; CTRL = Control with vehicles; RDE = treatment; CHIR = Active-Wnt signalling positive control. *P<0.05; **P<0.010; ***P<0.001; ****P<0.0001.

Interestingly, HT-29 was more resistant to the treatment, and only S6R protein phosphorylation (p-S6R p=0.0061, T-test vs CTRL) was modulated by RDE in a Rapamycin-dependent manner (data not

shown; ns= non-significant Dunnett's test vs CTRL). Rather than the simultaneous mutations in *APC* and *PI3KCA*, this finding has reason to be attributed to the mutation in *BRAF* (V600E), well known to confer tumor resistance to mTOR inhibitors treatment, such as *Everolimus* (He K. et al, 2016).

As expected, we found that Rapamycin, as a target inhibitor of mTOR, led to the inhibition of the pathway and its downstream targets in all the cell lines compared to CTRL [HEK293STF (**p-P70S6K**, R p=0.0420; RDE p=0.0487; **p-S6R,** R p<0.0001; RDE p<0.0001); HCT116 (**p-P70S6K**, R p=0.0253; RDE p=0.0020; **p-S6R,** R p<0.0109; RDE p<0.0094); SW480 (**p-P70S6K**, R p<0.0001; RDE p=0.0002; **p-S6R,** R p<0.0122; RDE p<0.0016)] (Fig.4.2 A; Fig.4.3 A-B). EGCG and DHA are also known to inhibit the PI3K/mTOR pathway (Van Aller G.S. et al., 2011; Vasudevan A. et al., 2014; Oh S. et al., 2014), however, we at the selected treatment condition we did not found a significant contribution to the downregulation of p-P70S6K and p-S6R.

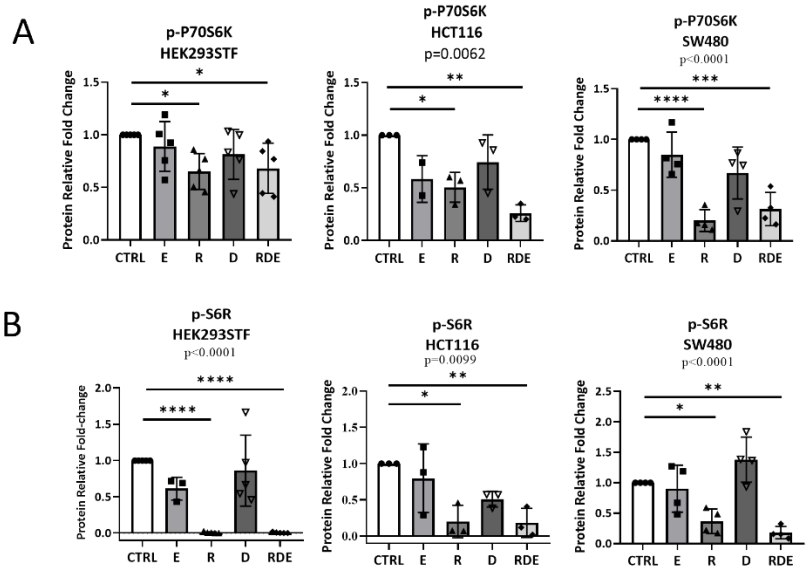

Figure 4.3. (A-B) Effect of RDE and single compounds on mTOR down-stream target proteins expression p-P70S6K and p-S6R in HEK293STF, HCT116 and SW480 cell lines evaluated by Western-Blot. P-P70S6K was normalized on the expression of total P70S6K protein; p-S6R was normalized to GAPDH protein. Proteins mean values relative fold changes were calculated using CTRL as reference sample. Data are expressed as means ± SD. Statistical significance was tested using One-Way ANOVA and the Dunnett's test for multiple comparisons vs CTRL. HEK293STF n = 5; HCT116 n= 3; SW480 n = 4. NC = Negative Control; CTRL = Control with vehicles; E = EGCG; R = Rapamycin; D = DHA; RDE = treatment; CHIR = Active-Wnt signalling positive control. *P<0.05; **P<0.010; ***P<0.001; ****P<0.0001.

Interestingly, we found that CHIR and RDE shared a similar inhibition of the PI3K/mTOR pathway in a mutation-independent manner (Fig.4.2 A; Fig.4.3 A-B). Indeed, it has been described that CHIR

treatment induced significant reduction in the phosphorylation of Akt and downregulated mTOR through TSC2/Rheb in a beta-catenin independent manner (Rethineswaran V. K. et al., 2021).

4.2 Wnt/β-catenin pathway modulation is influenced by genetic backgrounds.

The canonical Wnt/β-catenin and PI3K/mTOR pathways regulate each other through several mechanisms that define a wide cross-talk, usually associated with the occurrence of drug resistance. Thus, we decided to evaluate several genes and proteins involved in the Wnt/β-catenin functions and regulations.

In addition, it is well established that normal-mucosa (NM) -human-intestinal organoids require several growth factors, including Wnt3A and R-spondin1, to sustain *ex-vivo* growth and proliferation (Pleguezuelos-Manzano C. et al., 2020). After verifying that Wnt-supplement removal did not affect organoids viability and morphology for 48 hours, we treated the organoids in an essential culture media to better understand the RDE-dependent effects on the Wnt/β-catenin pathway, without the interference of exogenous Wnt signals (e.g. Wnt3A or R-spondin1).

After 48 and 24 hours we found that RDE treatment modulated the Wnt/β-catenin pathway differently among organoids and cell lines, respectively.

4.2.1 In FIT+- and CRC-NM wild-type organoids RDE induces activation of the Wnt/β-catenin pathway.

The healthy FIT+-NM organoids represented an appropriate *wild-type* setting to study the response to the treatment in the absence of aberrations involving the two pathways.

In this model, we found that compared to CTRL, RDE inactivated GSK3β by increasing the phosphorylation in Ser9 (p-GSK3β) (p=0.0263, T-test vs CTRL), affecting the functionality of the degradosome (Figure 4.4 A). As a result, we found an increase in non-phosphorylated (Active) (p=ns, T-test vs CTRL) and total β-catenin protein expression (p=ns, T-test vs CTRL) (Figure 4.4 B), which led the transcription of the Wnt/β-catenin target genes *AXIN2* (p=0.0222, T-test vs CTRL), *CCND1* (p=0.0006, T-test vs CTRL) and *C-MYC* (p=0.0016, T-test vs CTRL), confirming the activation of the pathway (Figure 4.4 C-D).

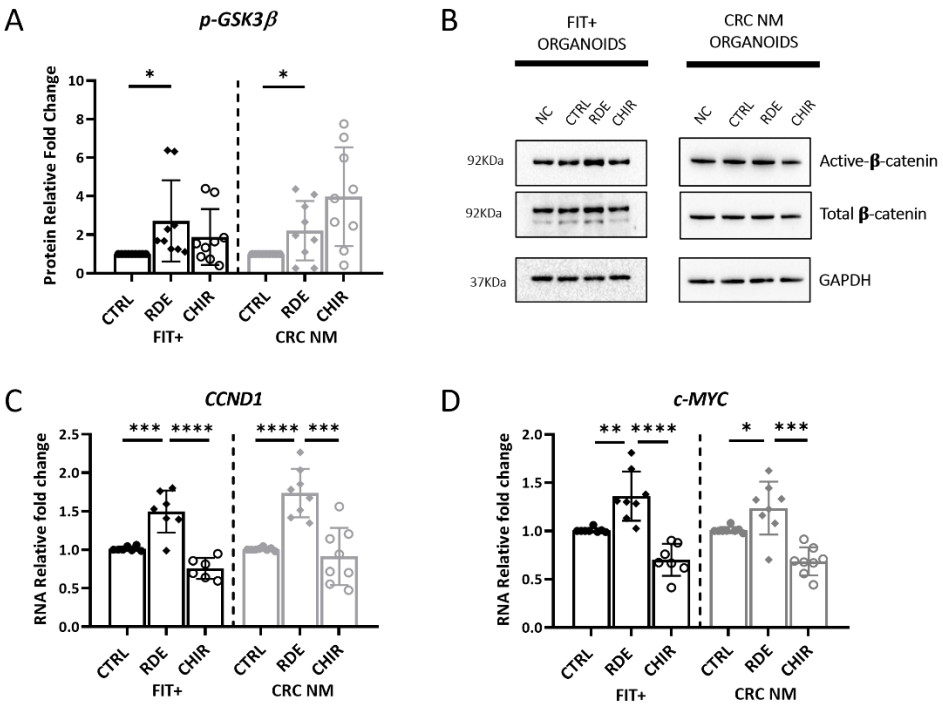

Figure 4.4. (A-B) Effect of RDE on GSK3β and β-catenin protein expression in FIT+ NM and CRC NM intestinal organoids evaluated by Western-Blot. P-GSK3β was normalized on the expression of total GSK3β protein; non-phosphorylated (Active) β-catenin was normalized to total β-catenin protein; total β-catenin protein was normalized to GAPDH protein. **(C-D)** Effect of RDE on *CCND1* and *c-MYC* mRNA expression assessed by qRT-PCR. *CCND1* and *c-MYC* mRNA expression was normalized to GAPDH mRNA expression. Proteins and RNA mean values relative fold changes were calculated using CTRL as reference sample. Data are expressed as means ± SD. Statistical significance was tested using unpaired T-test. FIT+ n=9; CRC NM=9. NC = Negative Control; CTRL = Control with vehicles; RDE = treatment; CHIR = Active-Wnt signalling positive control. *P<0.05; **P<0.010; ***P<0.001; ****P<0.0001

CRC-NM organoids were derived from NM tissues collected at a 5 cm distance from the corresponding tumors. We verified the absence of somatic mutations in the tissues through NGS analysis, thus we included this subset of organoids in the *wild-type* setting. Compared to CTRL we found that RDE induced Wnt/β-catenin signalling activation similar to FIT+-NM organoids, but with a more significant upregulation of β-catenin (p=0.0354, T-test vs CTRL) (Figure 4.4 A-D).

Despite the inactivation of GSK3β, the activation of the signalling in both FIT+-NM and CRC-NM organoids did not alter AXIN1 protein expression.

With a particular focus on CRC-NM organoids, compared to RDE, we found that CHIR despite GSK3β inactivation preserved an intact AXIN1 complex, whose function resulted unchanged. Indeed, we observed an increase in phosphorylated β-catenin (Ser33/37/Thr41) compared to RDE (p=0.0354, T-test RDE vs CHIR) and a reduction in the total β-catenin (p=0.0041, T-test RDE vs CHIR), and *CCND1*

(p=0.0003, T-test RDE vs CHIR) and *C-MYC* (p=0.0002, T-test RDE vs CHIR) target genes (Figure 4.4 A-D). These results were not surprising considering that the selected CHIR concentration (2.5 µM) is normally used in some media formulations for *ex-vivo* intestinal organoids cultures to support proliferation in a physiological manner.

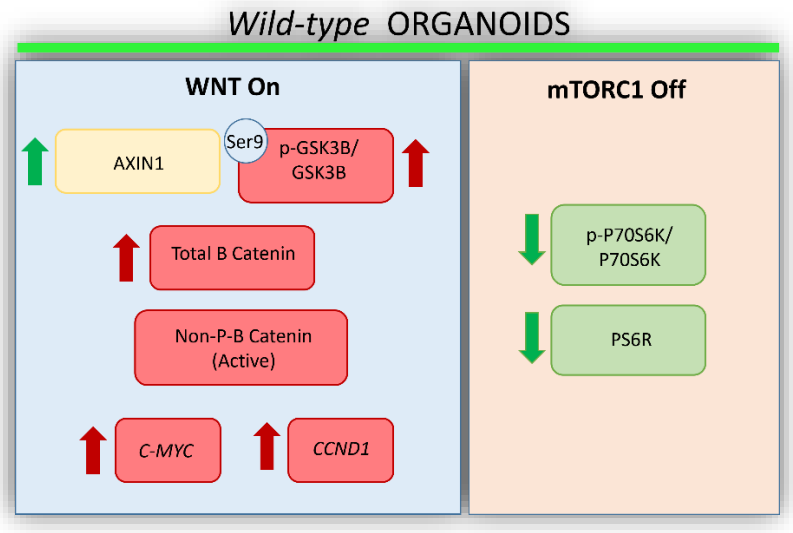

Figure 4.5. Summary of the effect of RDE on the Wnt/β-catenin and mTORC1 pathway in the wild-type organoids FIT+-NM and CRC-NM.

4.2.2 In HEK293STF wild-type cells RDE reduces CTNNB1 expression and partially inactivated the Wnt/β-catenin pathway.

We used the HEK293STF as a *wild-type* cell line model to explore the effects of RDE and the single compounds after 24 hours. We found that similar to FIT+ and CRC-NM organoids, RDE induced GSK3β phosphorylation (Ser9) compared to CTRL (p=ns, T-test vs CTRL). Rapamycin and DHA were mainly involved in the regulation of GSK3β (Fig.4.6 A) (p=ns, Dunnett's test vs CTRL). In addition, we found also that Rapamycin together with EGCG showed a trend in downregulating AXIN1 protein expression. Even if this result is not significant (p=ns, Dunnett's test vs CTRL) (Fig.4.6 B), it suggests a more severe dysregulation of the β-catenin destruction complex, which contributed to the accumulation of both cytoplasmic and nuclear β-catenin compared to CTRL (p=ns, Dunnett's test vs CTRL; p=ns, T-test RDE vs CTRL)(Fig.4.6 F-G). Despite the accumulation of active-β-catenin, we observed a significant downregulation of total β-catenin expression in RDE-treated HEK293STF (p=0.0453, T-test vs CTRL) (Fig.4.6 C-D).

We noticed that the modulation of both PI3K/mTOR and Wnt/β-catenin pathways was mainly post-translational. Indeed, both *RPS6* (encoding for S6R protein) and *AXIN1* gene transcripts were not altered by RDE compared to CTRL. In contrast, the protein expression of p-S6R and AXIN1 was significantly downregulated ($p<0.0001$, T-test vs CTRL; p=0.0072, Dunnett's test COMB vs CTRL) (Fig.4.6 B). We therefore hypothesized that the suppression of total-β-catenin induced by RDE was related more to post-translational mechanisms too.

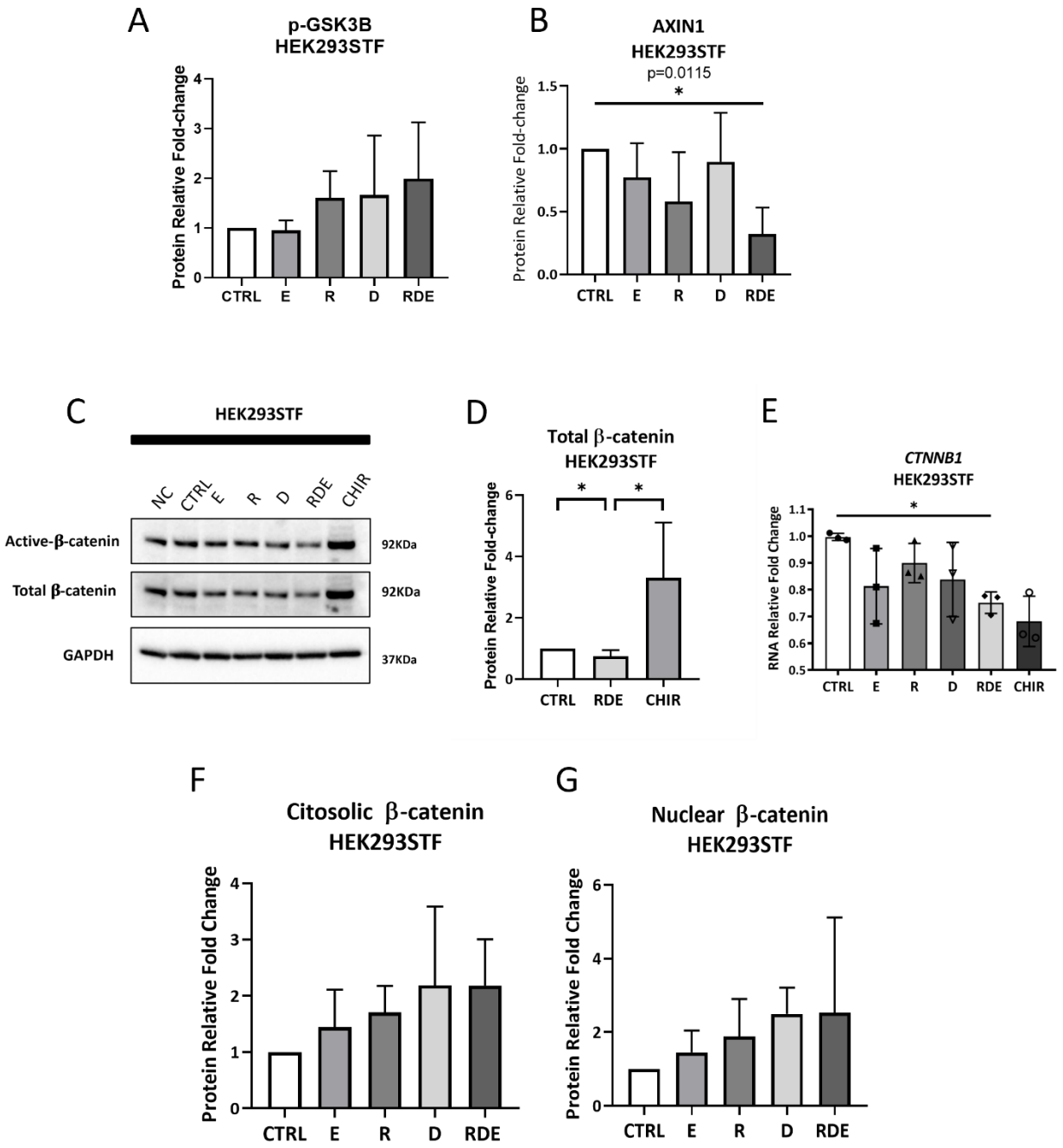

Figure 4.6. (A-B) Effect of RDE on GSK3β and AXIN1 protein expression in HEK293STF evaluated by Western Blot. P-GSK3β was normalized on the expression of total GSK3β protein; AXIN1 was normalized to GAPDH protein. **(C-D; F-G)** Effect of RDE on β-catenin protein expression in HEK293STF evaluated by Western-Blot. Non-phosphorylated (Active) β-catenin was normalized to total β-catenin protein; total and cytosolic β-catenin protein was normalized to GAPDH protein expression. Nuclear β-catenin protein was normalized to LAMINB1. **(E)** *CTNNB1* RNA expression assessed by qRT-PCR. GAPDH was use as reference gene. Proteins and RNA mean values relative fold changes were calculated using CTRL as reference sample. Data are expressed as means ± SD. Statistical significance was tested using unpaired T-test and One-Way ANOVA and the Dunnett's test for multiple comparisons vs CTRL. HEK293STF n = 3. NC = Negative Control; CTRL = Control with vehicles; E = EGCG;

R = Rapamycin; D = DHA; RDE = treatment; CHIR = Active-Wnt signalling positive control. *P<0.05; **P<0.010; ***P<0.001; ****P<0.0001. *P<0.05; **P<0.010; ***P<0.001; ****P<0.0001

Due to its key role in the regulation of the β-catenin protein into the canonical Wnt/β-catenin pathway, we started investigating the proteasome ubiquitination system to test this hypothesis. We treated HEK293STF with MG132 at 10 μM for 4 hours to inhibit the proteasomal degradation of ubiquitinated proteins and, as expected, we observed increased total β-catenin protein expression following the accumulation of phosphorylated β-catenin protein in MG132 treated samples compared to the non-treated ones. However, despite the proteasomal inhibition, we found that RDE still suppressed total β-catenin protein compared to the corresponding CTRL+MG132. Interestingly MG132 rescued AXIN1 protein in RDE treated cells compared to the non-MG132-treated ones, preventing its degradation also in CTRL+MG132 compared to CTRL (Fig.4.7), without impairing the phosphorylation of GSK3β (data not shown). Moreover, we found a significant induction of *c-MYC* expression in MG132-treated samples compared to the non-treated ones. Taken together these results suggested that the suppression of β-catenin protein was related to alternative mechanisms ad it was independent from AXIN1 and GSK3β protein dysregulation in the degradosome.

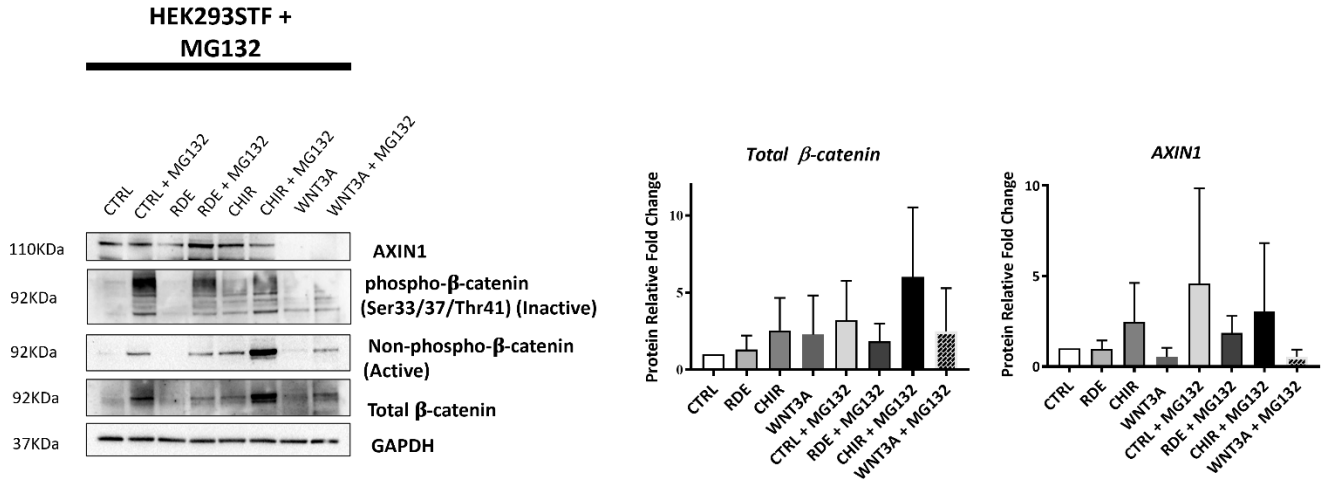

Figure 4.7. Effect of the proteasomal inhibition (MG132 10μM treatment) in HEK293STF. Evaluation of AXIN1 and β-catenin protein expression by Western-Blot. Phosphorylated (Inactive) and non-phosphorylated (Active) β-catenin were normalized to total β-catenin protein; total β-catenin and AXIN1 proteins were normalized to GAPDH protein. Proteins values relative fold changes were calculated using CTRL as reference sample. Data are expressed as means ± SD. Statistical significance was tested using unpaired T-test. HEK293STF n = 3. NC = Negative Control; CTRL = Control with vehicles; RDE = treatment; CHIR = Active-Wnt signalling positive control. WNT3A was used as exogenous signals to monitor Wnt signalling. *P<0.05; **P<0.010; ***P<0.001; ****P<0.0001.

Thus, we evaluated through qPCR the expression of *CTNNB1* gene, encoding β-catenin, and we found that RDE suppressed *CTNNB1* gene expression. Apparently, EGCG was mainly involved in this mechanism (Fig.4.6 E).

As a consequence of the reduction of the amount of total β-catenin, we found in RDE-treated HEK293STF a significant downregulation of *CCND1* gene expression (p=0.0047, T-test vs CTRL), compared to CTRL and *wild-type* organoids, but similar to organoids RDE still increased expression of *C-MYC* gene (p=0.0138, T-test vs CTRL). These evidence suggested that the RDE-dependent induction of *C-MYC* gene may not be directly related to the amount of β-catenin.

In addition, similar to NM organoids, CHIR did not impair AXIN1 protein level (Fig.4.6 C), and, despite the downregulation of *CTNNB1* gene expression, increased phosphorylated (Ser33/37/Thr41), active-, and total-β-catenin compared to RDE (p=0.0308, T-test CHIR vs RDE) (Fig.4.6 C-G). Indeed, we observed a higher accumulation of both cytoplasmic and nuclear β-catenin as well as induction of *AXIN2* (p=0.0041, T-test RDE vs CHIR) and *CCND1* gene transcription (p=0.0018, T-test RDE vs CHIR), compared to RDE, confirming a more post-translational regulation and induction of the pathway dependent on the inhibition of GSK3β.

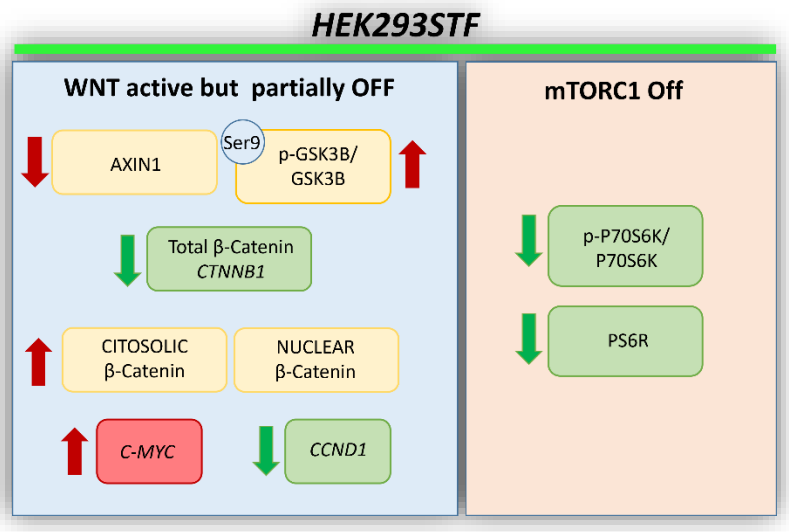

Figure 4.8. Summary of the effect of RDE on the Wnt/β-catenin and mTORC1 pathway in the wild-type cell line HEK293STF.

4.2.3 In FAP NM and ADENOMAS APC-mutated organoids RDE induces hyperactivation of Wnt/β-catenin pathway

FAP-NM organoids carried a single-hit-germline-mutations in the *APC* gene and FAP-ADENOMAS (A) organoids were characterized by the occurrence of somatic *APC* mutations, thus representing important genetic settings to investigate the role of the *APC* gene dysregulation in influencing the ability of RDE to target the Wnt/β-catenin pathway.

In FAP-NM and -A organoids, we found that RDE regulated the Wnt/β-catenin pathway similar to FIT+ and CRC-NM organoids, enhancing GSK3β inhibition ($p=0.0126$, T-test vs CTRL) (Fig.4.9 A), β-catenin stabilization (Fig.4.9 B), and the expression of *AXIN2* ($p=0.0044$, T-test vs CTRL), *CCND1* ($p=0.0044$, T-test vs CTRL) and *C-MYC* ($p=0.0093$, T-test vs CTRL) genes compared to CTRL (Fig.4.9 C-D). The hyperactivation of the Wnt/β-catenin pathway was found to be more significant in FAP-A organoids, which showed a significant accumulation of total β-catenin ($p=0.0086$, T-test vs CTRL) and increased expression of *CCND1* ($p<0.0001$, T-test vs CTRL) and *C-MYC* compared to CTRL ($p=0.0004$, T-test vs CTRL) (Fig.4.9 C-D), resulting from the APC protein inactivation and the basal higher activation of the pathway compared to the corresponding NM or the *wild-type* organoids. Despite the inactivation of GSK3β and the partial or complete dysregulation of APC protein function due to mutations, we also observed a contrasting increase in AXIN1 protein expression ($p=0.0328$, T-test vs CTRL).

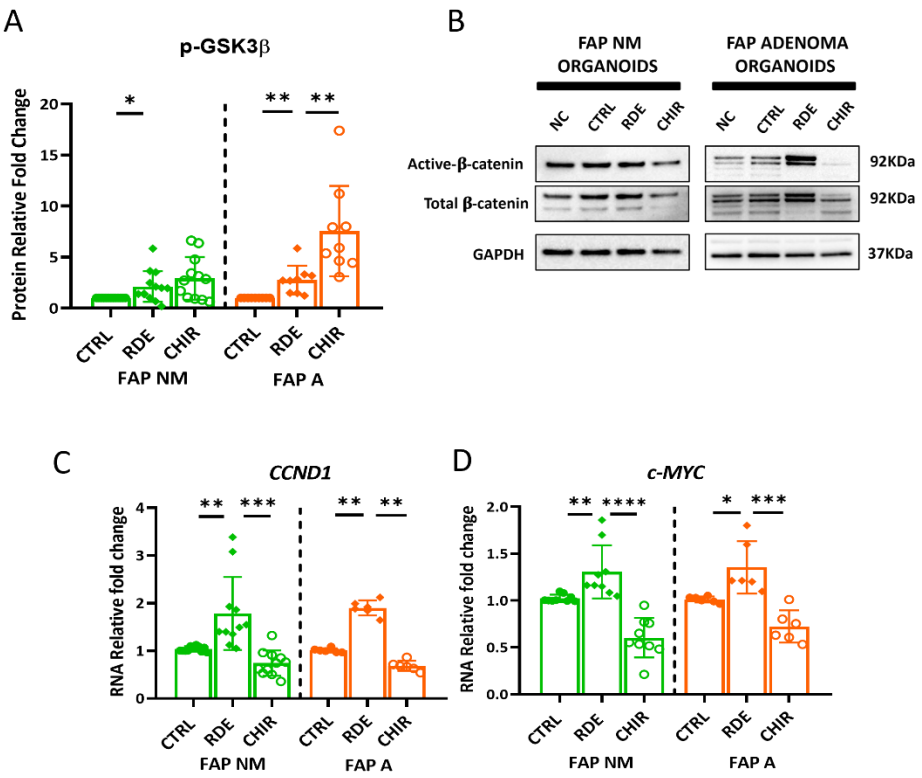

Figure 4.9. (A-B) Effect of RDE on GSK3β and β-catenin protein expression in FAP NM and FAP ADENOMA (A) intestinal organoids evaluated by Western-Blot. p-GSK3β was normalized on the expression of total GSK3β protein; non-phosphorylated (Active) β-catenin was normalized to total β-catenin protein; total β-catenin protein was normalized to GAPDH protein. **(C-D)** Effect of RDE on *CCND1* and *c-MYC* mRNA expression assessed by qRT-PCR. *CCND1* and *c-MYC* mRNA expression was normalized to GAPDH mRNA expression. Proteins and RNA mean values relative fold changes were calculated using CTRL as reference sample. Data are expressed as means ± SD. Statistical significance was tested using unpaired T-test. FAP NM n=10; FAP A n=9. NC = Negative Control; CTRL = Control with vehicles; RDE = treatment; CHIR = Active-Wnt signalling positive control. *P<0.05; **P<0.010; ***P<0.001; ****P<0.0001

In addition, it is to note that FAP organoids carried different germline mutation in the *APC* gene and, among all the organoids selected, two patients (FAP04 and FAP09) had a milder form of the syndrome referred to as attenuated FAP (AFAP). Interestingly, among all FAP organoids, in FAP03, RDE displayed a distinctive modulation in both NM and ADENOMAS with increased RNA expression of *AXIN2*, *CCND1* and *C-MYC*, but suppressed AXIN1 and total β-catenin protein expression (Fig.4.10 A-D).

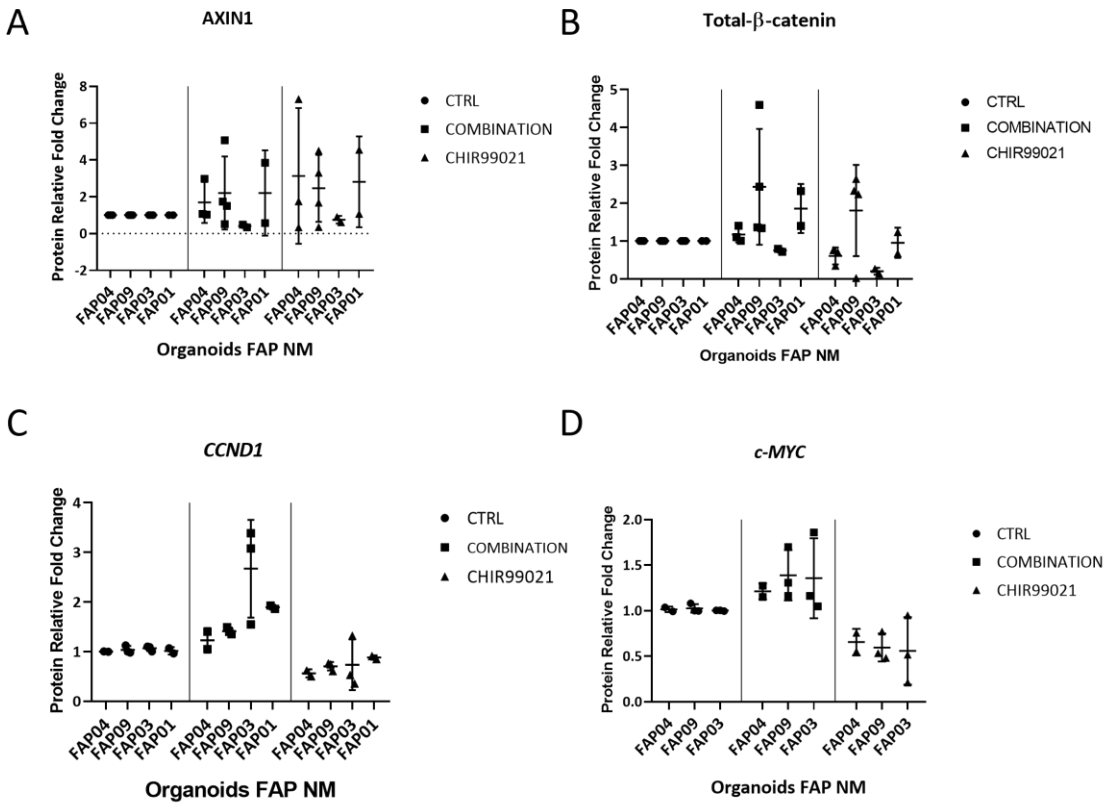

Figure 4.10. Graphical representation of how different germline-mutations of *APC* in FAP patients influence the response to RDE. **(A-B)** Western-Blot analysis of AXIN1 and β-catenin protein expression. AXIN1 and total β-catenin protein were normalized to GAPDH protein. **(C-D)** Effect on *CCND1* and *c-MYC* mRNA expression assessed by qRT-PCR. *CCND1* and *c-MYC* mRNA expression was normalized to GAPDH mRNA expression. Proteins and RNA mean values relative fold changes were calculated using CTRL as reference sample. Data are expressed as means ± SD. Statistical significance was tested using unpaired T-test. FAP01 n=2; FAP03 n=3; FAP04 n=3; FAP09 n=3. NC = Negative Control; CTRL = Control with vehicles; RDE = treatment; CHIR = Active-Wnt signalling positive control.

FAP03 organoids were the only carrying a non-sense germline mutation in the *APC* gene (c.847C>T (p.R283X)) compared to the other FAP organoids tissues carrying frameshift mutations. We tried to established organoids from other FAP tissues with non-sense mutations but after few passages the organoids started to die (data not shown). Thus, we hypothesized that the location and significance of the germline mutation is relevant to influence the response to RDE.

However, this feature appeared less important in influencing Wnt/β-catenin after CHIR treatment and despite a higher inactivation of GSK3β (p=0.0068, T-test RDE vs CHIR) we found that CHIR significantly downregulated the total-β-catenin compared to RDE (p=0.0009, T-test RDE vs CHIR), suppressing *CCND1* (p<0.0001, T-test RDE vs CHIR) and *C-MYC* gene transcription (p<0.0001, T-test RDE vs CHIR) in

all FAP-A organoids and in most of the FAP-NM organoids (Fig.4.9 A-D). The only exception was represented by FAP09-NM organoids, which nevertheless shared the same germline mutation with FAP04-NM organoids.

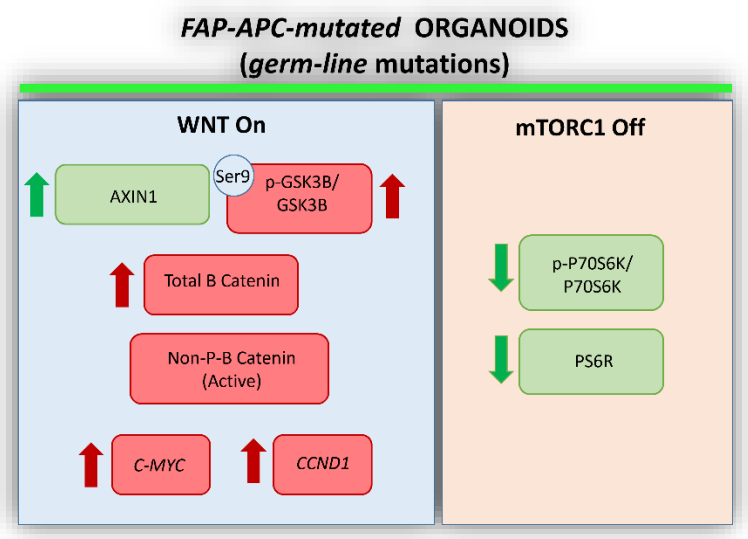

Figure 4.11. Summary of the effect of RDE on the Wnt/β-catenin and mTORC1 pathway in the *APC*-mutated pre-cancerous organoids FAP-NM and FAP-A.

4.2.4 RDE downregulated Wnt/β-catenin pathway in APC-mutated CRC-Cancer organoids and CRC cells.

Considering the effects of RDE in the *APC*-mutated FAP organoids, we further explored the treatment in *APC*-mutated CRC cancer (K) organoids. As previously described, we treated organoids derived from two different cancer tissues (PT13CRC-K and PT16CRC-K) with additional mutations in *TP53* and/or *PI3K* gene. Compared to CTRL, we found that RDE in CRC-K organoids increased the phosphorylation of GSK3β protein (p=ns, T-test vs CTRL) and *C-MYC* RNA expression (p=0.0087, T-test vs CTRL) as for FAP and *wild-type* settings, but downregulated AXIN1 protein (p=ns, T-test vs CTRL) (Fig.4.12 A-B). We expected a more severe upregulation of Wnt/β-catenin pathway, in contrast we found that the total β-catenin was downregulated compared to CTRL (p=ns, T-test vs CTRL) (Fig.4.12 C).

To further investigate the effects of RDE in CRC *APC*-driven tumoral settings, we selected the cell lines SW480 and HT-29, characterized by *TP53* and/or *PI3K* gene mutations too. Also in these models we found that RDE contributed to AXIN1 downregulation (p=ns, T-test vs CTRL) (Fig.4.12 B) and total β-catenin protein expression was suppressed too (SW480, p=0.0048, T-test vs CTRL; HT-29, p=ns, T-test vs CTRL) (Fig.4.12 C), with a significant decrease in nuclear β-catenin compared to CTRL (SW480, p=0.0253, T-test vs CTRL; HT-29, p=0.0002, T-test vs CTRL) (Fig.4.12 D). However, compared to HEK293STF, *CTNNB1* gene expression was barely involved, suggesting the occurrence of a more post-translation modulation in these mutated genetic backgrounds. Thus, we hypothesized that also in these genetic backgrounds RDE contributed to enhance alternative mechanisms involved in β-catenin degradation. As a result of degraded β-catenin, we found that *CCND1* gene expression was downregulated compared to CTRL, however we observed *c-MYC* RNA expression increased, as for the *wild-type*, FAP, and CRC-K organoids, suggesting a direct involvement of *C-MYC* gene transcript in mediating the response to RDE (SW480, p=ns, T-test vs CTRL; HT-29, p=0.0147, T-test vs CTRL). Indeed, we tried to evaluated the protein expression of this marker, but any significant variations had been detected (data not shown).

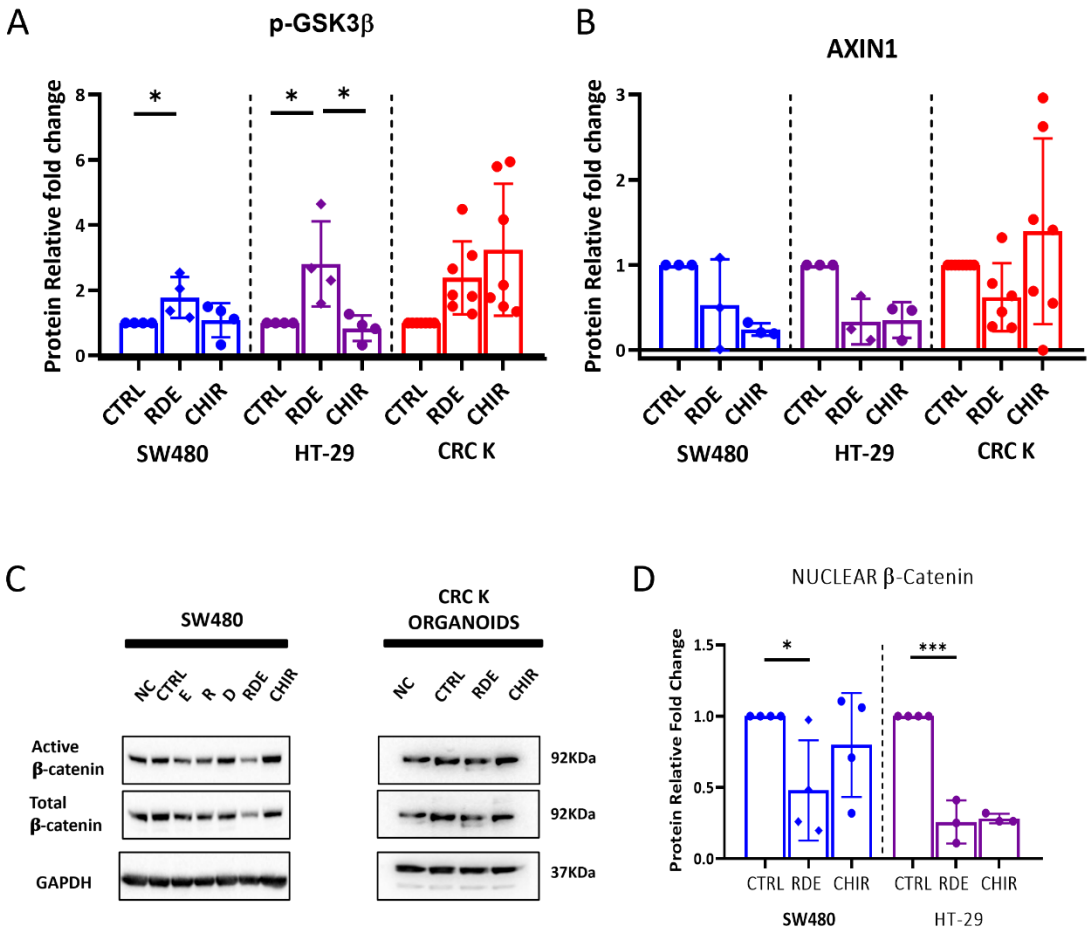

Figure 4.12. (A-D) Effect of RDE on AXIN1, GSK3β and β-catenin protein expression in CRC K organoids, SW480 and HT-29 cell lines evaluated by Western-Blot. P-GSK3β was normalized on the expression of total GSK3β protein; non-phosphorylated (Active) β-catenin was normalized to total β-catenin protein; AXIN1 and total β-catenin protein were normalized to GAPDH protein. Nuclear β-catenin was normalized to LAMINB1. Proteins mean values relative fold changes were calculated using CTRL as reference sample. Data are expressed as means ± SD. Statistical significance was tested using unpaired T-test. CRC K organoids n=6; SW480=4; HT-29=4. NC = Negative Control; CTRL = Control with vehicles; RDE = treatment; CHIR = Active-Wnt signalling positive control.

Importantly, RDE showed a stronger effect compared to the single compounds, suggesting a synergic reaction between Rapamycin, DHA and EGCG which contributed to the inhibition of the Wnt/β-catenin pathway. Since both SW480 and HT-29 carry also *KRAS* (G12D) and *BRAF* (V600E) mutations, respectively, these results suggested that RDE by activating the Wnt/β-catenin signaling succeeded in inhibiting more both the pathway in cancer settings when *APC*-mutated tumors had acquired additional mutations in genes involved in the regulation of the PI3K/mTOR pathway and *TP53*.

Conversely, CHIR showed less effectiveness in inhibiting the Wnt/β-catenin pathway and showed a huge variation among the CRC cells and CRC K-organoids, suggesting that targeting GSK3β was not sufficient to stably hyperactivate the signaling and enhance β-catenin degrading mechanism in the presence of additional mutations that influenced the PI3K/mTOR pathway.

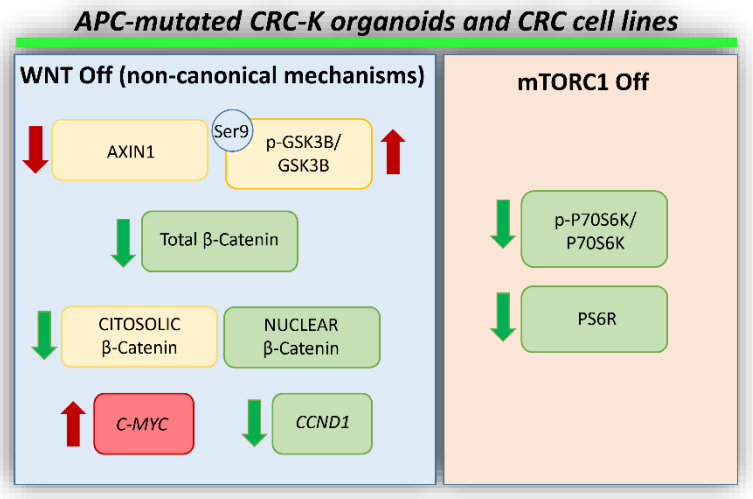

Figure 4.13. Summary of the effect of RDE on the Wnt/β-catenin and mTORC1 pathway in the *APC*-mutated CRC-K organoids, and *APC*-mutated CRC cell lines SW480 and HT-29.

4.2.5 RDE suppressed β-catenin protein expression and downregulated Wnt/β-catenin pathway in the non-APC-mutated HCT116 cell line.

To better investigate the relevance of *APC* mutations in mediating the suppression of β-catenin protein by RDE, we selected HCT116 CRC cell line. This CRC model is characterized by *PI3K* and *KRAS* mutations and β-catenin is constitutively activated due to a mutation in the β-catenin allele in exon 3 that deletes the GSK3β phosphorylation site, leading to the accumulation of Non-phosphorylated-(Active)-β-catenin in the cytoplasm and its nuclear translocation. Despite this characteristic, compared to CTRL we found that RDE significantly suppressed β-catenin protein expression ($p<0.001$, T-Test vs CTRL) and its nuclear translocation, without affecting *CTNNB1* gene transcription, as previously described for SW480 and HT-29 cells (Fig.4.14 C-E), supporting the hypothesis of a post-translational regulation of the pathway independent from the degradosome and *APC*-mutations. Interestingly, among all the settings analysed, in HCT116 RDE resulted less effective in enhancing p-GSK3β (Fig.4.14 A) or *c-MYC,* which exhibited a very modest increase compared to CTRL. The trend of these two markers induced by RDE was found to be consistent among the different genetic settings, including the non-mutated ones, thus we excluded the involvement of *CTNNB1* mutation in leading this attenuated response. HCT116 among the selected cells represent the only model with microsatellite instability (MSI), thus we speculated that this genetic feature could be responsible for these distinctive outcomes.

In contrast, the *CTNNB1* mutation seemed to impact the ability of CHIR to inhibit GSK3β compared to RDE ($p<0.0001$, T-Test RDE vs CHIR) and we observed accumulation of total- β-catenin ($p=0.0038$, T-Test RDE vs CHIR) and active Wnt/β-catenin signalling (Fig.4.14 A,C,D). However this seemed not to be enough to activate the same alternative mechanism enhanced by RDE or in FAP-A organoids.

Thus these results showed the RDE-effectiveness in inhibiting both the pathway resulted from the synergic action of all the three compounds, as for SW480 and HT-29.

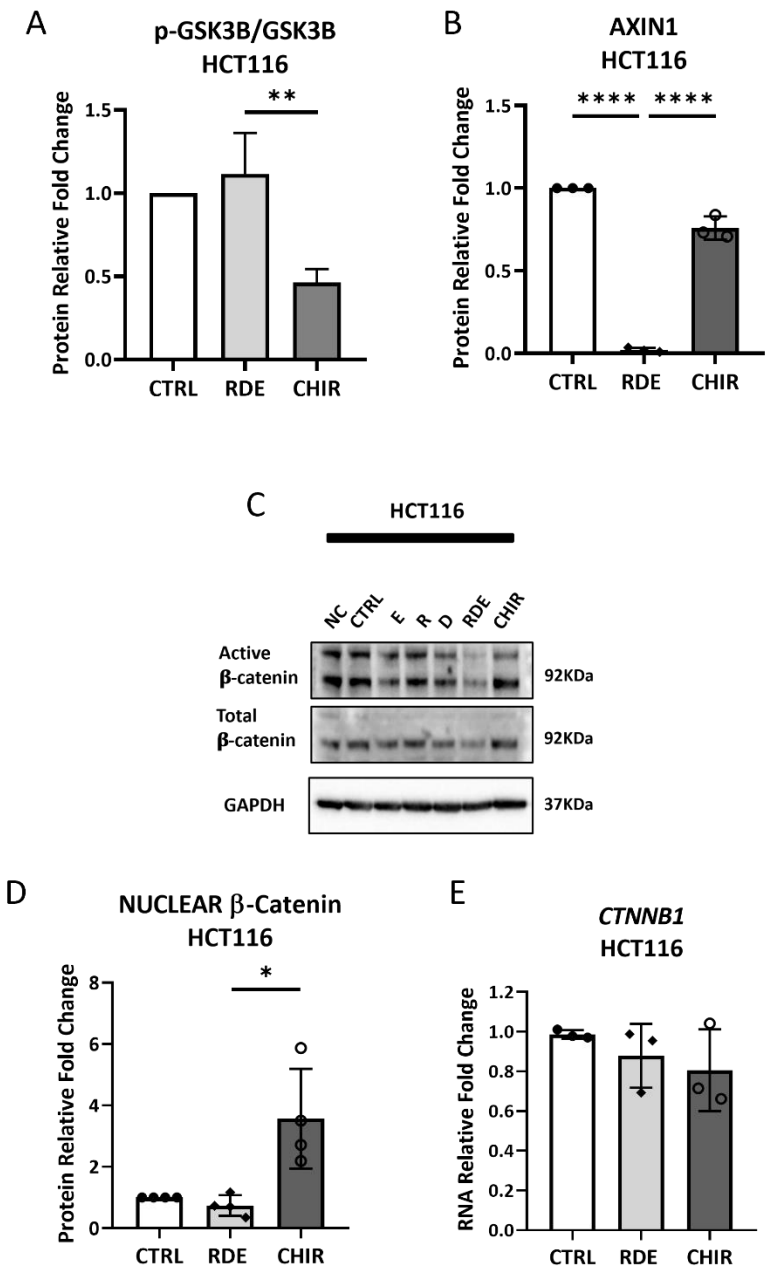

Figure 4.14. (A-D) Effect of RDE on GSK3β, AXIN1 and β-catenin protein expression in HCT116 cells by Western-Blot. P-GSK3β was normalized on the expression of total GSK3β protein; non-phosphorylated (Active) β-catenin was normalized to total β-catenin protein; AXIN1 and total β-catenin protein were normalized to GAPDH protein. Nuclear β-catenin protein was normalized to LAMINB1. **(E)** Effect of RDE on *CTNNB1* mRNA expression assessed by qRT-PCR. *CTNNB1* mRNA expression was normalized to GAPDH mRNA expression. Proteins and RNA mean values relative fold changes were calculated using CTRL as reference sample. Data are expressed as means ± SD. Statistical significance was tested using unpaired T-test. HCT116 n=4. Negative Control; CTRL = Control with vehicles; RDE = treatment; CHIR = Active-Wnt signalling positive control.

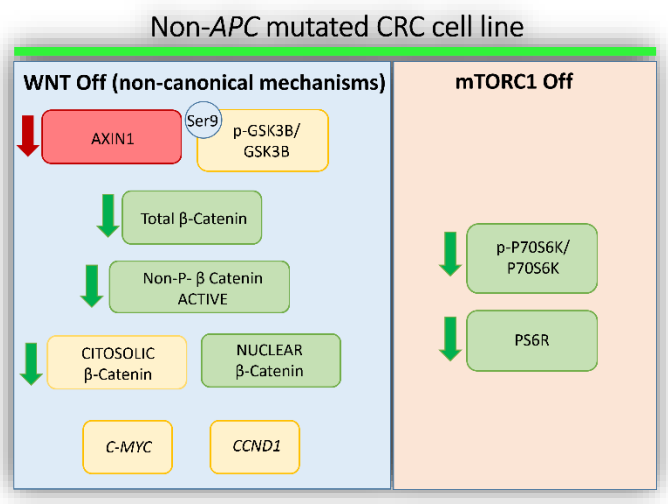

Figure 4.15. Summary of the effect of RDE on the Wnt/β-catenin and mTORC1 pathway in the Non-*APC*-mutated CRC cell lines HCT116.

4.3 RDE affected stemness, differentiation and cell viability

4.3.1 RDE suppressed LGR5 expression and induced differentiation in organoids.

We treated the organoids in a growing phase and with small dimension to better understand the influence of RDE in growing tissues. Under this conditions neither CTRL nor non-treated organoids (NC) were found to develop budding, due to the short experimental timing. After 48 hours of treatment RDE mediated the downregulation of organoids viability approximately 20% and CRC-K organoids were the more sensitive to the treatment compared to CTRL (Fig.4.16 A-B). Considering that most of the organoids treated were normal tissue-derived, a suppression in cell viability of around 20% appeared as non-cytotoxic and safe. However, we also observed a significant suppression in *LGR5* gene expression, even in organoids with increased Wnt/β-catenin signaling activation. Suppression of *LGR5* was followed by an increase in *KRT20* gene expression, suggesting a reduction in stemness in favour of a shift toward tissue differentiation compared to both CTRL and CHIR ($p<0.0001$, T-test RDE vs CHIR) (Fig.4.16 C-D). The latter, showed an opposite trend and despite the activation or inhibition of Wnt/β-catenin significantly increased *LGR5* and suppressed *KRT20* gene expression, suggesting the occurrence of a more direct regulation between GSK3β and *LGR5*.

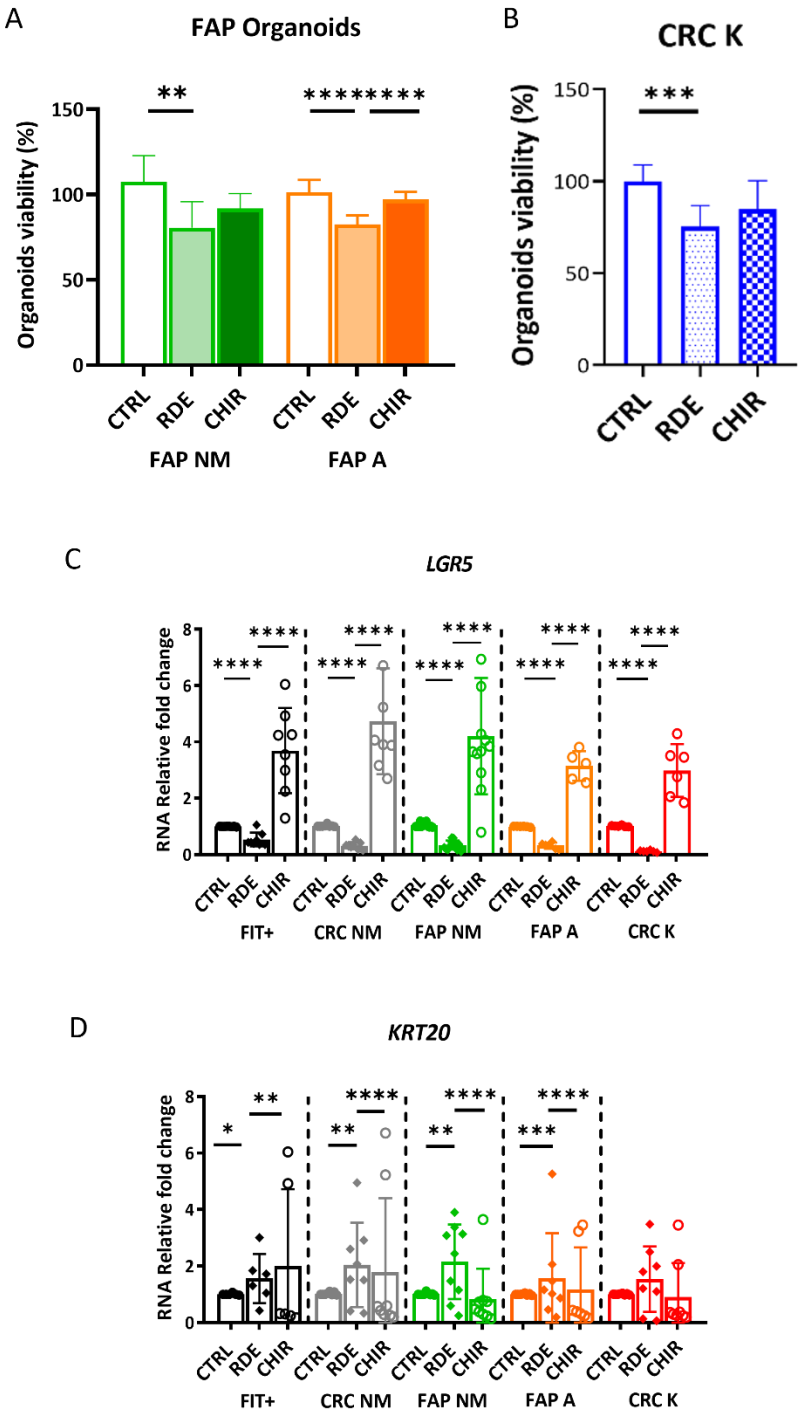

Figure 4.16. (A-B) Effect of RDE on organoids viability. **(C-D)** Effect of RDE on *LGR5* and *KRT20* mRNA expression assessed by qRT-PCR. *LGR5* and *KRT20* mRNA expression was normalized to GAPDH mRNA expression. Proteins and RNA mean values relative fold changes were calculated using CTRL as reference sample. Data are expressed as means ± SD. Statistical significance was tested using unpaired T-test. NC = Negative Control; CTRL = Control with vehicles; RDE = treatment; CHIR = Active-Wnt signalling positive control. Relative fold changes were calculated using CTRL as reference sample. Data are expressed as means ± SD. Statistical significance was

tested using unpaired T-test. FIT+NM n=6; CRC NM=6. FAP NM=9; FAP A = 6 CRCK=6. Negative Control; CTRL = Control with vehicles; RDE = treatment; CHIR = Active-Wnt signalling positive control.

4.3.2 RDE suppressed LGR5 gene expression and activated HCT116 cell apoptosis with a mechanism independent of Caspase 3/7 activation.

We confirmed that after 24 hours RDE targeted *LGR5* expression also in cell lines and resulted more significant in HE293STF and in HCT116 ($p<0.0001$, T-test RDE vs CHIR). We found that Rapamycin drove the inhibition of *LGR5* in RDE-treated HEK293STF; meanwhile, in HCT116, all the three compounds co-participated synergically in the final effects of RDE. Interestingly, in *APC*-mutated cell lines DHA was the main leader in suppressing *LGR5* expression. This results suggested a slightly involvement of Wnt/β-catenin signaling in the significant suppression of *LGR5*, since it didn't recapitulate the expression of the β-catenin protein and its translocation.

In all cell lines models we observed a co-suppression of both Wnt/β-catenin and PI3K/mTOR pathways, but we found reduced 50% cell viability only in HCT116. *APC*-mutated CRC cells HT-29 and SW480 were barely influenced, with a reduction in cell viability around 20% and 15% respectively as for *APC*-mutated CRC-K organoids (Fig.4.17 A).

Thereafter, we tested HCT116 for apoptosis by staining the cleaved (active) PARP by Western-Blot analysis, but we did not detect any protein expression. However, we found a significant decrease in SURVIVIN protein, an antiapoptotic factor and cell cycle regulator (Fig.4.12 B). We co-stained cells with Incucyte® Caspase-3/7 Dye and Incucyte® Annexin V Dye and we monitored cells for 36 hours. We found that RDE induced apoptosis after 3 hours of treatment with a mechanism independent from Caspase 3/7 activation. EGCG was the only compound that drove this mechanism, and neither Rapamycin nor DHA was found to activate apoptosis (Fig.4.17 B).

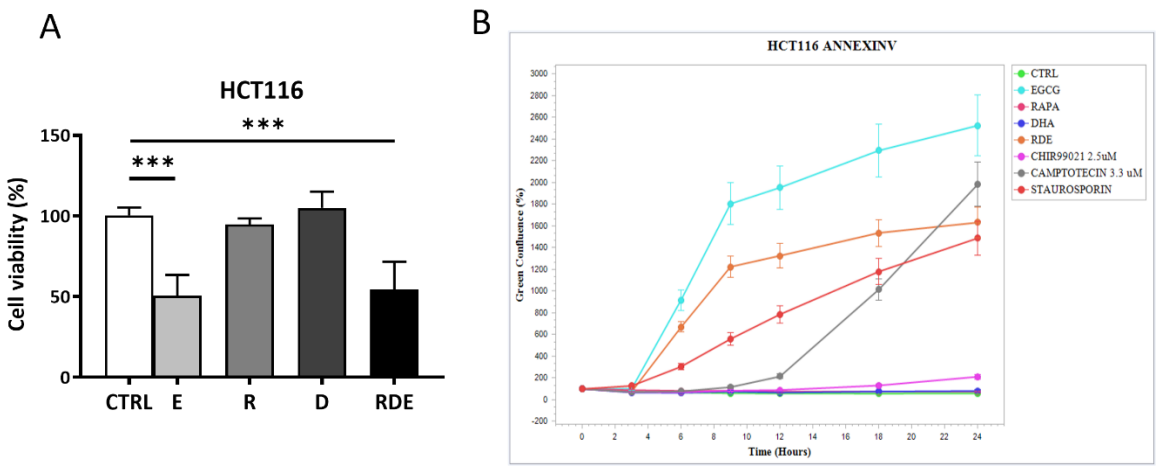

Figure 4.17. (A-B) Effect of RDE on HCT116 cell viability and Apoptosis. Mean values relative fold changes were calculated using CTRL as reference sample. Data are expressed as means ± SD. Statistical significance was tested using unpaired T-test and One-Way ANOVA Dunnett's test for multiple comparison vs CTRL. HCT116 = 3. NC = Negative Control; CTRL = Control with vehicles; RDE = treatment; CHIR = Active-Wnt signalling positive control. E = EGCG, R = Rapamycin; D = DHA.

5. Discussion and Conclusions

The primary endpoint of this study was to investigate how a combination (RDE) of Rapamycin, ω3-PUFA Docosahexaenoic Acid (DHA) and EGCG influences the activation of Wnt/β-catenin and PI3K/mTOR pathways. After analyzing several different genetic backgrounds, we dissected new insights into the cross-talk between the two pathways.

In the healthy intestinal background constituted by FIT+-NM organoids we could delve into the mechanisms of RDE treatment in the absence of aberrations involving the two pathways. Here, we found that 48h-RDE significantly inhibited the PI3K/mTORC1 pathway by suppressing the activation of mTOR (data not shown) and its final effectors p70S6K and S6R. Concomitantly with the suppression of the PI3K/mTORC1 pathway, we found induced activation of the Wnt/β-catenin pathway. Indeed, we reported a significant increase in active-non-phosphorylated and total-β-catenin expression that enhanced the expression of *AXIN2*, *CCND1* and *C-MYC* target genes. In accordance with common literature, upon Wnt/β-catenin pathway induction, we also found a significant inhibition of GSK3β with increased phosphorylation in Ser9, together with a (non-significant) slight decrease of AXIN1. We hypothesized that variations in AXIN1 expression levels across organoids and experiments were indicative of a partial inhibition of its binding into the degradosome complex, and that 48 hours treatment were not sufficient to completely inactivate the functionality of the degradosome, leading to a significant decrease shared between all patient-derived organoids tested. Due to the limited quantity of proteins available, we were not able to perform co-precipitation assays to confirm this information and clarify the integrity and interaction of the proteins into the degradosome. However, to partially analyze this mechanism, we tested RDE for 96 hours in FIT13+-NM organoids and we found a stronger suppression of both GSK3β and AXIN1 compared to CTRL (data not shown). Therefore, these results can preliminarily support our hypothesis and the previously reported findings about a time-dependent degradation of the AXIN1 scaffold protein upon Wnt/β-catenin pathway activation. Indeed, after the signaling activation, the ubiquitination of phosphorylated β-catenin has been reported to be initially blocked within an intact complex, leading to the saturation of the degradosome. As a results, newly synthesized non-phosphorylated β-catenin accumulates into the cytosol and subsequently translocate into the nucleus where activates the Wnt/β-catenin pathway target genes (Li V.S. et al., 2012; Azzolin L. et al., 2014).

In this study we found that, similar to FIT+ NM-organoids and despite the single-hit germline mutation in *APC* gene, in FAP NM-organoids RDE enhanced the activation of the Wnt/β-catenin pathway, leading to the accumulation of active-non-phosphorylated β-catenin and AXIN1 proteins. On one hand, these evidence confirmed that inactivating mutations in only one allele of *APC* gene are not sufficient to significantly impair the Wnt/β-catenin pathway. As a result, response of these tissues to treatments that alters the Wnt/β-catenin pathway can be compared in most of the cases to that of healthy ones. This is also true for NM in the proximity of sporadic CRC (5cm) tissues, that showed a basal enhanced transcriptional activation of the pathway resulting from stimuli released by surrounding cancer tissue. On the other hand, this data confirmed the detectability of the phenomenon of the saturation of the degradosome upon Wnt/β-catenin signaling induction in normal-like intestinal organoids. Although, Li et al. reported this phenomenon as a feature of CRC settings that exhibit mutations in Wnt/β-catenin signaling components (Li V.S. et al., 2012). This can partially explain why, upon RDE treatment, we found in FAP Adenomas-organoids a higher and significant accumulation of both β-catenin and AXIN1 proteins compared to NM-organoids, as a result of the complete inactivation of the *APC* gene. However, the location and the significance of the mutations along the *APC* gene have been associated to distinctive Wnt/β-catenin pathway activation statuses and tumor features (Christie M. et al, 2013). Through this study we confirmed that *APC* germline mutation can also influence the responses to treatments that trigger the Wnt/β-catenin signaling activation.

Moreover, opposed to the findings detailed above by Li et al., upon RDE treatment we found in all the CRC cell lines and CRC-K organoids in an *APC*-independent manner a downregulation of AXIN1 protein expression, together with suppression of β-catenin protein in both nuclear and cytoplasmatic compartments. Thus, we hypothesized that the hyperactivation of the Wnt/β-catenin signaling induced by RDE in Wnt-deranged settings lead to the occurrence of alternative post-translational mechanisms involved in the β-catenin degradation to counteract the toxicity of a Wnt/β-catenin signaling overactivation.

Through the analysis of the single compounds that composed RDE, we found that EGCG together with DHA were mainly involved in the modulation of components of the degradosome and in their protein expression. Oh S. et al. proposed a mechanism in which EGCG promoted the degradation of the β-catenin by inducing its phosphorylation at Ser33/37 residues through a mechanism independent of

GSK-3β and PP2A (protein phosphatase 2A). This mechanism has been reported as activated in SW480 CRC cell lines and promotes β-catenin degradation, resulting in anti-proliferative activity against SW480 CRC cells. Through our experiments, we confirmed this EGCG-driven effect in SW480 cell line. However, it resulted mostly true referred to EGCG as a single treatment, but not in combination with the other compounds that composed RDE. Indeed, Rapamycin and DHA probably interfere with the regulation of EGCG by activating further mechanisms that however supported an effective dowregulation of the Wnt signalling. Moreover, in the same work, Oh S. et al. reported that EGCG, in HEK293, attenuates Wnt/β-catenin signaling by decreasing the β-catenin protein level rather than by affecting its gene expression. By contrast, in the non-intestinal *wild-type* model HEK293, we found that RDE downregulated total β-catenin by directly suppressing *CTNNB1* gene expression in an EGCG-dependent manner. Among the regulatory mechanisms proposed for EGCG and involving the Wnt/β-catenin pathway, we firstly reported within this study a direct inhibition of the *CTNNB1* gene expression, thus identifying EGCG as a transcriptional regulator of β-catenin. Furthermore, Oh S. et al. described HCT116 as resistant to the mechanism. Nevertheless, in the present study we found a strong suppression of β-catenin protein driven by EGCG, both as single treatment and in combination, resulting in significant anti-proliferative and cytotoxic activities against HCT116.

We therefore hypothesized that RDE enhanced alternative non-canonical mechanisms involved in the β-catenin degradation. Among these we found Nur77 and Mule as potential candidate. Nur77 (also known as TR3 or NGFI-B), an orphan member of the nuclear receptor superfamily and an immediate early response gene, has been described to regulate cancer cell growth and survival, differentiation and apoptosis in response to a variety of stimuli such as growth factors, inflammatory stimuli, cytokines, peptide hormones, and cellular stress (Safe S. et al., 2008; Zhao Y. and Bruemmer D., 2010). Interestingly, Sun Z. et al. reported that cytoplasmic Nur77 inhibits the transcriptional activity of β-catenin on *CCND1* expression by enhancing β-catenin degradation via a GSK3β-independent mechanism that involved the proteasomal pathway. They described the effectiveness of Nur77 in suppressing β-catenin in both HCT116 and SW620, thus indicating that the regulation of Nur77 was not strictly linked to an *APC*-mutated setting. In addition, several studies provided insight into Nur77 extranuclear regulatory functions, and in particular Wilson A.J. et al. demonstrated in HCT116 that Nur77, in response to pro-apoptotic agents, interacts with the member of the Bcl-2 proapoptotic factors BAX, triggering the cytochrome c release from mitochondria and enhancing cellular apoptosis

(Wilson A.J. et al., 2003). Hence, these results have led to the speculation that RDE and EGCG functioned as pro-apoptotic factors that triggered this system in HCT116, consequently explaining their anti-proliferative and the higher cytotoxic activities in this CRC setting.

Conversely, Mule (Huwe1/Arf-BP1) is a E3 Ubiquitine ligase that in intestinal tissues is involved in the regulation of Wnt/β-catenin signaling. Mule has been described to modulate several component directly or indirectly related to the pathway, influencing the intestinal stem cell compartment. Dominguez-Brauer et al. demonstrated that Mule controls the gradient of receptor tyrosine kinase EphB3 proteins by enhancing their proteasomal and lysosomal degradation (Dominguenz-Brauer C. et al., 2016). In another study, de Groot R.E. et al reported the existence of a negative feedback loop that lead to a Mule-dependent ubiquitination of Dvl in a Wnt ligand-dependent manner. More importantly, in a recent work, Dominguez-Brauer et al. described a direct interaction between Mule and β-catenin which is responsible for the protein degradation under conditions of hyperactive Wnt/β-catenin pathway in a phosphorylation-independent manner. Indeed, they demonstrated *in-vitro* (including in the HCT116 cell line) and *in-vivo* that loss of Mule in deranged Wnt/β-catenin signalling activation leaded to increased β-catenin protein accumulation, promoting CRC tumour onset and progression (Dominguenz-Brauer C. et al., 2017). As a consequence, loss of Mule has been also associated to an increased in *LGR5* expression. Therefore, according to this model, we hypothesized that in CRC settings, RDE leads to the activation of Mule as a results of its activating modulatory effect on the Wnt/β-catenin signaling.

Further, an interaction between c-Myc and Mule has been described. Indeed c-Myc is a direct substrate of Mule, which mediates its degradation. Loss of Mule has been associated to c-Myc up-regulation at both transcriptional and protein level in a Wnt-activation-independent manner (Dominguenz-Brauer C. et al., 2016). This appears in contrast to our findings that demonstrated a transcriptional up-regulation of *c-MYC* induced by RDE in a mutated-independent manner. Thus, the effect on c-MYC transcriptional levels appears not related to a potential induction of Mule activation by RDE.

Indeed, we speculated that *c-MYC* was activated as a feed-back mechanism to sustain cell proliferation and counteract the effects of RDE on cell viability. Indeed, in HCT116, *c-MYC* expression was not up-regulated and in this model RDE induced 50% reduction in cell viability. Moreover, upon Wnt/β-catenin pathway activation, particularly in NM-organoids we expected an increase in cell

viability and proliferation. However, we found that RDE suppressed 22% cell viability. Indeed, this finding showed a relation with the mild activation of apoptotic mechanisms, which significantly induced ANNEXINV expression with a median fold of 1.2 compared to CTRL. Despite the upregulation of the Wnt/β-catenin pathway we also reported a significant inhibition in the gene expression of the intestinal marker *LGR5*, in favor of a slightly shift towards activation of the *KRT20* intestinal differentiation marker. We attributed these results to the mTOR inhibition. Therefore, we speculated that the RDE-induced activation of apoptosis occurs as a necessary strategy for healthy NM organoids to counteract the increased proliferative stimuli occurring in the stem cell niche, in a context of impaired metabolic functions resulting from mTOR inhibition. Thus, the inhibition of mechanisms like the protein synthesis cannot support the proliferative stimulus, leading to the partial suppression of the stem cell niche. Indeed, we found in the *wild-type* HEK293STF cells that Rapamycin as individual treatment led to a trend toward suppression of *LGR5* gene expression (mean fold 0.7, non-significant), along with a significant inhibition of cell viability (20%), despite limitations related to the model, which include the fact that HEK293 are a human embryonic kidney-derived model instead of an intestinal one. Importantly we found a significant inhibition of *LGR5* also in FAP-adenomas organoids and, even if less potent, in CRC settings. However, our findings about CHIR contrast with this theory. Indeed, we observed that CHIR 2.5µM, by selectively targeting GSKβ as part of its inhibitory pharmacological mechanism, activated the Wnt/β-catenin pathway and inhibited the PI3K/mTOR pathway similar to RDE and Rapamycin. Enhancement of Wnt/β-catenin signaling showed a more restrained activation compared to RDE, however CHIR sustained the transcriptional up-regulation of LGR5 and did not significantly affect cell viability. Thus, these results suggested that GSK3β more than other players may exert a central and direct role in regulating stemness and apoptosis in response to RDE, but it still to be clarified. LGR5 has been described as a controverse target, since its play an important role during CRC development or progression, but also its presence or ablation has been associated with long-term efficacy or failure of current chemotherapeutics. However, the inhibition of LGR5 in precancerous and cancerous lesions has demonstrated promising results in promoting the effectiveness of common target-therapies in resistant tissues.

The main limitations of the study include: (i) the use of commercial medium for intestinal organoids that does not provide a clear indication of its composition makes it difficult to understand whether there are other growth factors (e.g. EGF) that can influence the response to RDE activating or

inhibiting cross-talks with other pathways connected with the Wnt/β-catenin or PI3K/mTOR signaling; (ii) the limited material available for the development of intestinal organoids did not enable to clarify the contribution of the individual compounds in the final effect of RDE in 3D models. Further, the use of the 2D-cell line models to hypothesize the effect of the individual compounds limited the interpretation of the data, because 2D-cell line models lack more complex information relating to the spatial organization and/or the presence of the distinguished stem/differentiated compartments compared to intestinal organoids culture; (iii) the *wild-type* cell model HEK293STF, a non-colon cell line has proved not to be a good model for studying and comparing the effects of non-mutated models between 2D and 3D lines; (iv) most of the mechanisms hypothesized must be explored and investigated in depth.

In conclusion, with the combinatorial strategy of RDE we highlighted how the dual inhibition of Wnt/β-catenin and PI3K/mTOR is challenging and involved several different regulatory mechanisms in a Wnt-deregulated-dependent manner. However, our approach was found to be effective in CRC cell lines and CRC K- organoids through the activation of potential non-canonical mechanisms involved in the β-catenin regulation and degradation, contributing to the suppression of both the signaling. While in *APC*-mutated non-cancerous organoids (FAP adenomas) RDE affects markers of intestinal stemness and tissue differentiation, suggesting a potential therapeutic approach for both preventive and therapeutic strategies against CRC development and progression.

BIBLIOGRAPHY

Aberle H, Bauer A, Stappert J, Kispert A, Kemler R. beta-catenin is a target for the ubiquitin-proteasome pathway. EMBO J. 1997 Jul 1;16(13):3797-804. doi: 10.1093/emboj/16.13.3797. PMID: 9233789; PMCID: PMC1170003.

Aelvoet AS, Buttitta F, Ricciardiello L, Dekker E. Management of familial adenomatous polyposis and MUTYH-associated polyposis; new insights. Best Pract Res Clin Gastroenterol. 2022 Jun-Aug;58-59:101793. doi: 10.1016/j.bpg.2022.101793. Epub 2022 Mar 16. PMID: 35988966.

Alam M, Ali S, Ashraf GM, Bilgrami AL, Yadav DK, Hassan MI. Epigallocatechin 3-gallate: From green tea to cancer therapeutics. Food Chem. 2022 Jun 15;379:132135. doi: 10.1016/j.foodchem.2022.132135. Epub 2022 Jan 11. PMID: 35063850.

Albuquerque C, Breukel C, van der Luijt R, Fidalgo P, Lage P, Slors FJ, Leitão CN, Fodde R, Smits R. The 'just-right' signaling model: APC somatic mutations are selected based on a specific level of activation of the beta-catenin signaling cascade. Hum Mol Genet. 2002 Jun 15;11(13):1549-60. doi: 10.1093/hmg/11.13.1549. PMID: 12045208.

Alquati C, Prossomariti A, Piazzi G, Buttitta F, Bazzoli F, Laghi L, Ricciardiello L. Discovering the Mutational Profile of Early Colorectal Lesions: A Translational Impact. Cancers (Basel). 2021 Apr 25;13(9):2081. doi: 10.3390/cancers13092081. PMID: 33923068; PMCID: PMC8123354.

Arnold M, Abnet CC, Neale RE, Vignat J, Giovannucci EL, McGlynn KA, Bray F. Global Burden of 5 Major Types of Gastrointestinal Cancer. Gastroenterology. 2020 Jul;159(1):335-349.e15. doi: 10.1053/j.gastro.2020.02.068. Epub 2020 Apr 2. PMID: 32247694; PMCID: PMC8630546.

Aylett CH, Sauer E, Imseng S, Boehringer D, Hall MN, Ban N, Maier T. Architecture of human mTOR complex 1. Science. 2016 Jan 1;351(6268):48-52. doi: 10.1126/science.aaa3870. Epub 2015 Dec 17. PMID: 26678875.

Azzolin L, Panciera T, Soligo S, Enzo E, Bicciato S, Dupont S, Bresolin S, Frasson C, Basso G, Guzzardo V, Fassina A, Cordenonsi M, Piccolo S. YAP/TAZ incorporation in the β-catenin destruction complex orchestrates the Wnt response. Cell. 2014 Jul 3;158(1):157-70. doi: 10.1016/j.cell.2014.06.013. Epub 2014 Jun 26. PMID: 24976009.

Basu A, Haldar S. Combinatorial effect of epigallocatechin-3-gallate and TRAIL on pancreatic cancer cell death. Int J Oncol. 2009 Jan;34(1):281-6. PMID: 19082499.

Behrens J, von Kries JP, Kühl M, Bruhn L, Wedlich D, Grosschedl R, Birchmeier W. Functional interaction of beta-catenin with the transcription factor LEF-1. Nature. 1996 Aug 15;382(6592):638-42. doi: 10.1038/382638a0. PMID: 8757136.

Bernatoniene J, Kopustinskiene DM. The Role of Catechins in Cellular Responses to Oxidative Stress. Molecules. 2018 Apr 20;23(4):965. doi: 10.3390/molecules23040965. PMID: 29677167; PMCID: PMC6017297.

Bird RP. Observation and quantification of aberrant crypts in the murine colon treated with a colon carcinogen: preliminary findings. Cancer Lett. 1987 Oct 30;37(2):147-51. doi: 10.1016/0304-3835(87)90157-1. PMID: 3677050.

Boland CR, Thibodeau SN, Hamilton SR, Sidransky D, Eshleman JR, Burt RW, Meltzer SJ, Rodriguez-Bigas MA, Fodde R, Ranzani GN, Srivastava S. A National Cancer Institute Workshop on Microsatellite Instability for cancer detection and familial predisposition: development of international criteria for the determination of microsatellite instability in colorectal cancer. Cancer Res. 1998 Nov 15;58(22):5248-57. PMID: 9823339.

Boland CR, Goel A. Microsatellite instability in colorectal cancer. Gastroenterology. 2010 Jun;138(6):2073-2087.e3. doi: 10.1053/j.gastro.2009.12.064. PMID: 20420947; PMCID: PMC3037515.

Boparai KS, Dekker E, Van Eeden S, Polak MM, Bartelsman JF, Mathus-Vliegen EM, Keller JJ, van Noesel CJ. Hyperplastic polyps and sessile serrated adenomas as a phenotypic expression of MYH-associated polyposis. Gastroenterology. 2008 Dec;135(6):2014-8. doi: 10.1053/j.gastro.2008.09.020. Epub 2008 Sep 20. PMID: 19013464.

Brandt M, Grazioso TP, Fawal MA, Tummala KS, Torres-Ruiz R, Rodriguez-Perales S, Perna C, Djouder N. mTORC1 Inactivation Promotes Colitis-Induced Colorectal Cancer but Protects from APC Loss-Dependent Tumorigenesis. Cell Metab. 2018 Jan 9;27(1):118-135.e8. doi: 10.1016/j.cmet.2017.11.006. Epub 2017 Dec 21. PMID: 29275959.

Bratton SB, Salvesen GS. Regulation of the Apaf-1-caspase-9 apoptosome. J Cell Sci. 2010 Oct 1;123(Pt 19):3209-14. doi: 10.1242/jcs.073643. PMID: 20844150; PMCID: PMC2939798.

Brody H. Colorectal cancer. Nature. 2015 May 14;521(7551):S1. doi: 10.1038/521S1a. PMID: 25970450.

Browne GJ, Proud CG. A novel mTOR-regulated phosphorylation site in elongation factor 2 kinase modulates the activity of the kinase and its binding to calmodulin. Mol Cell Biol. 2004 Apr;24(7):2986-97. doi: 10.1128/MCB.24.7.2986-2997.2004. PMID: 15024086; PMCID: PMC371112.

Budanov AV, Karin M. p53 target genes sestrin1 and sestrin2 connect genotoxic stress and mTOR signaling. Cell. 2008 Aug 8;134(3):451-60. doi: 10.1016/j.cell.2008.06.028. Erratum in: Cell. 2009 Jan 23;136(2):378. PMID: 18692468; PMCID: PMC2758522.

Cadigan KM, Liu YI. Wnt signaling: complexity at the surface. J Cell Sci. 2006 Feb 1;119(Pt 3):395-402. doi: 10.1242/jcs.02826. PMID: 16443747.

Calder PC. Polyunsaturated fatty acids and inflammatory processes: New twists in an old tale. Biochimie. 2009 Jun;91(6):791-5. doi: 10.1016/j.biochi.2009.01.008. PMID: 19455748.

Calviello G, Serini S, Piccioni E. n-3 polyunsaturated fatty acids and the prevention of colorectal cancer: molecular mechanisms involved. Curr Med Chem. 2007;14(29):3059-69. doi: 10.2174/092986707782793934. PMID: 18220742.

Carrière A, Cargnello M, Julien LA, Gao H, Bonneil E, Thibault P, Roux PP. Oncogenic MAPK signaling stimulates mTORC1 activity by promoting RSK-mediated raptor phosphorylation. Curr Biol. 2008 Sep 9;18(17):1269-77. doi: 10.1016/j.cub.2008.07.078. Epub 2008 Aug 21. PMID: 18722121.

Carpten JD, Faber AL, Horn C, Donoho GP, Briggs SL, Robbins CM, Hostetter G, Boguslawski S, Moses TY, Savage S, Uhlik M, Lin A, Du J, Qian YW, Zeckner DJ, Tucker-Kellogg G, Touchman J, Patel K, Mousses S, Bittner M, Schevitz R, Lai MH, Blanchard KL, Thomas JE. A transforming mutation in the pleckstrin homology domain of AKT1 in cancer. Nature. 2007 Jul 26;448(7152):439-44. doi: 10.1038/nature05933. Epub 2007 Jul 4. PMID: 17611497.

Cho YE, Kim JH, Che YH, Kim YJ, Sung JY, Kim YW, Choe BG, Lee S, Park JH. Role of the WNT/β-catenin/ZKSCAN3 Pathway in Regulating Chromosomal Instability in Colon Cancer Cell lines and Tissues. Int J Mol Sci. 2022 Aug 18;23(16):9302. doi: 10.3390/ijms23169302. PMID: 36012568; PMCID: PMC9409321.

Choi YS, Zhang Y, Xu M, Yang Y, Ito M, Peng T, Cui Z, Nagy A, Hadjantonakis AK, Lang RA, Cotsarelis G, Andl T, Morrisey EE, Millar SE. Distinct functions for Wnt/β-catenin in hair follicle stem cell proliferation and survival and interfollicular epidermal homeostasis. Cell Stem Cell. 2013 Dec 5;13(6):720-33. doi: 10.1016/j.stem.2013.10.003. PMID: 24315444; PMCID: PMC3900235.

Choi JW, Kim P, Kim JK, Kim YR, Fukumura D, Yun SH. Longitudinal Tracing of Spontaneous Regression and Anti-angiogenic Response of Individual Microadenomas during Colon Tumorigenesis. Theranostics. 2015 Apr 1;5(7):724-32. doi: 10.7150/thno.10734. PMID: 25897337; PMCID: PMC4402496.

Christie M, Jorissen RN, Mouradov D, Sakthianandeswaren A, Li S, Day F, Tsui C, Lipton L, Desai J, Jones IT, McLaughlin S, Ward RL, Hawkins NJ, Ruszkiewicz AR, Moore J, Burgess AW, Busam D, Zhao Q, Strausberg RL, Simpson AJ, Tomlinson IP, Gibbs P, Sieber OM. Different APC genotypes in proximal and distal sporadic colorectal cancers suggest distinct WNT/β-catenin signalling thresholds for tumourigenesis. Oncogene. 2013 Sep 26;32(39):4675-82. doi: 10.1038/onc.2012.486. Epub 2012 Oct 22. PMID: 23085758; PMCID: PMC3787794.

Clapper ML, Chang WL, Cooper HS. Dysplastic Aberrant Crypt Foci: Biomarkers of Early Colorectal Neoplasia and Response to Preventive Intervention. Cancer Prev Res (Phila). 2020 Mar;13(3):229-240. doi: 10.1158/1940-6207.CAPR-19-0316. PMID: 32132117; PMCID: PMC7080315.

Clevers H, Loh KM, Nusse R. Stem cell signaling. An integral program for tissue renewal and regeneration: Wnt signaling and stem cell control. Science. 2014 Oct 3;346(6205):1248012. doi: 10.1126/science.1248012. Epub 2014 Oct 2. PMID: 25278615.

Colussi D, Brandi G, Bazzoli F, Ricciardiello L. Molecular pathways involved in colorectal cancer: implications for disease behavior and prevention. Int J Mol Sci. 2013 Aug 7;14(8):16365-85. doi: 10.3390/ijms140816365. PMID: 23965959; PMCID: PMC3759916.

Curia MC, Catalano T, Aceto GM. MUTYH: Not just polyposis. World J Clin Oncol. 2020 Jul 24;11(7):428-449. doi: 10.5306/wjco.v11.i7.428. PMID: 32821650; PMCID: PMC7407923.

de la Chapelle A. The incidence of Lynch syndrome. Fam Cancer. 2005;4(3):233-7. doi: 10.1007/s10689-004-5811-3. PMID: 16136383.

de Lau W, Peng WC, Gros P, Clevers H. The R-spondin/Lgr5/Rnf43 module: regulator of Wnt signal strength. Genes Dev. 2014 Feb 15;28(4):305-16. doi: 10.1101/gad.235473.113. PMID: 24532711; PMCID: PMC3937510.

De Palma FDE, D'Argenio V, Pol J, Kroemer G, Maiuri MC, Salvatore F. The Molecular Hallmarks of the Serrated Pathway in Colorectal Cancer. Cancers (Basel). 2019 Jul 20;11(7):1017. doi: 10.3390/cancers11071017. PMID: 31330830; PMCID: PMC6678087.

Deming DA, Leystra AA, Nettekoven L, Sievers C, Miller D, Middlebrooks M, Clipson L, Albrecht D, Bacher J, Washington MK, Weichert J, Halberg RB. PIK3CA and APC mutations are synergistic in the development of intestinal cancers. Oncogene. 2014 Apr 24;33(17):2245-54. doi: 10.1038/onc.2013.167. Epub 2013 May 27. PMID: 23708654; PMCID: PMC3883937.

Di Agostino S, Strano S, Emiliozzi V, Zerbini V, Mottolese M, Sacchi A, Blandino G, Piaggio G. Gain of function of mutant p53: the mutant p53/NF-Y protein complex reveals an aberrant transcriptional mechanism of cell cycle regulation. Cancer Cell. 2006 Sep;10(3):191-202. doi: 10.1016/j.ccr.2006.08.013. PMID: 16959611.

Dominguez-Valentin M, Sampson JR, Seppälä TT, Ten Broeke SW, Plazzer JP, Nakken S, Engel C, Aretz S, Jenkins MA, Sunde L, Bernstein I, Capella G, Balaguer F, Thomas H, Evans DG, Burn J, Greenblatt M, Hovig E, de Vos Tot Nederveen Cappel WH, Sijmons RH, Bertario L, Tibiletti MG, Cavestro GM, Lindblom A, Della Valle A, Lopez-Köstner F, Gluck N, Katz LH, Heinimann K, Vaccaro CA, Büttner R, Görgens H, Holinski-Feder E, Morak M, Holzapfel S, Hüneburg R, Knebel Doeberitz MV, Loeffler M, Rahner N, Schackert HK, Steinke-Lange V, Schmiegel W, Vangala D, Pylvänäinen K, Renkonen-Sinisalo L, Hopper JL, Win AK, Haile RW, Lindor NM, Gallinger S, Le Marchand L, Newcomb PA, Figueiredo JC, Thibodeau SN, Wadt K, Therkildsen C, Okkels H, Ketabi Z, Moreira L, Sánchez A, Serra-Burriel M, Pineda M, Navarro M, Blanco I, Green K, Lalloo F, Crosbie EJ, Hill J, Denton OG, Frayling IM, Rødland EA, Vasen H, Mints M, Neffa F, Esperon P, Alvarez K, Kariv R, Rosner G, Pinero TA, Gonzalez ML, Kalfayan P, Tjandra D, Winship IM, Macrae F, Möslein G, Mecklin JP, Nielsen M, Møller P. Cancer risks by gene, age, and gender in 6350 carriers of pathogenic mismatch repair variants: findings from the

Prospective Lynch Syndrome Database. Genet Med. 2020 Jan;22(1):15-25. doi: 10.1038/s41436-019-0596-9. Epub 2019 Jul 24. Erratum in: Genet Med. 2020 Sep;22(9):1569. PMID: 31337882; PMCID: PMC7371626.

Dowling RJ, Topisirovic I, Alain T, Bidinosti M, Fonseca BD, Petroulakis E, Wang X, Larsson O, Selvaraj A, Liu Y, Kozma SC, Thomas G, Sonenberg N. mTORC1-mediated cell proliferation, but not cell growth, controlled by the 4E-BPs. Science. 2010 May 28;328(5982):1172-6. doi: 10.1126/science.1187532. PMID: 20508131; PMCID: PMC2893390.

Edwards IJ, O'Flaherty JT. Omega-3 Fatty Acids and PPARgamma in Cancer. PPAR Res. 2008;2008:358052. doi: 10.1155/2008/358052. PMID: 18769551; PMCID: PMC2526161.

Emery S, Häberling I, Berger G, Walitza S, Schmeck K, Albert T, Baumgartner N, Strumberger M, Albermann M, Drechsler R. Omega-3 and its domain-specific effects on cognitive test performance in youths: A meta-analysis. Neurosci Biobehav Rev. 2020 May;112:420-436. doi: 10.1016/j.neubiorev.2020.02.016. Epub 2020 Feb 15. PMID: 32070694.

Faller WJ, Jackson TJ, Knight JR, Ridgway RA, Jamieson T, Karim SA, Jones C, Radulescu S, Huels DJ, Myant KB, Dudek KM, Casey HA, Scopelliti A, Cordero JB, Vidal M, Pende M, Ryazanov AG, Sonenberg N, Meyuhas O, Hall MN, Bushell M, Willis AE, Sansom OJ. mTORC1-mediated translational elongation limits intestinal tumour initiation and growth. Nature. 2015 Jan 22;517(7535):497-500. doi: 10.1038/nature13896. Epub 2014 Nov 5. PMID: 25383520; PMCID: PMC4304784

Fearnhead NS, Britton MP, Bodmer WF. The ABC of APC. Hum Mol Genet. 2001 Apr;10(7):721-33. doi: 10.1093/hmg/10.7.721. PMID: 11257105.

Fearon ER, Vogelstein B. A genetic model for colorectal tumorigenesis. Cell. 1990 Jun 1;61(5):759-67. doi: 10.1016/0092-8674(90)90186-i. PMID: 2188735.

Feitelson MA, Arzumanyan A, Kulathinal RJ, Blain SW, Holcombe RF, Mahajna J, Marino M, Martinez-Chantar ML, Nawroth R, Sanchez-Garcia I, Sharma D, Saxena NK, Singh N, Vlachostergios PJ, Guo S, Honoki K, Fujii H, Georgakilas AG, Bilsland A, Amedei A, Niccolai E, Amin A, Ashraf SS, Boosani CS, Guha G, Ciriolo MR, Aquilano K, Chen S, Mohammed SI, Azmi AS, Bhakta D, Halicka D, Keith WN, Nowsheen S. Sustained proliferation in cancer: Mechanisms and novel therapeutic targets. Semin Cancer Biol. 2015 Dec;35 Suppl(Suppl):S25-S54. doi: 10.1016/j.semcancer.2015.02.006. Epub 2015 Apr 17. PMID: 25892662; PMCID: PMC4898971.

Fidler MM, Bray F, Vaccarella S, Soerjomataram I. Assessing global transitions in human development and colorectal cancer incidence. Int J Cancer. 2017 Jun 15;140(12):2709-2715. doi: 10.1002/ijc.30686. Epub 2017 Mar 24. PMID: 28281292.

Fiedler M, Mendoza-Topaz C, Rutherford TJ, Mieszczanek J, Bienz M. Dishevelled interacts with the DIX domain polymerization interface of Axin to interfere with its function in down-regulating β-

catenin. Proc Natl Acad Sci U S A. 2011 Feb 1;108(5):1937-42. doi: 10.1073/pnas.1017063108. Epub 2011 Jan 18. PMID: 21245303; PMCID: PMC3033301.

Findeisen P, Kloor M, Merx S, Sutter C, Woerner SM, Dostmann N, Benner A, Dondog B, Pawlita M, Dippold W, Wagner R, Gebert J, von Knebel Doeberitz M. T25 repeat in the 3' untranslated region of the CASP2 gene: a sensitive and specific marker for microsatellite instability in colorectal cancer. Cancer Res. 2005 Sep 15;65(18):8072-8. doi: 10.1158/0008-5472.CAN-04-4146. PMID: 16166278.

Foley TM, Payne SN, Pasch CA, Yueh AE, Van De Hey DR, Korkos DP, Clipson L, Maher ME, Matkowskyj KA, Newton MA, Deming DA. Dual PI3K/mTOR Inhibition in Colorectal Cancers with *APC* and *PIK3CA* Mutations. Mol Cancer Res. 2017 Feb 9;15(3):317-327. doi: 10.1158/1541-7786.MCR-16-0256. Epub ahead of print. PMID: 28184015; PMCID: PMC5550373.

Fujishita T, Aoki K, Lane HA, Aoki M, Taketo MM. Inhibition of the mTORC1 pathway suppresses intestinal polyp formation and reduces mortality in ApcDelta716 mice. Proc Natl Acad Sci U S A. 2008 Sep 9;105(36):13544-9. doi: 10.1073/pnas.0800041105. Epub 2008 Sep 3. PMID: 18768809; PMCID: PMC2533226.

Gammons MV, Renko M, Johnson CM, Rutherford TJ, Bienz M. Wnt Signalosome Assembly by DEP Domain Swapping of Dishevelled. Mol Cell. 2016 Oct 6;64(1):92-104. doi: 10.1016/j.molcel.2016.08.026. Epub 2016 Sep 29. PMID: 27692984; PMCID: PMC5065529.

Gaubitz C, Oliveira TM, Prouteau M, Leitner A, Karuppasamy M, Konstantinidou G, Rispal D, Eltschinger S, Robinson GC, Thore S, Aebersold R, Schaffitzel C, Loewith R. Molecular Basis of the Rapamycin Insensitivity of Target Of Rapamycin Complex 2. Mol Cell. 2015 Jun 18;58(6):977-88. doi: 10.1016/j.molcel.2015.04.031. Epub 2015 May 28. PMID: 26028537.

Giannakis M, Hodis E, Jasmine Mu X, Yamauchi M, Rosenbluh J, Cibulskis K, Saksena G, Lawrence MS, Qian ZR, Nishihara R, Van Allen EM, Hahn WC, Gabriel SB, Lander ES, Getz G, Ogino S, Fuchs CS, Garraway LA. RNF43 is frequently mutated in colorectal and endometrial cancers. Nat Genet. 2014 Dec;46(12):1264-6. doi: 10.1038/ng.3127. Epub 2014 Oct 26. PMID: 25344691; PMCID: PMC4283570.

Goentoro L, Kirschner MW. Evidence that fold-change, and not absolute level, of beta-catenin dictates Wnt signaling. Mol Cell. 2009 Dec 11;36(5):872-84. doi: 10.1016/j.molcel.2009.11.017. PMID: 20005849; PMCID: PMC2921914.

Goodenberger M, Lindor NM. Lynch syndrome and MYH-associated polyposis: review and testing strategy. J Clin Gastroenterol. 2011 Jul;45(6):488-500. doi: 10.1097/MCG.0b013e318206489c. PMID: 21325953.

Grady WM, Carethers JM. Genomic and epigenetic instability in colorectal cancer pathogenesis. Gastroenterology. 2008 Oct;135(4):1079-99. doi: 10.1053/j.gastro.2008.07.076. Epub 2008 Sep 4. PMID: 18773902; PMCID: PMC2866182.

Gulhati P, Cai Q, Li J, Liu J, Rychahou PG, Qiu S, Lee EY, Silva SR, Bowen KA, Gao T, Evers BM. Targeted inhibition of mammalian target of rapamycin signaling inhibits tumorigenesis of colorectal cancer. Clin Cancer Res. 2009 Dec 1;15(23):7207-16. doi: 10.1158/1078-0432.CCR-09-1249. Epub 2009 Nov 24. PMID: 19934294; PMCID: PMC2898570.

Gupta S, Hastak K, Afaq F, Ahmad N, Mukhtar H. Essential role of caspases in epigallocatechin-3-gallate-mediated inhibition of nuclear factor kappa B and induction of apoptosis. Oncogene. 2004 Apr 1;23(14):2507-22. doi: 10.1038/sj.onc.1207353. PMID: 14676829.

Habib SJ, Chen BC, Tsai FC, Anastassiadis K, Meyer T, Betzig E, Nusse R. A localized Wnt signal orients asymmetric stem cell division in vitro. Science. 2013 Mar 22;339(6126):1445-8. doi: 10.1126/science.1231077. Erratum in: Science. 2013 May 24;340(6135):924. PMID: 23520113; PMCID: PMC3966430.

Hagen RM, Chedea VS, Mintoff CP, Bowler E, Morse HR, Ladomery MR. Epigallocatechin-3-gallate promotes apoptosis and expression of the caspase 9a splice variant in PC3 prostate cancer cells. Int J Oncol. 2013 Jul;43(1):194-200. doi: 10.3892/ijo.2013.1920. Epub 2013 Apr 24. PMID: 23615977.

Hardiman KM, Liu J, Feng Y, Greenson JK, Fearon ER. Rapamycin inhibition of polyposis and progression to dysplasia in a mouse model. PLoS One. 2014 Apr 24;9(4):e96023. doi: 10.1371/journal.pone.0096023. PMID: 24763434; PMCID: PMC3999114.

Harris WS, Mozaffarian D, Lefevre M, Toner CD, Colombo J, Cunnane SC, Holden JM, Klurfeld DM, Morris MC, Whelan J. Towards establishing dietary reference intakes for eicosapentaenoic and docosahexaenoic acids. J Nutr. 2009 Apr;139(4):804S-19S. doi: 10.3945/jn.108.101329. Epub 2009 Feb 25. PMID: 19244379; PMCID: PMC6459058.

Hawcroft G, Loadman PM, Belluzzi A, Hull MA. Effect of eicosapentaenoic acid on E-type prostaglandin synthesis and EP4 receptor signaling in human colorectal cancer cells. Neoplasia. 2010 Aug;12(8):618-27. doi: 10.1593/neo.10388. PMID: 20689756; PMCID: PMC2915406.

He K, Chen D, Ruan H, Li X, Tong J, Xu X, Zhang L, Yu J. BRAFV600E-dependent Mcl-1 stabilization leads to everolimus resistance in colon cancer cells. Oncotarget. 2016 Jul 26;7(30):47699-47710. doi: 10.18632/oncotarget.10277. PMID: 27351224; PMCID: PMC5216972.

Hernández AR, Klein AM, Kirschner MW. Kinetic responses of β-catenin specify the sites of Wnt control. Science. 2012 Dec 7;338(6112):1337-40. doi: 10.1126/science.1228734. Epub 2012 Nov 8. PMID: 23138978.

Holz MK, Ballif BA, Gygi SP, Blenis J. mTOR and S6K1 mediate assembly of the translation preinitiation complex through dynamic protein interchange and ordered phosphorylation events. Cell. 2005 Nov 18;123(4):569-80. doi: 10.1016/j.cell.2005.10.024. PMID: 16286006.

Huang YL, Niehrs C. Polarized Wnt signaling regulates ectodermal cell fate in Xenopus. Dev Cell. 2014 Apr 28;29(2):250-7. doi: 10.1016/j.devcel.2014.03.015. PMID: 24780739.

Inoki K, Zhu T, Guan KL. TSC2 mediates cellular energy response to control cell growth and survival. Cell. 2003 Nov 26;115(5):577-90. doi: 10.1016/s0092-8674(03)00929-2. PMID: 14651849.

Hull MA. Omega-3 polyunsaturated fatty acids. Best Pract Res Clin Gastroenterol. 2011 Aug;25(4-5):547-54. doi: 10.1016/j.bpg.2011.08.001. PMID: 22122770.

Inoki K, Li Y, Xu T, Guan KL. Rheb GTPase is a direct target of TSC2 GAP activity and regulates mTOR signaling. Genes Dev. 2003 Aug 1;17(15):1829-34. doi: 10.1101/gad.1110003. Epub 2003 Jul 17. PMID: 12869586; PMCID: PMC196227.

Janda CY, Waghray D, Levin AM, Thomas C, Garcia KC. Structural basis of Wnt recognition by Frizzled. Science. 2012 Jul 6;337(6090):59-64. doi: 10.1126/science.1222879. Epub 2012 May 31. PMID: 22653731; PMCID: PMC3577348.

Janda CY, Dang LT, You C, Chang J, de Lau W, Zhong ZA, Yan KS, Marecic O, Siepe D, Li X, Moody JD, Williams BO, Clevers H, Piehler J, Baker D, Kuo CJ, Garcia KC. Surrogate Wnt agonists that phenocopy canonical Wnt and β-catenin signalling. Nature. 2017 May 11;545(7653):234-237. doi: 10.1038/nature22306. Epub 2017 May 3. PMID: 28467818; PMCID: PMC5815871.

Jia W, Slominski BA, Guenter W, Humphreys A, Jones O. The effect of enzyme supplementation on egg production parameters and omega-3 fatty acid deposition in laying hens fed flaxseed and canola seed. Poult Sci. 2008 Oct;87(10):2005-14. doi: 10.3382/ps.2007-00474. PMID: 18809863.

Kaidanovich-Beilin O, Woodgett JR. GSK-3: Functional Insights from Cell Biology and Animal Models. Front Mol Neurosci. 2011 Nov 16;4:40. doi: 10.3389/fnmol.2011.00040. PMID: 22110425; PMCID: PMC3217193.

Kale A, Gawande S, Kotwal S, Netke S, Roomi W, Ivanov V, Niedzwiecki A, Rath M. Studies on the effects of oral administration of nutrient mixture, quercetin and red onions on the bioavailability of epigallocatechin gallate from green tea extract. Phytother Res. 2010 Jan;24 Suppl 1:S48-55. doi: 10.1002/ptr.2899. Erratum in: Phytother Res. 2010 Apr;24(4):632. PMID: 19585479.

Kanth P, Grimmett J, Champine M, Burt R, Samadder NJ. Hereditary Colorectal Polyposis and Cancer Syndromes: A Primer on Diagnosis and Management. Am J Gastroenterol. 2017 Oct;112(10):1509-1525. doi: 10.1038/ajg.2017.212. Epub 2017 Aug 8. PMID: 28786406.

Kantor M, Sobrado J, Patel S, Eiseler S, Ochner C. Hereditary Colorectal Tumors: A Literature Review on MUTYH-Associated Polyposis. Gastroenterol Res Pract. 2017;2017:8693182. doi: 10.1155/2017/8693182. Epub 2017 Sep 25. PMID: 29147111; PMCID: PMC5632881.

Kaur N, Chugh V, Gupta AK. Essential fatty acids as functional components of foods- a review. J Food Sci Technol. 2014 Oct;51(10):2289-303. doi: 10.1007/s13197-012-0677-0. Epub 2012 Mar 21. PMID: 25328170; PMCID: PMC4190204.

Kerr SE, Thomas CB, Thibodeau SN, Ferber MJ, Halling KC. APC germline mutations in individuals being evaluated for familial adenomatous polyposis: a review of the Mayo Clinic experience with 1591 consecutive tests. J Mol Diagn. 2013 Jan;15(1):31-43. doi: 10.1016/j.jmoldx.2012.07.005. Epub 2012 Nov 14. PMID: 23159591.

Khan N, Afaq F, Saleem M, Ahmad N, Mukhtar H. Targeting multiple signaling pathways by green tea polyphenol (-)-epigallocatechin-3-gallate. Cancer Res. 2006 Mar 1;66(5):2500-5. doi: 10.1158/0008-5472.CAN-05-3636. PMID: 16510563.

Kim DH, Sarbassov DD, Ali SM, King JE, Latek RR, Erdjument-Bromage H, Tempst P, Sabatini DM. mTOR interacts with raptor to form a nutrient-sensitive complex that signals to the cell growth machinery. Cell. 2002 Jul 26;110(2):163-75. doi: 10.1016/s0092-8674(02)00808-5. PMID: 12150925.

Kim LC, Cook RS, Chen J. mTORC1 and mTORC2 in cancer and the tumor microenvironment. Oncogene. 2017 Apr 20;36(16):2191-2201. doi: 10.1038/onc.2016.363. Epub 2016 Oct 17. PMID: 27748764; PMCID: PMC5393956.

Knudsen AL, Bisgaard ML, Bülow S. Attenuated familial adenomatous polyposis (AFAP). A review of the literature. Fam Cancer. 2003;2(1):43-55. doi: 10.1023/a:1023286520725. PMID: 14574166.

Kohler EM, Chandra SH, Behrens J, Schneikert J. Beta-catenin degradation mediated by the CID domain of APC provides a model for the selection of APC mutations in colorectal, desmoid and duodenal tumours. Hum Mol Genet. 2009 Jan 15;18(2):213-26. doi: 10.1093/hmg/ddn338. Epub 2008 Oct 14. PMID: 18854359.

Korkut C, Ataman B, Ramachandran P, Ashley J, Barria R, Gherbesi N, Budnik V. Trans-synaptic transmission of vesicular Wnt signals through Evi/Wntless. Cell. 2009 Oct 16;139(2):393-404. doi: 10.1016/j.cell.2009.07.051. PMID: 19837038; PMCID: PMC2785045.

Krausova M, Korinek V. Wnt signaling in adult intestinal stem cells and cancer. Cell Signal. 2014 Mar;26(3):570-9. doi: 10.1016/j.cellsig.2013.11.032. Epub 2013 Dec 2. PMID: 24308963.

Laird PW. Cancer epigenetics. Hum Mol Genet. 2005 Apr 15;14 Spec No 1:R65-76. doi: 10.1093/hmg/ddi113. PMID: 15809275.

Lambert JD, Kim DH, Zheng R, Yang CS. Transdermal delivery of (-)-epigallocatechin-3-gallate, a green tea polyphenol, in mice. J Pharm Pharmacol. 2006 May;58(5):599-604. doi: 10.1211/jpp.58.5.0004. PMID: 16640828.

Lambert JD, Elias RJ. The antioxidant and pro-oxidant activities of green tea polyphenols: a role in cancer prevention. Arch Biochem Biophys. 2010 Sep 1;501(1):65-72. doi: 10.1016/j.abb.2010.06.013. Epub 2010 Jun 15. PMID: 20558130; PMCID: PMC2946098.

Lamlum H, Ilyas M, Rowan A, Clark S, Johnson V, Bell J, Frayling I, Efstathiou J, Pack K, Payne S, Roylance R, Gorman P, Sheer D, Neale K, Phillips R, Talbot I, Bodmer W, Tomlinson I. The type of somatic mutation at APC in familial adenomatous polyposis is determined by the site of the germline mutation: a new facet to Knudson's 'two-hit' hypothesis. Nat Med. 1999 Sep;5(9):1071-5. doi: 10.1038/12511. PMID: 10470088.

Landgraf KE, Pilling C, Falke JJ. Molecular mechanism of an oncogenic mutation that alters membrane targeting: Glu17Lys modifies the PIP lipid specificity of the AKT1 PH domain. Biochemistry. 2008 Nov 25;47(47):12260-9. doi: 10.1021/bi801683k. PMID: 18954143; PMCID: PMC2919500.

Lands B. Dietary omega-3 and omega-6 fatty acids compete in producing tissue compositions and tissue responses. Mil Med. 2014 Nov;179(11 Suppl):76-81. doi: 10.7205/MILMED-D-14-00149. PMID: 25373089.

Larsson SC, Kumlin M, Ingelman-Sundberg M, Wolk A. Dietary long-chain n-3 fatty acids for the prevention of cancer: a review of potential mechanisms. Am J Clin Nutr. 2004 Jun;79(6):935-45. doi: 10.1093/ajcn/79.6.935. PMID: 15159222.

Lauby-Secretan B, Vilahur N, Bianchini F, Guha N, Straif K; International Agency for Research on Cancer Handbook Working Group. The IARC Perspective on Colorectal Cancer Screening. N Engl J Med. 2018 May 3;378(18):1734-1740. doi: 10.1056/NEJMsr1714643. Epub 2018 Mar 26. PMID: 29580179; PMCID: PMC6709879.

Lee CJ, Rana MS, Bae C, Li Y, Banerjee A. *In vitro* reconstitution of Wnt acylation reveals structural determinants of substrate recognition by the acyltransferase human Porcupine. J Biol Chem. 2019 Jan 4;294(1):231-245. doi: 10.1074/jbc.RA118.005746. Epub 2018 Nov 12. PMID: 30420431; PMCID: PMC6322882.

Lee-Six H, Olafsson S, Ellis P, Osborne RJ, Sanders MA, Moore L, Georgakopoulos N, Torrente F, Noorani A, Goddard M, Robinson P, Coorens THH, O'Neill L, Alder C, Wang J, Fitzgerald RC, Zilbauer M, Coleman N, Saeb-Parsy K, Martincorena I, Campbell PJ, Stratton MR. The landscape of somatic mutation in normal colorectal epithelial cells. Nature. 2019 Oct;574(7779):532-537. doi: 10.1038/s41586-019-1672-7. Epub 2019 Oct 23. PMID: 31645730.

Lengauer C, Kinzler KW, Vogelstein B. Genetic instabilities in human cancers. Nature. 1998 Dec 17;396(6712):643-9. doi: 10.1038/25292. PMID: 9872311.

Li J, Wang R, Zhou X, Wang W, Gao S, Mao Y, Wu X, Guo L, Liu H, Wen L, Fu W, Tang F. Genomic and transcriptomic profiling of carcinogenesis in patients with familial adenomatous polyposis. Gut. 2020 Jul;69(7):1283-1293. doi: 10.1136/gutjnl-2019-319438. Epub 2019 Nov 19. PMID: 31744909; PMCID: PMC7306982.

Li VS, Ng SS, Boersema PJ, Low TY, Karthaus WR, Gerlach JP, Mohammed S, Heck AJ, Maurice MM, Mahmoudi T, Clevers H. Wnt signaling through inhibition of β-catenin degradation in an intact Axin1 complex. Cell. 2012 Jun 8;149(6):1245-56. doi: 10.1016/j.cell.2012.05.002. PMID: 22682247.

Lipton L, Tomlinson I. The genetics of FAP and FAP-like syndromes. Fam Cancer. 2006;5(3):221-6. doi: 10.1007/s10689-005-5673-3. PMID: 16998667.

Liu C, Li Y, Semenov M, Han C, Baeg GH, Tan Y, Zhang Z, Lin X, He X. Control of beta-catenin phosphorylation/degradation by a dual-kinase mechanism. Cell. 2002 Mar 22;108(6):837-47. doi: 10.1016/s0092-8674(02)00685-2. PMID: 11955436.

Liu P, Gan W, Chin YR, Ogura K, Guo J, Zhang J, Wang B, Blenis J, Cantley LC, Toker A, Su B, Wei W. PtdIns(3,4,5)P3-Dependent Activation of the mTORC2 Kinase Complex. Cancer Discov. 2015 Nov;5(11):1194-209. doi: 10.1158/2159-8290.CD-15-0460. Epub 2015 Aug 20. PMID: 26293922; PMCID: PMC4631654.

Loeb LA, Loeb KR, Anderson JP. Multiple mutations and cancer. Proc Natl Acad Sci U S A. 2003 Feb 4;100(3):776-81. doi: 10.1073/pnas.0334858100. Epub 2003 Jan 27. PMID: 12552134; PMCID: PMC298677

Long X, Lin Y, Ortiz-Vega S, Yonezawa K, Avruch J. Rheb binds and regulates the mTOR kinase. Curr Biol. 2005 Apr 26;15(8):702-13. doi: 10.1016/j.cub.2005.02.053. PMID: 15854902.

Lustig B, Jerchow B, Sachs M, Weiler S, Pietsch T, Karsten U, van de Wetering M, Clevers H, Schlag PM, Birchmeier W, Behrens J. Negative feedback loop of Wnt signaling through upregulation of conductin/axin2 in colorectal and liver tumors. Mol Cell Biol. 2002 Feb;22(4):1184-93. doi: 10.1128/MCB.22.4.1184-1193.2002. PMID: 11809809; PMCID: PMC134640.

Markowitz SD, Bertagnolli MM. Molecular origins of cancer: Molecular basis of colorectal cancer. N Engl J Med. 2009 Dec 17;361(25):2449-60. doi: 10.1056/NEJMra0804588. PMID: 20018966; PMCID: PMC2843693.

Mármol I, Sánchez-de-Diego C, Pradilla Dieste A, Cerrada E, Rodriguez Yoldi MJ. Colorectal Carcinoma: A General Overview and Future Perspectives in Colorectal Cancer. Int J Mol Sci. 2017 Jan 19;18(1):197. doi: 10.3390/ijms18010197. PMID: 28106826; PMCID: PMC5297828.

Mashima T, Taneda Y, Jang MK, Mizutani A, Muramatsu Y, Yoshida H, Sato A, Tanaka N, Sugimoto Y, Seimiya H. mTOR signaling mediates resistance to tankyrase inhibitors in Wnt-driven colorectal cancer. Oncotarget. 2017 Jul 18;8(29):47902-47915. doi: 10.18632/oncotarget.18146. PMID: 28615517; PMCID: PMC5564614.

McGough IJ, Vincent JP. APC Moonlights to Prevent Wnt Signalosome Assembly. Dev Cell. 2018 Mar 12;44(5):535-537. doi: 10.1016/j.devcel.2018.02.018. PMID: 29533767; PMCID: PMC5861992.

Medina Pabón MA, Babiker HM. A Review of Hereditary Colorectal Cancers. [Updated 2022 Sep 26]. In: StatPearls. Treasure Island (FL): StatPearls Publishing; 2023 Jan-. Available from: https://www.ncbi.nlm.nih.gov/books/NBK538195/

Mehta CC, Bhatt HG. Tankyrase inhibitors as antitumor agents: a patent update (2013 - 2020). Expert Opin Ther Pat. 2021 Jul;31(7):645-661. doi: 10.1080/13543776.2021.1888929. Epub 2021 Mar 2. PMID: 33567917.

Molenaar M, van de Wetering M, Oosterwegel M, Peterson-Maduro J, Godsave S, Korinek V, Roose J, Destrée O, Clevers H. XTcf-3 transcription factor mediates beta-catenin-induced axis formation in Xenopus embryos. Cell. 1996 Aug 9;86(3):391-9. doi: 10.1016/s0092-8674(00)80112-9. PMID: 8756721.

Molinari F, Frattini M. Functions and Regulation of the PTEN Gene in Colorectal Cancer. Front Oncol. 2014 Jan 16;3:326. doi: 10.3389/fonc.2013.00326. PMID: 24475377; PMCID: PMC3893597.

Morin PJ, Sparks AB, Korinek V, Barker N, Clevers H, Vogelstein B, Kinzler KW. Activation of beta-catenin-Tcf signaling in colon cancer by mutations in beta-catenin or APC. Science. 1997 Mar 21;275(5307):1787-90. doi: 10.1126/science.275.5307.1787. PMID: 9065402.

Ng Y, Barhoumi R, Tjalkens RB, Fan YY, Kolar S, Wang N, Lupton JR, Chapkin RS. The role of docosahexaenoic acid in mediating mitochondrial membrane lipid oxidation and apoptosis in colonocytes. Carcinogenesis. 2005 Nov;26(11):1914-21. doi: 10.1093/carcin/bgi163. Epub 2005 Jun 23. PMID: 15975958; PMCID: PMC4477626.

Nguyen HT, Duong HQ. The molecular characteristics of colorectal cancer: Implications for diagnosis and therapy. Oncol Lett. 2018 Jul;16(1):9-18. doi: 10.3892/ol.2018.8679. Epub 2018 May 9. PMID: 29928381; PMCID: PMC6006272.

Nguyen HTL, Soragni A. Patient-Derived Tumor Organoid Rings for Histologic Characterization and High-Throughput Screening. STAR Protoc. 2020 Sep 18;1(2):100056. doi: 10.1016/j.xpro.2020.100056. Epub 2020 Jun 27. PMID: 33043307; PMCID: PMC7546514.

Nusse R, Clevers H. Wnt/β-Catenin Signaling, Disease, and Emerging Therapeutic Modalities. Cell. 2017 Jun 1;169(6):985-999. doi: 10.1016/j.cell.2017.05.016. PMID: 28575679.

Ogino S, Cantor M, Kawasaki T, Brahmandam M, Kirkner GJ, Weisenberger DJ, Campan M, Laird PW, Loda M, Fuchs CS. CpG island methylator phenotype (CIMP) of colorectal cancer is best characterised by quantitative DNA methylation analysis and prospective cohort studies. Gut. 2006 Jul;55(7):1000-6. doi: 10.1136/gut.2005.082933. Epub 2006 Jan 11. PMID: 16407376; PMCID: PMC1856352.

Oh S, Gwak J, Park S, Yang CS. Green tea polyphenol EGCG suppresses Wnt/β-catenin signaling by promoting GSK-3β- and PP2A-independent β-catenin phosphorylation/degradation. Biofactors. 2014 Nov-Dec;40(6):586-95. doi: 10.1002/biof.1185. Epub 2014 Oct 29. PMID: 25352148; PMCID: PMC4285564.

Pancione M, Remo A, Colantuoni V. Genetic and epigenetic events generate multiple pathways in colorectal cancer progression. Patholog Res Int. 2012;2012:509348. doi: 10.1155/2012/509348. Epub 2012 Jul 24. PMID: 22888469; PMCID: PMC3409552.

Pandurangan AK. Potential targets for prevention of colorectal cancer: a focus on PI3K/Akt/mTOR and Wnt pathways. Asian Pac J Cancer Prev. 2013;14(4):2201-5. doi: 10.7314/apjcp.2013.14.4.2201. PMID: 23725112.

Park YL, Kim HP, Cho YW, Min DW, Cheon SK, Lim YJ, Song SH, Kim SJ, Han SW, Park KJ, Kim TY. Activation of WNT/β-catenin signaling results in resistance to a dual PI3K/mTOR inhibitor in colorectal cancer cells harboring PIK3CA mutations. Int J Cancer. 2019 Jan 15;144(2):389-401. doi: 10.1002/ijc.31662. Epub 2018 Nov 29. PMID: 29978469; PMCID: PMC6587482.

Parvani JG, Davuluri G, Wendt MK, Espinosa C, Tian M, Danielpour D, Sossey-Alaoui K, Schiemann WP. Deptor enhances triple-negative breast cancer metastasis and chemoresistance through coupling to survivin expression. Neoplasia. 2015 Mar;17(3):317-28. doi: 10.1016/j.neo.2015.02.003. PMID: 25810016; PMCID: PMC4372649.

Peltomäki P, Nyström M, Mecklin JP, Seppälä TT. Lynch Syndrome Genetics and Clinical Implications. Gastroenterology. 2023 Apr;164(5):783-799. doi: 10.1053/j.gastro.2022.08.058. Epub 2023 Jan 24. PMID: 36706841.

Pino MS, Chung DC. The chromosomal instability pathway in colon cancer. Gastroenterology. 2010 Jun;138(6):2059-72. doi: 10.1053/j.gastro.2009.12.065. PMID: 20420946; PMCID: PMC4243705.

Pleguezuelos-Manzano C, Puschhof J, van den Brink S, Geurts V, Beumer J, Clevers H. Establishment and Culture of Human Intestinal Organoids Derived from Adult Stem Cells. Curr Protoc Immunol. 2020 Sep;130(1):e106. doi: 10.1002/cpim.106. PMID: 32940424; PMCID: PMC9285512.

Pronobis MI, Rusan NM, Peifer M. A novel GSK3-regulated APC:Axin interaction regulates Wnt signaling by driving a catalytic cycle of efficient βcatenin destruction. Elife. 2015 Sep 22;4:e08022. doi: 10.7554/eLife.08022. PMID: 26393419; PMCID: PMC4568445.

Prossomariti A, Piazzi G, Alquati C, Ricciardiello L. Are Wnt/β-Catenin and PI3K/AKT/mTORC1 Distinct Pathways in Colorectal Cancer? Cell Mol Gastroenterol Hepatol. 2020;10(3):491-506. doi: 10.1016/j.jcmgh.2020.04.007. Epub 2020 Apr 22. PMID: 32334125; PMCID: PMC7369353.

Prossomariti A, Scaioli E, Piazzi G, Fazio C, Bellanova M, Biagi E, Candela M, Brigidi P, Consolandi C, Balbi T, Chieco P, Munarini A, Pariali M, Minguzzi M, Bazzoli F, Belluzzi A, Ricciardiello L. Short-term treatment with eicosapentaenoic acid improves inflammation and affects colonic differentiation markers and microbiota in patients with ulcerative colitis. Sci Rep. 2017 Aug 7;7(1):7458. doi: 10.1038/s41598-017-07992-1. PMID: 28785079; PMCID: PMC5547132.

Rajalingam K, Schreck R, Rapp UR, Albert S. Ras oncogenes and their downstream targets. Biochim Biophys Acta. 2007 Aug;1773(8):1177-95. doi: 10.1016/j.bbamcr.2007.01.012. Epub 2007 Jan 28. PMID: 17428555.

Reis LB, Konzen D, Netto CBO, Braghini PMB, Prolla G, Ashton-Prolla P. Tuberous Sclerosis Complex with rare associated findings in the gastrointestinal system: a case report and review of the literature. BMC Gastroenterol. 2020 Nov 23;20(1):394. doi: 10.1186/s12876-020-01481-y. PMID: 33225890; PMCID: PMC7682061.

Rethineswaran VK, Kim DY, Kim YJ, Jang W, Ji ST, Van LTH, Giang LTT, Ha JS, Yun J, Jung J, Kwon SM. CHIR99021 Augmented the Function of Late Endothelial Progenitor Cells by Preventing Replicative Senescence. Int J Mol Sci. 2021 Apr 30;22(9):4796. doi: 10.3390/ijms22094796. Erratum in: Int J Mol Sci. 2022 Oct 27;23(21): PMID: 33946516; PMCID: PMC8124445.

Ricciardiello L, Ferrari C, Cameletti M, Gaianill F, Buttitta F, Bazzoli F, Luigi de'Angelis G, Malesci A, Laghi L. Impact of SARS-CoV-2 Pandemic on Colorectal Cancer Screening Delay: Effect on Stage Shift and Increased Mortality. Clin Gastroenterol Hepatol. 2021 Jul;19(7):1410-1417.e9. doi: 10.1016/j.cgh.2020.09.008. Epub 2020 Sep 6. PMID: 32898707; PMCID: PMC7474804.

Rios-Esteves J, Resh MD. Stearoyl CoA desaturase is required to produce active, lipid-modified Wnt proteins. Cell Rep. 2013 Sep 26;4(6):1072-81. doi: 10.1016/j.celrep.2013.08.027. Epub 2013 Sep 19. PMID: 24055053; PMCID: PMC3845236.

Roberts DM, Pronobis MI, Poulton JS, Waldmann JD, Stephenson EM, Hanna S, Peifer M. Deconstructing the ßcatenin destruction complex: mechanistic roles for the tumor suppressor APC in regulating Wnt signaling. Mol Biol Cell. 2011 Jun 1;22(11):1845-63. doi: 10.1091/mbc.E10-11-0871. Epub 2011 Apr 6. PMID: 21471006; PMCID: PMC3103401.

Roncucci L, Stamp D, Medline A, Cullen JB, Bruce WR. Identification and quantification of aberrant crypt foci and microadenomas in the human colon. Hum Pathol. 1991 Mar;22(3):287-94. doi: 10.1016/0046-8177(91)90163-j. PMID: 1706308.

Rosset C, Netto CBO, Ashton-Prolla P. TSC1 and TSC2 gene mutations and their implications for treatment in Tuberous Sclerosis Complex: a review. Genet Mol Biol. 2017 Jan-Mar;40(1):69-79. doi: 10.1590/1678-4685-GMB-2015-0321. Epub 2017 Feb 20. PMID: 28222202; PMCID: PMC5409767.

Saito-Diaz K, Benchabane H, Tiwari A, Tian A, Li B, Thompson JJ, Hyde AS, Sawyer LM, Jodoin JN, Santos E, Lee LA, Coffey RJ, Beauchamp RD, Williams CS, Kenworthy AK, Robbins DJ, Ahmed Y, Lee E. APC Inhibits Ligand-Independent Wnt Signaling by the Clathrin Endocytic Pathway. Dev Cell. 2018 Mar 12;44(5):566-581.e8. doi: 10.1016/j.devcel.2018.02.013. PMID: 29533772; PMCID: PMC5884143.

Salahshor S, Woodgett JR. The links between axin and carcinogenesis. J Clin Pathol. 2005 Mar;58(3):225-36. doi: 10.1136/jcp.2003.009506. Erratum in: J Clin Pathol. 2005 Dec;58(12):1344. PMID: 15735151; PMCID: PMC1770611.

Samowitz WS, Albertsen H, Herrick J, Levin TR, Sweeney C, Murtaugh MA, Wolff RK, Slattery ML. Evaluation of a large, population-based sample supports a CpG island methylator phenotype in colon cancer. Gastroenterology. 2005 Sep;129(3):837-45. doi: 10.1053/j.gastro.2005.06.020. PMID: 16143123.

Sancak Y, Thoreen CC, Peterson TR, Lindquist RA, Kang SA, Spooner E, Carr SA, Sabatini DM. PRAS40 is an insulin-regulated inhibitor of the mTORC1 protein kinase. Mol Cell. 2007 Mar 23;25(6):903-15. doi: 10.1016/j.molcel.2007.03.003. PMID: 17386266.

Saxton RA, Sabatini DM. mTOR Signaling in Growth, Metabolism, and Disease. Cell. 2017 Mar 9;168(6):960-976. doi: 10.1016/j.cell.2017.02.004. Erratum in: Cell. 2017 Apr 6;169(2):361-371. PMID: 28283069; PMCID: PMC5394987.

Scheid MP, Marignani PA, Woodgett JR. Multiple phosphoinositide 3-kinase-dependent steps in activation of protein kinase B. Mol Cell Biol. 2002 Sep;22(17):6247-60. doi: 10.1128/MCB.22.17.6247-6260.2002. PMID: 12167717; PMCID: PMC134003.

Schwarz-Romond T, Fiedler M, Shibata N, Butler PJ, Kikuchi A, Higuchi Y, Bienz M. The DIX domain of Dishevelled confers Wnt signaling by dynamic polymerization. Nat Struct Mol Biol. 2007 Jun;14(6):484-92. doi: 10.1038/nsmb1247. Epub 2007 May 27. PMID: 17529994.

Sehgal R, Sheahan K, O'Connell PR, Hanly AM, Martin ST, Winter DC. Lynch syndrome: an updated review. Genes (Basel). 2014 Jun 27;5(3):497-507. doi: 10.3390/genes5030497. PMID: 24978665; PMCID: PMC4198913.

Sekine S, Yamashita S, Tanabe T, Hashimoto T, Yoshida H, Taniguchi H, Kojima M, Shinmura K, Saito Y, Hiraoka N, Ushijima T, Ochiai A. Frequent PTPRK-RSPO3 fusions and RNF43 mutations in colorectal traditional serrated adenoma. J Pathol. 2016 Jun;239(2):133-8. doi: 10.1002/path.4709. Epub 2016 Apr 9. PMID: 26924569.

Serhan CN, Chiang N. Endogenous pro-resolving and anti-inflammatory lipid mediators: a new pharmacologic genus. Br J Pharmacol. 2008 Mar;153 Suppl 1(Suppl 1):S200-15. doi: 10.1038/sj.bjp.0707489. Epub 2007 Oct 29. PMID: 17965751; PMCID: PMC2268040.

Seshagiri S, Stawiski EW, Durinck S, Modrusan Z, Storm EE, Conboy CB, Chaudhuri S, Guan Y, Janakiraman V, Jaiswal BS, Guillory J, Ha C, Dijkgraaf GJ, Stinson J, Gnad F, Huntley MA, Degenhardt JD, Haverty PM, Bourgon R, Wang W, Koeppen H, Gentleman R, Starr TK, Zhang Z, Largaespada DA, Wu TD, de Sauvage FJ. Recurrent R-spondin fusions in colon cancer. Nature. 2012 Aug 30;488(7413):660-4. doi: 10.1038/nature11282. PMID: 22895193; PMCID: PMC3690621.

Shankar S, Ganapathy S, Srivastava RK. Green tea polyphenols: biology and therapeutic implications in cancer. Front Biosci. 2007 Sep 1;12:4881-99. doi: 10.2741/2435. PMID: 17569617.

Shen L, Toyota M, Kondo Y, Lin E, Zhang L, Guo Y, Hernandez NS, Chen X, Ahmed S, Konishi K, Hamilton SR, Issa JP. Integrated genetic and epigenetic analysis identifies three different subclasses of colon cancer. Proc Natl Acad Sci U S A. 2007 Nov 20;104(47):18654-9. doi: 10.1073/pnas.0704652104. Epub 2007 Nov 14. PMID: 18003927; PMCID: PMC2141832.

Shussman N, Wexner SD. Colorectal polyps and polyposis syndromes. Gastroenterol Rep (Oxf). 2014 Feb;2(1):1-15. doi: 10.1093/gastro/got041. Epub 2014 Jan 23. PMID: 24760231; PMCID: PMC3920990.

Siegel RL, Miller KD, Fuchs HE, Jemal A. Cancer statistics, 2022. CA Cancer J Clin. 2022 Jan;72(1):7-33. doi: 10.3322/caac.21708. Epub 2022 Jan 12. PMID: 35020204.

Smith G, Carey FA, Beattie J, Wilkie MJ, Lightfoot TJ, Coxhead J, Garner RC, Steele RJ, Wolf CR. Mutations in APC, Kirsten-ras, and p53--alternative genetic pathways to colorectal cancer. Proc Natl Acad Sci U S A. 2002 Jul 9;99(14):9433-8. doi: 10.1073/pnas.122612899. Epub 2002 Jul 1. PMID: 12093899; PMCID: PMC123158.

Sieber OM, Tomlinson IP, Lamlum H. The adenomatous polyposis coli (APC) tumour suppressor--genetics, function and disease. Mol Med Today. 2000 Dec;6(12):462-9. doi: 10.1016/s1357-4310(00)01828-1. Erratum in: Mol Med Today 2001 Jan;7(1):40. PMID: 11099951.

Smith G, Bounds R, Wolf H, Steele RJ, Carey FA, Wolf CR. Activating K-Ras mutations outwith 'hotspot' codons in sporadic colorectal tumours - implications for personalised cancer medicine. Br J Cancer. 2010 Feb 16;102(4):693-703. doi: 10.1038/sj.bjc.6605534. PMID: 20147967; PMCID: PMC2837563.

Solberg NT, Waaler J, Lund K, Mygland L, Olsen PA, Krauss S. TANKYRASE Inhibition Enhances the Antiproliferative Effect of PI3K and EGFR Inhibition, Mutually Affecting β-CATENIN and AKT Signaling in Colorectal Cancer. Mol Cancer Res. 2018 Mar;16(3):543-553. doi: 10.1158/1541-7786.MCR-17-0362. Epub 2017 Dec 8. PMID: 29222171.

Srinivas KP, Viji R, Dan VM, Sajitha IS, Prakash R, Rahul PV, Santhoshkumar TR, Lakshmi S, Pillai MR. DEPTOR promotes survival of cervical squamous cell carcinoma cells and its silencing induces apoptosis through downregulating PI3K/AKT and by up-regulating p38 MAP kinase. Oncotarget. 2016 Apr 26;7(17):24154-71. doi: 10.18632/oncotarget.8131. PMID: 26992219; PMCID: PMC5029691.

Stamos JL, Weis WI. The β-catenin destruction complex. Cold Spring Harb Perspect Biol. 2013 Jan 1;5(1):a007898. doi: 10.1101/cshperspect.a007898. PMID: 23169527; PMCID: PMC3579403.

Stamos JL, Chu ML, Enos MD, Shah N, Weis WI. Structural basis of GSK-3 inhibition by N-terminal phosphorylation and by the Wnt receptor LRP6. Elife. 2014 Mar 18;3:e01998. doi: 10.7554/eLife.01998. PMID: 24642411; PMCID: PMC3953950.

Stekrova J, Sulova M, Kebrdlova V, Zidkova K, Kotlas J, Ilencikova D, Vesela K, Kohoutova M. Novel APC mutations in Czech and Slovak FAP families: clinical and genetic aspects. BMC Med Genet. 2007 Apr 5;8:16. doi: 10.1186/1471-2350-8-16. PMID: 17411426; PMCID: PMC1853078.

Stracka D, Jozefczuk S, Rudroff F, Sauer U, Hall MN. Nitrogen source activates TOR (target of rapamycin) complex 1 via glutamine and independently of Gtr/Rag proteins. J Biol Chem. 2014 Sep 5;289(36):25010-20. doi: 10.1074/jbc.M114.574335. Epub 2014 Jul 25. PMID: 25063813; PMCID: PMC4155668.

Sun Z, Cao X, Jiang MM, Qiu Y, Zhou H, Chen L, Qin B, Wu H, Jiang F, Chen J, Liu J, Dai Y, Chen HF, Hu QY, Wu Z, Zeng JZ, Yao XS, Zhang XK. Inhibition of β-catenin signaling by nongenomic action of orphan nuclear receptor Nur77. Oncogene. 2012 May 24;31(21):2653-67. doi: 10.1038/onc.2011.448. Epub 2011 Oct 10. PMID: 21986938; PMCID: PMC3257393.

Suzuki A, Hayashida M, Ito T, Kawano H, Nakano T, Miura M, Akahane K, Shiraki K. Survivin initiates cell cycle entry by the competitive interaction with Cdk4/p16(INK4a) and Cdk2/cyclin E complex activation. Oncogene. 2000 Jul 6;19(29):3225-34. doi: 10.1038/sj.onc.1203665. PMID: 10918579.

Takagaki A, Nanjo F. Metabolism of (-)-epigallocatechin gallate by rat intestinal flora. J Agric Food Chem. 2010 Jan 27;58(2):1313-21. doi: 10.1021/jf903375s. PMID: 20043675.

Tang Y, Zhao DY, Elliott S, Zhao W, Curiel TJ, Beckman BS, Burow ME. Epigallocatechin-3 gallate induces growth inhibition and apoptosis in human breast cancer cells through survivin suppression. Int J Oncol. 2007 Oct;31(4):705-11. PMID: 17786300.

Tauriello DV, Jordens I, Kirchner K, Slootstra JW, Kruitwagen T, Bouwman BA, Noutsou M, Rüdiger SG, Schwamborn K, Schambony A, Maurice MM. Wnt/β-catenin signaling requires interaction of the Dishevelled DEP domain and C terminus with a discontinuous motif in Frizzled. Proc Natl Acad Sci U S A. 2012 Apr 3;109(14):E812-20. doi: 10.1073/pnas.1114802109. Epub 2012 Mar 12. PMID: 22411803; PMCID: PMC3325702.

Tee AR, Manning BD, Roux PP, Cantley LC, Blenis J. Tuberous sclerosis complex gene products, Tuberin and Hamartin, control mTOR signaling by acting as a GTPase-activating protein complex toward Rheb. Curr Biol. 2003 Aug 5;13(15):1259-68. doi: 10.1016/s0960-9822(03)00506-2. Erratum in: Curr Biol. 2022 Feb 7;32(3):733-734. PMID: 12906785.

Thibodeau SN, Bren G, Schaid D. Microsatellite instability in cancer of the proximal colon. Science. 1993 May 7;260(5109):816-9. doi: 10.1126/science.8484122. PMID: 8484122.

Thomas LE, Hurley JJ, Meuser E, Jose S, Ashelford KE, Mort M, Idziaszczyk S, Maynard J, Brito HL, Harry M, Walters A, Raja M, Walton SJ, Dolwani S, Williams GT, Morgan M, Moorghen M, Clark SK, Sampson JR. Burden and Profile of Somatic Mutation in Duodenal Adenomas from Patients with Familial Adenomatous- and *MUTYH*-associated Polyposis. Clin Cancer Res. 2017 Nov 1;23(21):6721-6732. doi: 10.1158/1078-0432.CCR-17-1269. Epub 2017 Aug 8. PMID: 28790112.

Thorne CA, Wichaidit C, Coster AD, Posner BA, Wu LF, Altschuler SJ. GSK-3 modulates cellular responses to a broad spectrum of kinase inhibitors. Nat Chem Biol. 2015 Jan;11(1):58-63. doi: 10.1038/nchembio.1690. Epub 2014 Nov 17. PMID: 25402767; PMCID: PMC4270937.

Thorpe LM, Yuzugullu H, Zhao JJ. PI3K in cancer: divergent roles of isoforms, modes of activation and therapeutic targeting. Nat Rev Cancer. 2015 Jan;15(1):7-24. doi: 10.1038/nrc3860. PMID: 25533673; PMCID: PMC4384662.

Turk HF, Chapkin RS. Membrane lipid raft organization is uniquely modified by n-3 polyunsaturated fatty acids. Prostaglandins Leukot Essent Fatty Acids. 2013 Jan;88(1):43-7. doi: 10.1016/j.plefa.2012.03.008. Epub 2012 Apr 18. PMID: 22515942; PMCID: PMC3404206.

Turk HF, Barhoumi R, Chapkin RS. Alteration of EGFR spatiotemporal dynamics suppresses signal transduction. PLoS One. 2012;7(6):e39682. doi: 10.1371/journal.pone.0039682. Epub 2012 Jun 27. PMID: 22761867; PMCID: PMC3384615.

Tian T, Li X, Zhang J. mTOR Signaling in Cancer and mTOR Inhibitors in Solid Tumor Targeting Therapy. Int J Mol Sci. 2019 Feb 11;20(3):755. doi: 10.3390/ijms20030755. PMID: 30754640; PMCID: PMC6387042.

Tsai YH, Czerwinski M, Wu A, Dame MK, Attili D, Hill E, Colacino JA, Nowacki LM, Shroyer NF, Higgins PDR, Kao JY, Spence JR. A Method for Cryogenic Preservation of Human Biopsy Specimens and Subsequent Organoid Culture. Cell Mol Gastroenterol Hepatol. 2018 May 30;6(2):218-222.e7. doi: 10.1016/j.jcmgh.2018.04.008. PMID: 30105282; PMCID: PMC6085494.

Van Aller GS, Carson JD, Tang W, Peng H, Zhao L, Copeland RA, Tummino PJ, Luo L. Epigallocatechin gallate (EGCG), a major component of green tea, is a dual phosphoinositide-3-kinase/mTOR inhibitor. Biochem Biophys Res Commun. 2011 Mar 11;406(2):194-9. doi: 10.1016/j.bbrc.2011.02.010. Epub 2011 Feb 15. PMID: 21300025.

Valvezan A.J., Zhang F., Diehl J.A., Klein P.S. Adenomatous polyposis coli (APC) regulates multiple signaling pathways by enhancing glycogen synthase kinase-3 (GSK-3) activity. *J Biol Chem.* 2012;287:3823–3832.

Valvezan AJ, Huang J, Lengner CJ, Pack M, Klein PS. Oncogenic mutations in adenomatous polyposis coli (Apc) activate mechanistic target of rapamycin complex 1 (mTORC1) in mice and zebrafish. Dis Model Mech. 2014 Jan;7(1):63-71. doi: 10.1242/dmm.012625. Epub 2013 Oct 2. PMID: 24092877; PMCID: PMC3882049.

Valvezan AJ, Turner M, Belaid A, Lam HC, Miller SK, McNamara MC, Baglini C, Housden BE, Perrimon N, Kwiatkowski DJ, Asara JM, Henske EP, Manning BD. mTORC1 Couples Nucleotide Synthesis to Nucleotide Demand Resulting in a Targetable Metabolic Vulnerability. Cancer Cell. 2017 Nov

13;32(5):624-638.e5. doi: 10.1016/j.ccell.2017.09.013. Epub 2017 Oct 19. PMID: 29056426; PMCID: PMC5687294.

Vilar E, Gruber SB. Microsatellite instability in colorectal cancer-the stable evidence. Nat Rev Clin Oncol. 2010 Mar;7(3):153-62. doi: 10.1038/nrclinonc.2009.237. Epub 2010 Feb 9. PMID: 20142816; PMCID: PMC3427139.

Vivanco I, Sawyers CL. The phosphatidylinositol 3-Kinase AKT pathway in human cancer. Nat Rev Cancer. 2002 Jul;2(7):489-501. doi: 10.1038/nrc839. PMID: 12094235.

Voutsadakis IA. The Landscape of PIK3CA Mutations in Colorectal Cancer. Clin Colorectal Cancer. 2021 Sep;20(3):201-215. doi: 10.1016/j.clcc.2021.02.003. Epub 2021 Feb 19. PMID: 33744168.

Wall R, Ross RP, Fitzgerald GF, Stanton C. Fatty acids from fish: the anti-inflammatory potential of long-chain omega-3 fatty acids. Nutr Rev. 2010 May;68(5):280-9. doi: 10.1111/j.1753-4887.2010.00287.x. PMID: 20500789.

Wang C, Aikemu B, Shao Y, Zhang S, Yang G, Hong H, Huang L, Jia H, Yang X, Zheng M, Sun J, Li J. Genomic signature of MTOR could be an immunogenicity marker in human colorectal cancer. BMC Cancer. 2022 Jul 26;22(1):818. doi: 10.1186/s12885-022-09901-w. PMID: 35883111; PMCID: PMC9327395.

Wang Q, Zhou Y, Rychahou P, Harris JW, Zaytseva YY, Liu J, Wang C, Weiss HL, Liu C, Lee EY, Evers BM. Deptor Is a Novel Target of Wnt/β-Catenin/c-Myc and Contributes to Colorectal Cancer Cell Growth. Cancer Res. 2018 Jun 15;78(12):3163-3175. doi: 10.1158/0008-5472.CAN-17-3107. Epub 2018 Apr 17. PMID: 29666061; PMCID: PMC6004255.

Ward R, Meagher A, Tomlinson I, O'Connor T, Norrie M, Wu R, Hawkins N. Microsatellite instability and the clinicopathological features of sporadic colorectal cancer. Gut. 2001 Jun;48(6):821-9. doi: 10.1136/gut.48.6.821. PMID: 11358903; PMCID: PMC1728324.

Weisenberger DJ, Siegmund KD, Campan M, Young J, Long TI, Faasse MA, Kang GH, Widschwendter M, Weener D, Buchanan D, Koh H, Simms L, Barker M, Leggett B, Levine J, Kim M, French AJ, Thibodeau SN, Jass J, Haile R, Laird PW. CpG island methylator phenotype underlies sporadic microsatellite instability and is tightly associated with BRAF mutation in colorectal cancer. Nat Genet. 2006 Jul;38(7):787-93. doi: 10.1038/ng1834. Epub 2006 Jun 25. PMID: 16804544.

Wilson AJ, Arango D, Mariadason JM, Heerdt BG, Augenlicht LH. TR3/Nur77 in colon cancer cell apoptosis. Cancer Res. 2003 Sep 1;63(17):5401-7. PMID: 14500374.

Win AK, Jenkins MA, Dowty JG, Antoniou AC, Lee A, Giles GG, Buchanan DD, Clendenning M, Rosty C, Ahnen DJ, Thibodeau SN, Casey G, Gallinger S, Le Marchand L, Haile RW, Potter JD, Zheng Y, Lindor NM, Newcomb PA, Hopper JL, MacInnis RJ. Prevalence and Penetrance of Major Genes and Polygenes

for Colorectal Cancer. Cancer Epidemiol Biomarkers Prev. 2017 Mar;26(3):404-412. doi: 10.1158/1055-9965.EPI-16-0693. Epub 2016 Oct 31. PMID: 27799157; PMCID: PMC5336409.

Wu AH, Yu MC, Tseng CC, Hankin J, Pike MC. Green tea and risk of breast cancer in Asian Americans. Int J Cancer. 2003 Sep 10;106(4):574-579. doi: 10.1002/ijc.11259. PMID: 12845655.

Yang E, Tacchelly-Benites O, Wang Z, Randall MP, Tian A, Benchabane H, Freemantle S, Pikielny C, Tolwinski NS, Lee E, Ahmed Y. Wnt pathway activation by ADP-ribosylation. Nat Commun. 2016 May 3;7:11430. doi: 10.1038/ncomms11430. PMID: 27138857; PMCID: PMC4857404.

Yang J, Zhang W, Evans PM, Chen X, He X, Liu C. Adenomatous polyposis coli (APC) differentially regulates beta-catenin phosphorylation and ubiquitination in colon cancer cells. J Biol Chem. 2006 Jun 30;281(26):17751-7. doi: 10.1074/jbc.M600831200. Epub 2006 May 3. PMID: 16798748.

Yu J, Chia J, Canning CA, Jones CM, Bard FA, Virshup DM. WLS retrograde transport to the endoplasmic reticulum during Wnt secretion. Dev Cell. 2014 May 12;29(3):277-91. doi: 10.1016/j.devcel.2014.03.016. Epub 2014 Apr 24. PMID: 24768165.

Zhang J, Roberts TM, Shivdasani RA. Targeting PI3K signaling as a therapeutic approach for colorectal cancer. Gastroenterology. 2011 Jul;141(1):50-61. doi: 10.1053/j.gastro.2011.05.010. PMID: 21723986.

Zhang HR, Chen JM, Zeng ZY, Que WZ. Knockdown of DEPTOR inhibits cell proliferation and increases chemosensitivity to melphalan in human multiple myeloma RPMI-8226 cells via inhibiting PI3K/AKT activity. J Int Med Res. 2013 Jun;41(3):584-95. doi: 10.1177/0300060513480920. Epub 2013 Apr 15. PMID: 23613505.

Zhao Y, Bruemmer D. NR4A orphan nuclear receptors: transcriptional regulators of gene expression in metabolism and vascular biology. Arterioscler Thromb Vasc Biol. 2010 Aug;30(8):1535-41. doi: 10.1161/ATVBAHA.109.191163. PMID: 20631354; PMCID: PMC2907171

Zeng H, Lu B, Zamponi R, Yang Z, Wetzel K, Loureiro J, Mohammadi S, Beibel M, Bergling S, Reece-Hoyes J, Russ C, Roma G, Tchorz JS, Capodieci P, Cong F. mTORC1 signaling suppresses Wnt/β-catenin signaling through DVL-dependent regulation of Wnt receptor FZD level. Proc Natl Acad Sci U S A. 2018 Oct 30;115(44):E10362-E10369. doi: 10.1073/pnas.1808575115. Epub 2018 Oct 8. PMID: 30297426; PMCID: PMC6217415.

Zinzalla V, Stracka D, Oppliger W, Hall MN. Activation of mTORC2 by association with the ribosome. Cell. 2011 Mar 4;144(5):757-68. doi: 10.1016/j.cell.2011.02.014. PMID: 21376236.